Polymeric self-assembled cucurbit[*n*]urils: synthesis, structures and applications

Dan Yang[a], Ming Liu[a], Xin Xiao*[a], Zhu Tao[a], Carl Redshaw*[b]

[a] *Key Laboratory of Macrocyclic and Supramolecular Chemistry of Guizhou Province, Guizhou University, Guiyang 550025, China.*

[b] *Department of Chemistry and Biochemistry, University of Hull, Hull HU6 7RX, U.K.*

**Corresponding authors. Tel./fax: +86 15519089928*

E-mail addresses: gyhxxiaoxin@163.com (X. Xiao); c.redshaw@hull.ac.uk (C. Redshaw)

Abstract: In recent years, cucurbit[*n*]urils (CB[*n*] or Q[*n*]s) have attracted considerable attention on account of their unique structural and host-guest binding properties. In this review, we provide an overview of their self-assembly into polymeric species via Q[*n*]-mediated tertiary host-guest interactions, and where appropriate, focus on potential applications. The first part of the review describes systems in terms of their structural type from the adoption of tertiary complexes through to microcapsules and vesicles, whilst the second part of the review discusses the systems by way of differing applications. Within each section, systems are arranged in terms of Q[*n*] size, with n = 5 to 14, and the type of bonding involved, namely the use of either covalent bonding or non-covalent bonding in combination with host-guest interactions.

Keywords: cucurbit[*n*]urils, polymer, self-assembly, host-guest, covalent bond, non-covalent bond, applications.

Contents

1. Introduction

Cucurbit[*n*]urils (Q[*n*] = 5–8, 10, 13–15), also often abbreviated as CB[*n*]s, herein we will use the term Q[*n*], where discovered back in 1905 by Behrend *et al*. [1], and are a family of macrocyclic molecules derived from the acid catalyzed condensation of glycoluril with formaldehyde. However, it was not until the 1980s that the exact nature of the structure became clear with the characterization of the Q[6] derivative, and in subsequent years other larger derivatives were isolated [2-5]. Much of the interest in this macrocycle family stems from the remarkable aqueous host–guest chemistry they exhibit. The structures, properties and applications of some Q[*n*]s have been the subject of a number of reviews. [6-15] In terms of supramolecular Q[*n*]-based polymers, Zhang and coworkers published a focus review on the n = 8 system, describing systems built up

from small molecules, polymers, dendrimers and proteins [16]. Wang and Li also review the Q[8] system, focusing on polymer and networks formed in water [17]. More recently, Zou, Wang *et al* brought the Q[8] supramolecular story more up-to-date, and described a number of microcapsules, hydrogels, micelles, vesicles and colloids [18]. Tuncel *et al* have reviewed a number of nanostructures constructed either via host-guest chemistry or post-modification [19]. The same group have also reviewed supramolecular Q[*n*] assemblies incorporating photoactive, π-conjugated chromophores [20]. Research progress in the Scherman group in the area of host-guest Q[*n*] supramolecular chemistry has also been reviewed [21]. It is clear from all the work to-date that the carbonyl-lined portals and the hydrophobic cavities of the Q[*n*]s are central to the construction of these polymeric systems, with the release of water molecules from the latter playing a pivotal role in host-guest complexation. The size of the cavity increases with the number of glycoluril units, with internal cavity diameters typically in the range 4.4 – 12.6 Å. In this review, we give an up-to-date overview of the field of polymeric Q[*n*] chemistry, with focus on synthesis, structure and applications. Representations of the structures of the Q[*n*]s described in this review are given in Chart 1.

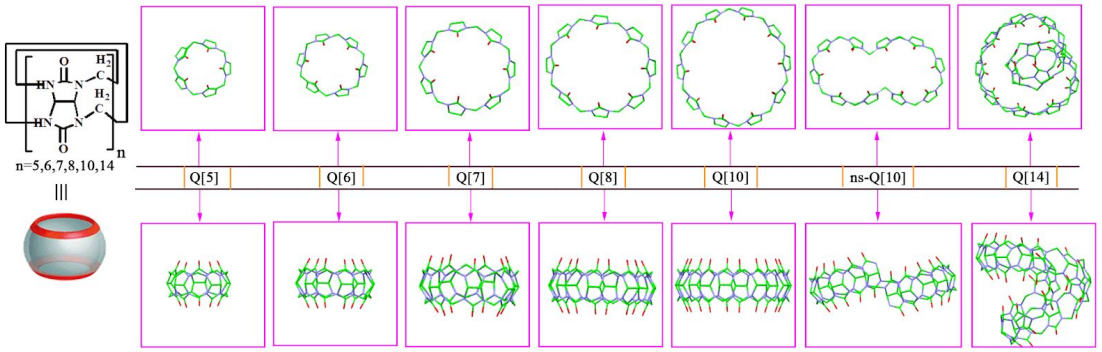

Chart 1. Types of cucurbiturils reviewed herein.

2. Tertiary complexes

2.1 Non-Covalent Q[8] systems

A group that has been very active in this area is Scherman *et al*., and in the area of non-covalent Q[8]-based systems, their studies included Q[8]-mediated supramolecular non-covalent protein-polymer complex formation [22]. To achieve this, the protein requires a pendant function

that can interact with Q[8], and this was accomplished by using viologen and naphthalene functionalized PEG bovine serum albumin. Tertiary host-guest complexes were formed in aqueous solution, and DOSY experiments confirmed that all three entities present moved at the same rate. UV-vis and fluorescence spectral and ITC measurements also confirmed the formation of the tertiary complex.

The same group investigated the mass spectra of a series of tertiary Q[8] species with a view to gleaning information about their stability in the gas phase [23]. Two types of '*tris*' molecules bearing arms with terminal methyl viologens were selected as the first guest and combined with three lots of Q[8] and of the second guest, the latter included anilines and PEG-containing species (figure 1). Results revealed that the nature of the second guest, and it's ability to hydrogen bond and form electrostatic interactions, played a large role in the gas phase stability of the respective tertiary complexes.

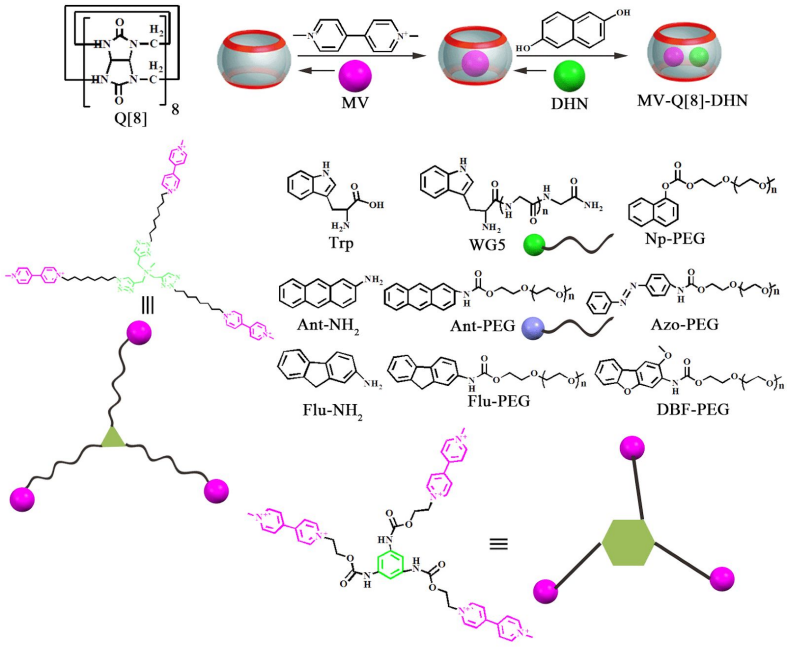

Figure 1. Guests employed to probe the gas phase stability of Q[8] tertiary complexes.

Jonkheijm, Huskens *et al*. studied the interaction of phenylalanine-based peptides of differing length with Q[8] by use of calorimetry and NMR spectroscopy in order to evaluate the degree of cooperativity [24]. For both peptides used, which had either two or six glycine residues, the first step in forming a tertiary complex was enthalpy driven, whilst the second step entropy driven. The smaller peptide chain exhibited a greater affinity for the Q[8] cavity as a result of its ability

to curve and optimize dipole-dipole interactions with the Q[8] carbonyl amide protons. The results obtained in this study suggest a non-cooperative binding situation.

A 2-ureido-4-pyrimidinone containing peptide, the *N*-terminal phenylalanine of which allowed for complexation with Q[8], was utilized by Dankers *et al*. [25]. Formation of a ternary complex was accomplished on further reaction with a fluorescent protein at the surface of a thermoplastic elastomer (figure 2). Products were formed as drop-cast films which were analyzed by XPS and MALDI-ToF though it proved problematic to identify a ternary complex. Results from fluorescence spectroscopy suggested that the ternary complex formed reversibly at the surface. It was clear that proteins could selectively be immobilized onto the surfaces, however the dynamics of the assembly present a challenge in terms of future use.

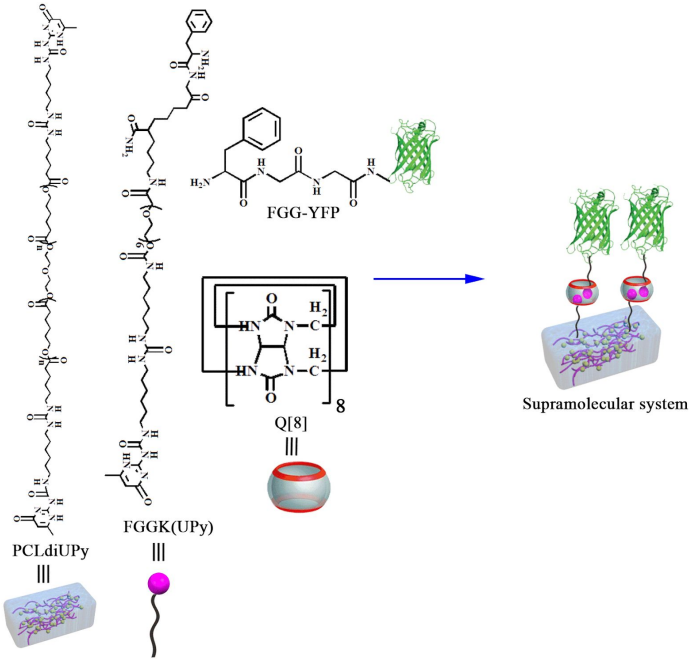

Figure 2. Use of peptide/proteins in a dynamic system.

3. Oligomers

3.1 Covalent Q[6] systems

Wittenberg and Isaacs reported that a Q[6] dimer, in the presence of low molecular weight (≤3500) polyethylene glycol guests, can self-assemble into cyclic oligomers (figure 3). The shorter the guest, the lower the degree of oligomerization. When the guest had increased molecular weight (10000), the self-assembled product was more polymeric in nature with 36

repeat units, although over time (2 weeks) this was found to decrease to 22. This slow change was associated with hexanediammonium motif dissociation rate constant when departing from the Q[6] cavity [26].

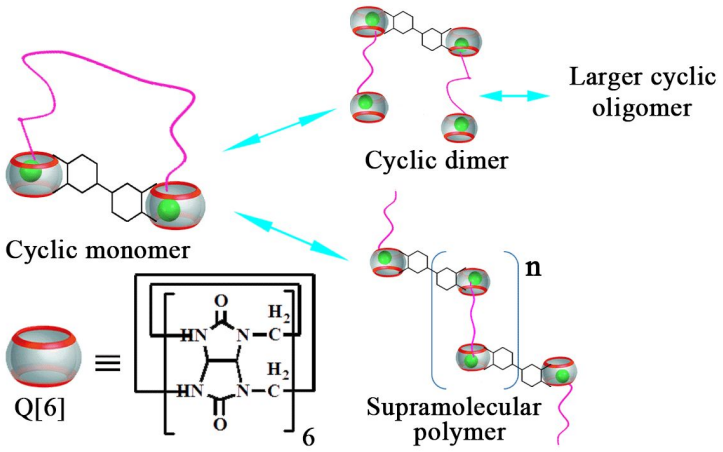

Figure 3. Oligomeric structures derived from a Q[6] dimer and polyethylene glycol guests.

3.2 Covalent Q[8] systems

A bifunctional monomer in which a central octaethylene glycol was capped either side by Phe-Gly-Gly residues was employed by Wang, Zhang *et al*. On mixing with Q[8] in a 1:1 ratio in water, the aromatic protons associated with the Phe underwent upfield shifts in the ^{1}H NMR spectrum consistent with encapsulation, and no terminal groups could be observed. In the MALDI-ToF spectrum, species with 20 repeat units were evident, whilst AFM-based single-molecule force spectroscopy suggested a length of 263 nm, corresponding to 50–60 repeat units [27].

3.3 Covalent other systems

Nally and Isaacs, in the hope of targeting supramolecular polymeric structures, investigated the interaction of *nor-seco*-Q[10], which contains two identical cavities, with potential guests bearing two adamantylammonium-containing substituents linked via *ortho*-, *meta*- or *para*-xylylene motifs. From the ^{1}H NMR spectra, it was clear that different types of products were formed, *i.e*. *ortho*- and *meta*-substituted guests led to broad spectra, whereas *para*-substituted guests afforded well-defined spectra. The observed chemical shift changes and the integrations were consisted with the presence of 1:1, 2:2 complexes as well as larger possibly oligomeric or polymeric

species. In particular, use of DOSY experiments confirmed the respective stoichiometries for the various combinations of *nor-seco*-Q[10] and guests, although the determination of definitive structures for the higher nuclearity species proved problematic. If a biphenyl linker was employed in the guest (between the two adamantylammonium-containing substituents), then, based on ^{1}H NMR spectra and diffusion coefficients, the preferred structured was 2:2 in nature resulting from a cyclization. In an attempt to avoid such a cyclization, an unsymmetrical guest containing very different potential binding sites was synthesized (one was an adamantylamine type site the other a hexanediammonium function). NMR and mass spectral data were consistent with the formation of 2:2 diastereomers when equimolar amounts of *nor-seco*-Q[10] and guest were employed. A change in stoichiometry to 1:2 (*nor-seco*-Q[10]:guest) afforded the inclusion complex *nor-seco*-Q[10]@(guest)$_2$. This change in product could be reversed by manipulation of the ratio of reactants. Interestingly, on addition of Q[6], the product *nor-seco*-Q[10]@(guest)$_2$@Q[6]$_2$ was identified, which on further addition of Q[7] kicked out the *nor-seco*-Q[10] forming Q[7]@guest@Q[6] [28].

4. Bottle brush polymers

Zhao *et al*. produced a 'bottlebrush' polymer (figure 4) using the viologen capped monomer with a backbone possessing *para* orientated isopropyl groups on a central aromatic motif that they had previously characterized by X-ray diffraction and was shown to a adopt a head-to-tail arrangement [29]. By combining it with a monomer containing a central phenylene motif bearing two tetraethylene glycol chains and two methoxy-containing naphthalene groups, in the presence of Q[8], a supramolecular polymer was obtained via π-π interactions of naphthalene groups with the viologen. ^{1}H NMR spectra were broad but integrations were consistent with a 1:1:2 ratio for monomer:monomer:Q[8]. DLS and DOSY data were consistent with the formation of a supramolecular 'bottlebrush' polymer in water [30].

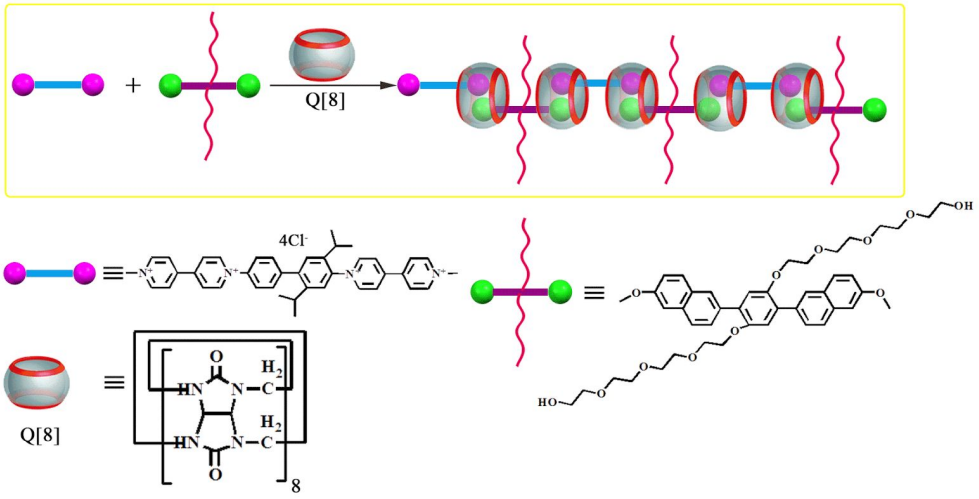

Figure 4. Formation of a supramolecular 'bottlebrush' polymer.

5. Supramolecular polymers

5.1 Covalent systems

5.1.1 Covalent Q[5] systems

The construction, via self-assembly in water, of a supramolecular polymer from an ammonium-substituted tetraphenylethylene (TPE) and a Q[5] derivative containing cyclopentano groups (CyP5TD[5]) was reported by Wang *et al*. The result was restricted rotation such that the new supramolecular polymers exhibited increased fluorescence as a result of aggregation induced emission (AIE), see figure 5. The formation and properties of the polymers was investigated by UV-vis spectroscopy, ITC and 2D DOSY ^{1}H NMR spectroscopy. Furthermore, the morphology and size was examined using TEM, and for a 1:2 ratio of TPE to CyP5TD[5] (concentration 0.1 mM) square-like particles were observed with lengths over the range 200 to 400 nm. Analysis of the data from dynamic light scattering experiments on the supramolecular polymers indicated that the distribution of the hydrodynamic parameter of the polymers had a peak centered at 260 nm *versus* 1 nm for TPE [31].

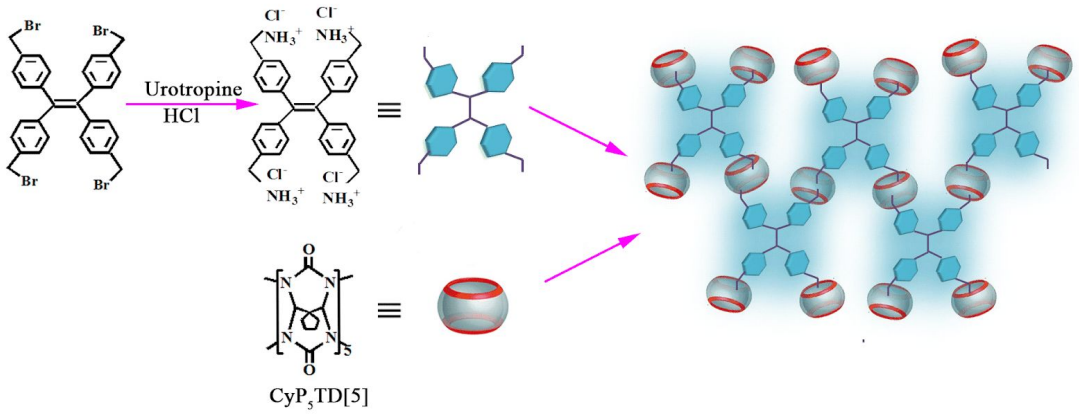

Figure 5. Formation of a supramolecular polymer from TPE and (CyP5TD[5]).

5.1.2 Covalent Q[6] systems

In the mid-1990s, Kim *et al* utilized the high affinity of Q[*n*]s for dialkyl diammonium ions to construct polyrotaxane polymers with high structural regularity. The structure was confirmed by X-ray crystallography and every repeating unit containing a cyclic component. The preparation involves the mixing of Q[6] with *N*,*N*-bis(4-pyridylmethyl)-1,4-diaminobutane dihydrochloride (L) followed by subsequent addition of $Cu(NO_3)_2$ (see figure 6). The resulting coordination polymer incorporated square pyramidal copper ions which as well as being bound to two pyridines of two of the Ls, is bound by three water molecules; nitrates provide the counterion (four for each repeating unit). The *cis* pyridine nature of the bonding at the copper centres results in an overall zig-zag shape for the polymeric structure. Each Q[6] is held in place via H-bonding with the protonated ammonium centres. The use of other first row transition metal failed to afford similar polyrotaxane polymers [32].

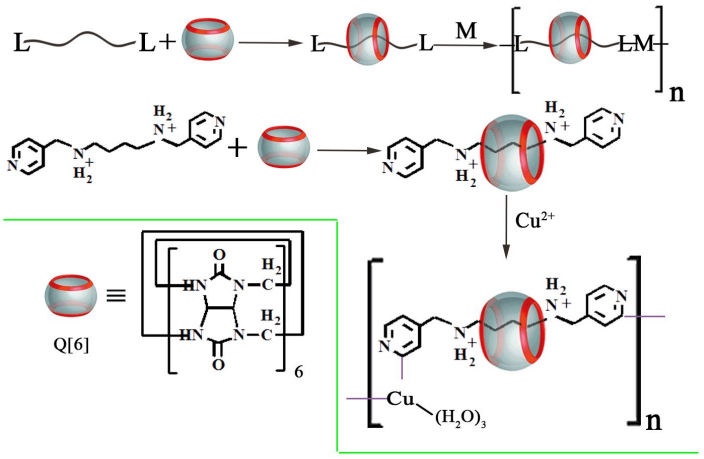

Figure 6. Formation of a polyrotaxane polymers from Q[6] *N*,*N*-bis(4-pyridylmethyl)-1,4-diaminobutane dihydrochloride and $Cu(NO_3)_2$.

Tan *et al*. then reported a system involving a block polypseudorotaxane comprising methoxypoly(ethyleneglycol)-β-poly-[N1-(4-vinylbenzyl)-pentane-1,5-diaminedihydrochloride]-β-methoxy poly(ethyleneglycol) in which the Q[6] was localized on the pentamethylene units of the side chains (figure 7). By varying the amount of Q[6] added, it proved possible to control the amount of threading such that 0.25 to 1.0 Q[6] per repeating unit was possible. Increased threading led to increases in the intensity of observed UV-vis bands, fluorescence and average hydrodynamic radius. The system also exhibited a degree of variation with temperature, with a drop-in fluorescence intensity [33].

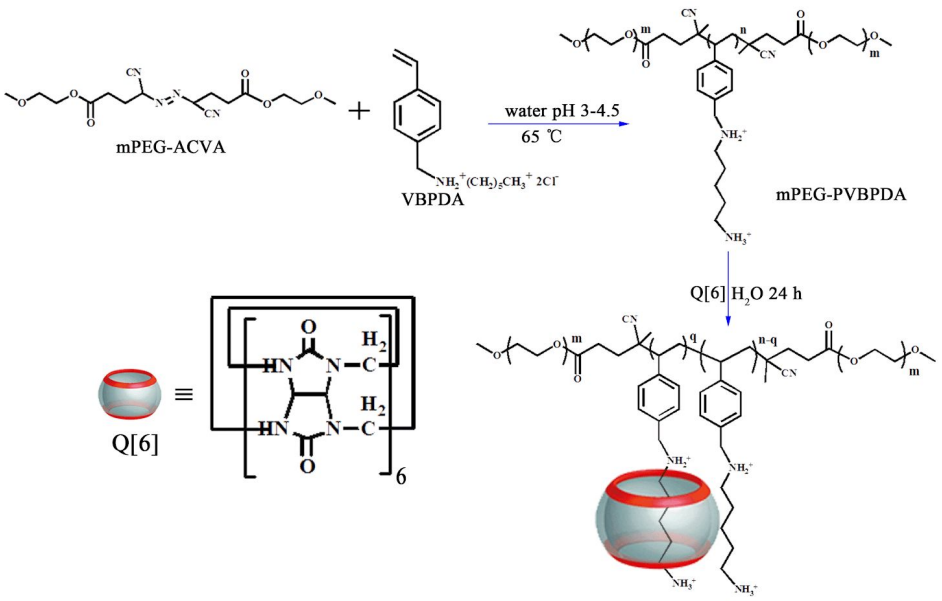

Figure 7. Synthesis of block polypseudorotaxane derived from methoxypoly(ethyleneglycol)-β-poly-[N1-(4-vinylbenzyl)-pentane-1,5-diaminedihydrochloride]-β-methoxy poly(ethyleneglycol).

Chen *et al* studied the affect of anions, namely SCN^-, Cl^- and NO_3^-, on the type of coordination product formed on reaction of Cu(II) salts with Q[6] in water. [34] In the case of the strongly coordinating thiocyanate anion, the product Q[6] $\cdot\{Cu[(SCN)_4(H_3O)]\}_2\cdot 2(H_3O)\cdot 35H_2O$, in which coordination of Q[6] with Cu(II) is prevented. For each Q[6], there are six close $[Cu(SCN)_4(H_3O)]^-$ anions, and each anion is involved in C – H ⋯ N and C – H ⋯ S with Q[6]s to afford a 2D sheet. When the chloride anion is present, a 1D polycationic chain $\{[Cu(H_2O)_3(Cl)]_2\cdot Q[6]\}n$ is formed in which two $[Cu(H_2O)_3Cl)$ bridges link Q[6]s. In the case of non-coordinating nitrate, the binuclear $(H_2O)_2Cu(\mu\text{-}H_2O)Cu(H_2O)_2$ motif is bound to the Q[6], and in the solid state these stack to form a 1D channels occupied by nitrate and water molecules.

5.1.3 Covalent Q[7] systems

Polyaniline, also known as PANI, has been known for well over a century but in recent years has attracted attention given its high electrical conductivity. The neutral form is known as emeraldine, and can be doped with acid to afford radical cations and desirable conduction. The stabilization of said radicals is an area of interest, and so threading Q[*n*]s along PANI was an attractive project.

With this in mind, the combination of polyaniline and Q[7] in aqueous HCl afforded, following work-up, the polypseudorotaxane in 65% yield (figure 8). Liu *et al*. employed a variety of techniques to investigate the properties of this polypseudorotaxane, and found for example that this polypseudorotaxane exhibited enhanced stability and greater water solubility *versus* PANI. Analysis of the shifts in the ^{1}H NMR spectra was consistent with the Q[7] residing on the doped parts of the PANI backbone. The size of the backbone was estimated from TEM images and these suggested that around 880 aniline formed the backbone (length *ca.* 500nm). In the TEM images, it was also evident that the structure comprised linear rods lying side-by-side. At weaker concentrations, AFM images revealed that the rods started to bend. The redox behaviour of the system was monitored by UV-Vis-NIR spectroscopy as NaOH was added. As the colour changed from green to blue, there was a significant shift and enhancement in the π-π transition of the PANI chain, which signified formation of the undoped form. By adding HCl, it proved possible to revert back to the doped form. These changes at differing pHs were faster in the parent PANI. EPR and cyclic voltammetry studies also indicated increased stability of the polypseudorotaxane *versus* free PANI [35].

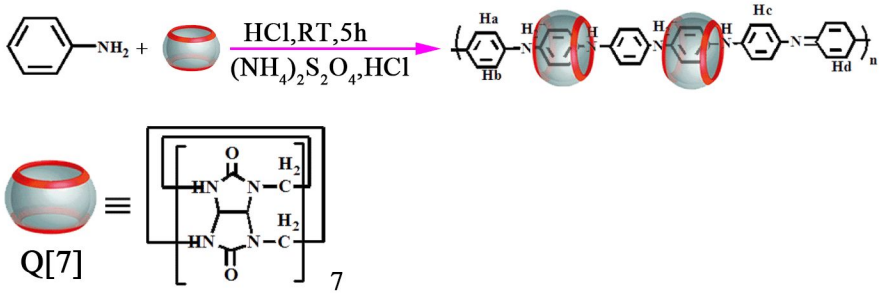

Figure 8. A polypseudorotaxane based on Q[7] and polyaniline.

A bifunctional monomer containing a central *p*-phenylene grouping sandwiched between two naphthalene group, which possessed the ability to self-sort (figure 9) was prepared by Zhang *et al*. The monomer was combined with equimolar amounts of Q[7] and Q[8], and consistent with a self-sorting process, the Q[7] favours the *p*-phenylene grouping, whilst the Q[8] seeks out the naphthalene groups. ITC studies were employed to elucidate a plausible mechanism involving

Q[7] allowing Q[8] access to the naphthalene groups. Use of excess Q[7] initially involves an intermediate whereby all sites are occupied by Q[7], *i.e.* a 3:1 complex, but as more Q[7] is added, it preferentially binds to *p*-phenylene, *i.e.* a 1:1 complex. On subsequent treatment with Q[8], the naphthalene sites are complexed by Q[8]. Diffusion-ordered NMR and ^{1}H NMR spectroscopy indicated the formation of a high molecular weight supramolecular polymer. The molecular weight, as determined by asymmetric flow field flow fractionation, was calculated to be 9.7 x 10^{4} $gmol^{-1}$ with a polydispersity of 1.5. the rigidity of the system can be controlled by controlling the amount of Q[7] added [36].

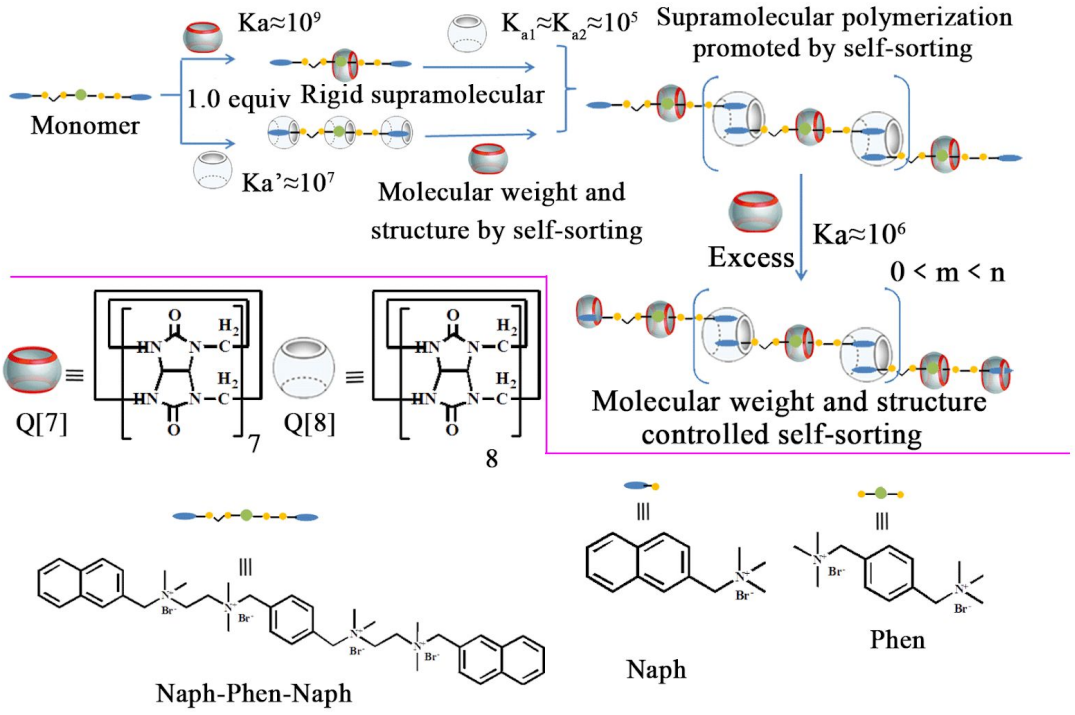

Figure 9. Interaction of a guest with a central *p*-phenylene grouping sandwiched between two naphthalene groups and Q[7] and Q[8].

Building on earlier studies, Zhang *et al*. made use of a bifunctional monomer which contained a central carbon backbone (alkyl chain) bearing 4, 6, 8 or 10 carbons and naphthalenyl end groups. In much the same way as the earlier work mentioned above involving a central *p*-phenylene [36], the addition of Q[7] and Q[8] to this monomer resulted in self-sorting with the Q[7] associated with the alkyl backbone and Q[8]s with the naphthalenyl end groups. In this way, linear supramolecular polymerization was achieved, and it proved possible to control the molecular weights which fell in the range 10 kDa to 50 kDa by adjusting the reaction stoichiometry, in

particular the amount of Q[7] added. The length of the carbon backbone was also a factor with those with too short or too long a backbone resulting in a lower degree of supramolecular polymerization. In fact, the optimum chain length was judged to be a hexyl chain [37].

5.1.4 Covalent Q[8] systems

Dong, Liu *et al*. prepared an *N*-terminal phenylalanine–glycine–glycine-derivatized peptide guest which included a tyrosine residue to allow for coupling, and reacted it with Q[8]. The resulting so-called supramonomer, contained two of the guests, and ^{1}H NMR spectroscopic studies indicated that the terminal phenyl groups were encapsulated within the Q[8] cavity. The system was then treated with the enzyme horseradish peroxidase (HRP) in the presence of H_2O_2. Within 20 minutes, a supramolecular polymer had formed, via coupling of the tyrosine groups, in near quantitative yield. From AFM and TEM measurements, the polymer was found to have a fibrillar type structure of length *ca*. 400 to 500 nm, suggesting a molecular weight of the order of 10^5. The height of the fibrillars (1.46 nm) is close to that of Q[8] and so a single strand polymeric structure was proposed. At concentrations, the fibrils became nanofibers and eventually coils comprised of tightly twisted nanofibers [38].

5.1.5 Covalent other systems

Scherman, Isaacs *et al*. as part of their studies on *nor-seco*-Q[10] extended work to its interaction with the polymeric guest poly(diallyldimethylammonium) chloride, for which the molecular weight was in the range 100,000–200,000 g/mol. The addition of *nor-seco*-Q[10] to this guest resulted in the formation of a supramolecular polymer, and the structure of the polymeric guest was somewhat disentangled from its parent state, particularly at high concentrations [39].

5.2 Non-Covalent

5.2.1 Non-covalent Q[8] systems

By employing anthracene derivatives with Q[8], it proved possible to utilize $\pi - \pi$ interactions for the construction of supramolecular polymers. To illustrate this, Zhang *et al* employed the monomers 1-(anthracen-2-ylmethyl)-pyridinium bromide and

4,4′-(propane-1,3-diyl)bis[1-(anthracen-2-ylmethyl)pyridinium] bromide [40]. As π – π stacking within the Q[8] cavity is the favoured mode, the first monomer results in a 2:1 (monomer :Q[8]) host-guest complex as confirmed by a Jobs plot and mass spectra, whilst the second favours the adoption of a polymeric structure with a 1:1 ratio (again confirmed by a Jobs plot). Changes in the UV/Vis and fluorescence spectroscopy were consistent with enhanced π – π interactions within the Q[8] cavity. The length of the polymers was dependent on the concentration, and the more concentrated the solution, the longer the polymer.

Following work using *N*,*N*,*N*-trimethyl-1-(naphthalen-2-yl)methanaminium bromide, which was found to form a 2:1 host-guest complex with Q[8] via π - π interactions, Zhang *et al*. extended their studies to the bifunctional monomer, 1,4-bis(naphthalene-2-ylmethyl)-1,4-diazabicyclo-[2.2.2]octane-1,4-diium bromide [41]. DOSY experiments confirmed the formation of a supramolecular polymer formed via π - π interactions, and was estimated to be 64x the length of the aforementioned 2:1 host-guest complex involving *N*,*N*,*N*-trimethyl-1-(naphthalen-2-yl)methanaminium bromide. Interestingly, addition of *N*,*N*,*N*-trimethyl-1-(naphthalen-2-yl)methanaminium bromide to the supramolecular polymeric system caused it to collapse showing that the process was reversible.

The combination of a naphthol-modified β-cyclodextrin and an adamantane–viologen in the presence of Q[8] was found to afford a linear supramolecular polymer [42]. GPC measurements indicated the formation of a high molecular weight polymer with *M*w 28.3 x 10^4 Da. On addition of a competing guest such as 1-adamantaneamine, the polymeric structure is disrupted.

Click chemistry was employed by the same group to connect a tertiary complex derived from Phe-Gly-Gly-propargyl amide and Q[8] (2:1) with a diazido-terminated poly(ethylene glycol) to form a supramolecular polymer [43]. The success of the reaction relied on the orthogonality between the click reaction and the host–guest interaction. The molecular weight of the polymer

was *ca*. 87.3 KDa as determined by MALDI-ToF mass spectra. The addition of triethylamine led to disruption of the polymeric structure.

Xiao *et al*. reported two types of stick-like supramolecular polymers by employing different types of viologen capped monomers, one with a backbone possessing *para* orientated isopropyl groups on a central aromatic motif, the other comprising a tris-viologen [44]. On the basis of ^{1}H NMR spectroscopic studies, a Jobs plot and ITC data, 1:1 binding stoichiometries was confirmed for both monomers with Q[8]. An X-ray crystal structure of the first monomer revealed a structure in which 4,4′-bipyridin-1-ium units were aligned in head-to-tail fashion. On the basis of this off-set face-to-face stacking, a structure for the supramolecular polymer was proposed whereby the aromatic stacking of the monomer was encapsulated within the Q[8] cavity. ^{1}H NMR NOESY spectroscopy was consistent with this postulated structure. TEM and AFM studies revealed the adoption of stick-like structures of a length of several hundred nm.

A supramolecular polymer was prepared by Zhang *et al*. by employing a thiol–ene click reaction combining supermonomers in a host-guest tertiary complex, the latter being formed via the Q[8] encapsulation of the phenyl end groups of two tetrapeptides, namely Phe-Gly-Gly-Cys [45]. The resulting supermonomers were then reacted via the terminal thiol with maleimide terminated poly(ethylene glycol) in an equimolar ratio under catalyst free conditions. The rate of polymerization can be controlled by the pH. The molecular weight of the supramolecular polymer was estimated to be between 2.1×10^4 and 3.5×10^4 g mol^{-1}.

Jin, Zhang, Kuang *et al*. employed a mono-naphthyl substituted boron dipyrromethene which also possessed three oligo(ethyleneglycol) chains for solubility purposes, and a related di-naphthyl derivative to access either a supramolecular dimer or a linear supramolecular dendronized polymer (figure 10), respectively, on interaction with Q[8] [46]. For the polymer, ^{1}H NMR spectroscopic studies revealed that two naphthyl groups were encapsulated by each Q[8], and the poor resolution of the peaks was consistent with polymer formation. AFM indicated that some of the chains were 150 nm in length, with a max diameter of 1.75 nm consistent with that of a Q[8]. AFM-based single molecule force spectroscopy indicated that the polymer length of a

random sample was 38.7 nm. In the case of the mono-naphthyl guest, Nuclear Overhauser effects were used to elucidate the structure, and data were consistent with supramolecular dimer formation.

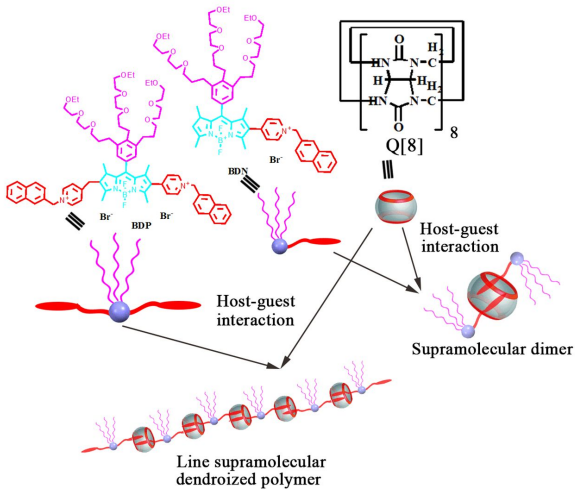

Figure 10. Formation of a supramolecular dimer or a linear supramolecular dendronized polymer using boron dipyrromethene derivatives.

5.2.2 Non-Covalent other systems

Perrier *et al*. initially prepared a linear peptide of type H_2N-*L*-Lys(Boc)-*D*-Leu-*L*-Lys(N3)-*D*-Leu-*L*-Lys(Boc)-*D*-Leu-*L*-Trp(Boc)-*D*-Leu-COOH which was then cyclized via a deprotection route before two phenylalanine moieties were introduced. This was then converted to a more soluble PEGalated peptide polymer conjugate, which via H-bonding assumed the form of a tubular supramolecular polymer. Addition of Q[7] resulted in disassembly of the tubular supramolecular polymer, but could be reformed on addition of the competing guest [47].

The synthesis of supramolecular carbohydrate polymers was described by Salah *et al*. which involved first encapsulating parts of the alkyl chain of dequalinium chloride hydrate with two shuttling Q[7]s, *i.e*. a 1:2 host-guest complex, and then this was covalently linked to the sugar chitosan via the NH_2 groups. The system exhibited Förster resonance energy transfer (FRET), upon mixing with 2-anilinonaphthalene-6-sulfonic acid, the latter acting as the acceptor. By comparison with model systems, it was clear that the FRET between donor and acceptor was enhanced by the presence of Q[7]. The FRET proved to be temperature sensitive, with measurements being conducted over the temperature range 298K to 368K, which revealed that the FRET could be turned on and off by simply adjusting the surrounding temperature. This

response to temperature was attributed to the increased ability of Q[7] to shuttle along the dequalinium chloride hydrate backbone as the temperature increased. This temperature control negated the need to adjust the ratio of donor:acceptor, which is the usual method of FRET control in other systems [48].

A self-sorting methodology to assemble linear, high molecular weight supramolecular polymers based on nor-seco-CB[10] (*versus* Q[7]) was employed by Ni *et al*. [49]. A bifunctional guest was employed which comprised a central phenylene moiety and naphthylene end groups (figure 11). On mixing the monomer with Q[7] and Q[10] in a 1:1:1 ratio in water, the assembly process could be followed by ^{1}H NMR spectroscopy and DOSY, and from the latter the molecular weight of the polymer was determined to be 5.6 x 10^{4} Da. The amount of Q[7] present dictated the molecular weight, with the largest polymer observed for 1.0 equiv. of Q[7]. The presence of Q[7] also helped avoid unwanted dimerization and cyclization processes occurring by encapsulating the phenylene moiety and imparting rigidity and directionality. However, the presence of too much Q[7] resulted in it acting as a competing host.

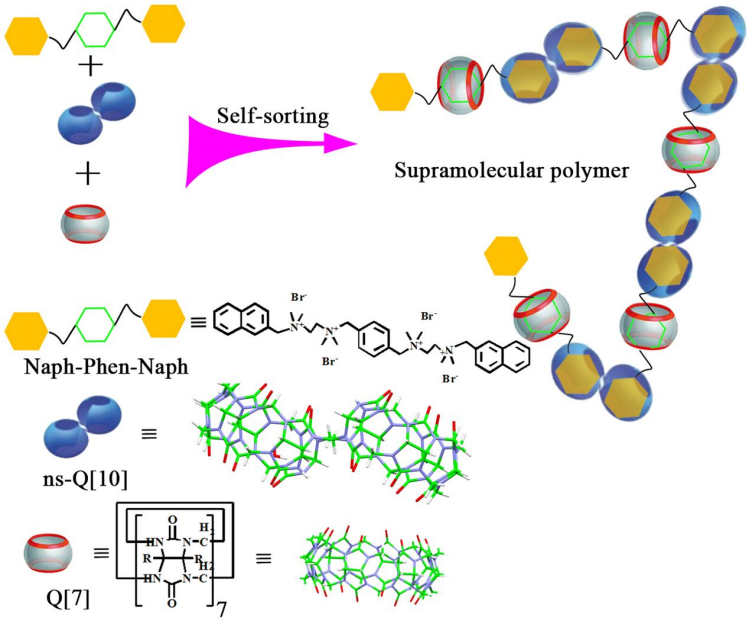

Figure 11. The fabrication of the ns-CB[10] based supramolecular polymer via self-sorting.

The combination of Q[8] with a monomer containing both hydrophilic (oliogoglycol) and hydrophobic (alkyl) chains, resulted in the formation of an amphiphilic supramolecular polymer

[50]. The polymer was capable of further concentration dependent self-assembly and could form either nanotubes and 2D films. Using ^{1}H NMR spectroscopy, the pH responsiveness of the polymer was investigated and it was found that under acidic conditions, polymer breakdown occurred whereas under basic conditions the polymeric structure could be recovered.

6. 2D polymers and layered structures

6.1 Covalent Q[5] systems

The reaction of lanthanum, cerium or neodynium nitrate hexahydrates with the dicarboxylic acids glutaric acid (H_2GT) and diglycolic acid (H_2DGC) and with Q[5] was reported by Zhang *et al*. The nature of the products was confirmed by X-ray crystallography, and it was found that a range of structures including a one-dimensional polymer, three two-dimensional polymers with a unique honeycomb-type topology, as well as both di- and tetra-metallic species were adopted. The compounds were further analyzed by Raman spectroscopy which revealed shifts to higher wavenumbers for the Q[5] upon coordination the Ln^{3+} ions, consistent with the presence of slightly more inelastic Q[5]. Optical absorption spectroscopy revealed strong ligand charge transfer bands (223 – 232 nm) and metal to ligand transfer bands (268 – 304 nm) [51].

6.2 Covalent Q[6] systems

The dipyridine *N,N′*-bis(4-pyridylmethyl)-1,4-diaminobutane dihydronitrate can be reacted with Q[6] and subsequently $AgNO_3$ to afford a 2D coordination polymer network. In the product, edge sharing hexagons (adopting chair-like conformations) are present which have at each corner an Ag(I) ion, whilst at each edge, there is a dipyridyl molecule linking two Ag(I) ions. Three of the Q[6]/dialkyl diammonium bis(pyridine) constructs bind to each of the Ag(I) ions, the latter sitting on a mirror plane. The distorted tetrahedral geometry is completed by a nitrate ion. The 2D coordination polymer network stack along the [011] direction at a distance apart of 9.87 Å, whilst a second 2D coordination polymer network interlocks with the first in near perpendicular fashion to afford novel polycatenated 2D polyrotaxane nets. Further experiments revealed that anions played a key role in dictating the structure formed, for example the use of silver tosylate resulted in the formation of a 1D polyrotaxane coordination polymer (figure 12) [52].

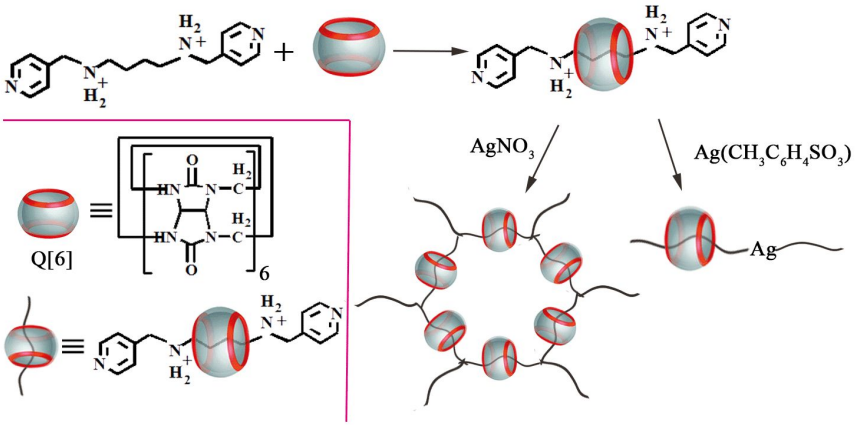

Figure 12. Formation of 2D and 1D polyrotaxane coordination polymers based on Ag(I) salts.

The formation of layered thin sheets by employing a covalent and supramolecular polymerization approach was communicated by Stoddart *et al*. In particular, by conducting a Q[6]-templated azide–alkyne polymerization in the presence of a β-cyclodextrin, hydrogen bonded networks are formed (figure 13). Introducing 2,9-diazaperopyrenium dications into the equation allows for stacking of the sheets to occur, *viz* $\pi-\pi$ interactions with the perylene core of a neighbouring dication at angles of 60–70°. The dimerization ability (criss-cross fashion) of the aromatic core of the dication led to the formation of an extended polymer network [53].

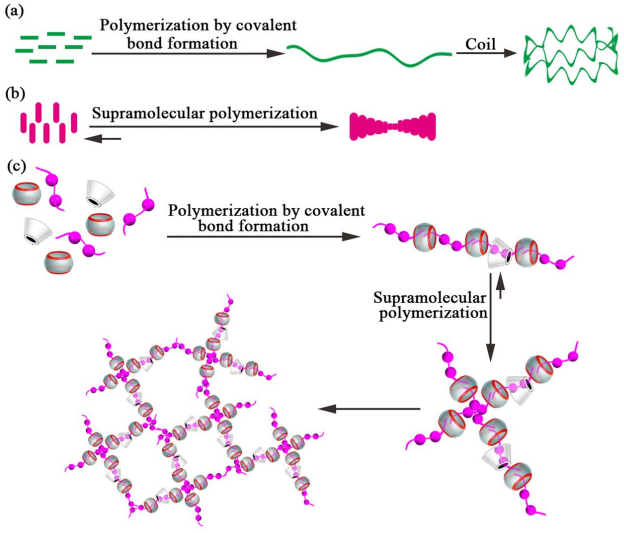

Figure 13. Formation of an extended polymer network employing (a) a covalent bond formation (b) a supramolecular polymerization approach, and (c) a combination of both approaches.

6.3 Other Q[n]-based systems

Xiao, Jiang *et al*. probed the potential of the four-arm guest 5,10,15,20-tetrakis(*N*-butyl-4-pyridinium)porphyrin tetrabromide, and combined it with the twisted cucurbituril Q[14] in aqueous solution (figure 14). ^{1}H NMR spectroscopic studies and ITC measurements were consistent with a product possessing a 2:1 ratio (Q[14]:guest). Competition experiments using KCl revealed that it was possible to displace the 'four-arm' guest and form a new inclusion complex between Q[14] and KCl [54].

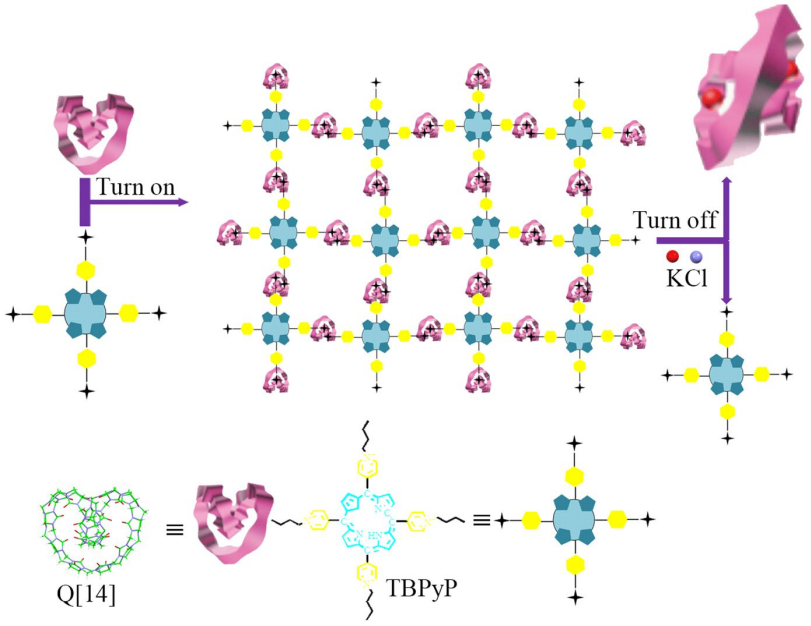

Figure 14. Interaction of Q[14] with the four-arm guest 5,10,15,20-tetrakis(*N*-butyl-4-pyridinium)porphyrin tetrabromide and KCl.

6.4 Non-Covalent Q[8] systems

A three-arm monomer, 1,10,100-(benzene-1,3,5-triyltris(methylene))-tris(3-(naphthalen-2-ylmethyl)-1H-imidazol-3-ium) bromide, BTNI, (figure 15), formed from the reaction of 2-(bromomethyl) naphthalene with 1,3,5-tris((1H-imidazol-1-yl)methyl)benzene, and its reaction with Q[8] at pH 4.75 (acetate buffer) to afford a product with a 2:3 ratio of monomer:Q[8] was reported by Zhang *et al*. [55]. UV-vis and fluorescence spectroscopy data was consistent with a product in which the naphthalene groups π-π stack within the Q[8] cavities. Furthermore, DOSY experiments suggested that the product is one large polymeric entity, and DLS measurements were consistent with hyper-branched polymers. The formation of this product is reversible and addition of ferrocenylmethyl-trimethylammonium iodide resulted in depolymerization.

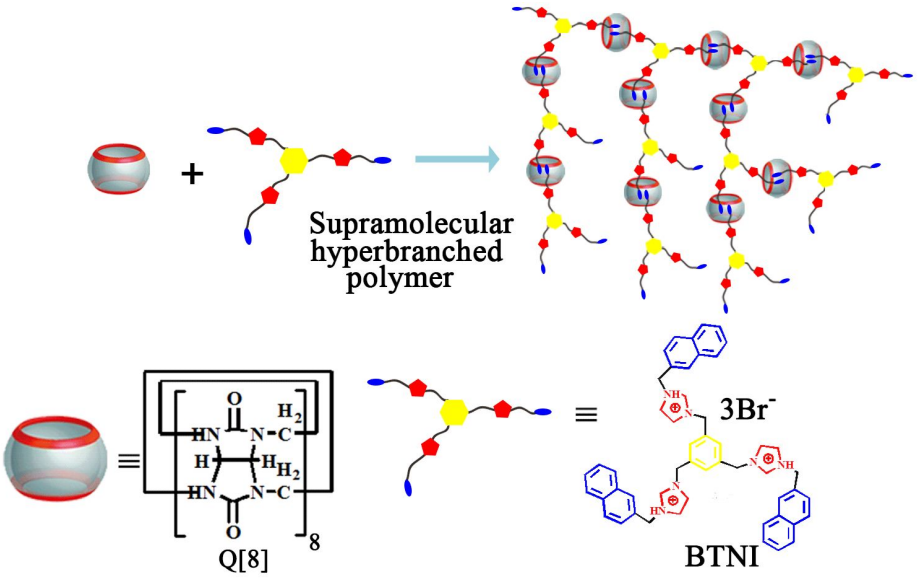

Figure 15. Hyper-branched polymers from a 3-arm monomer.

Supramolecular hyperbranched polymers (figure 16) were produced simply by mixing a naphthyl-substituted tetraphenylethylene with Q[8] in aqueous solution, which resulted in encapsulation of the naphthyl motifs as evidenced by the UV-vis spectra [56]. Whilst the parent tetraphenylethylene exhibited only weak emission (fluorescence quantum yield 16.49%), that of the supramolecular hyperbranched polymers was far stronger (fluorescence quantum yield 24.77%), as a result of restricted rotation of the phenyl rings. Indeed, yellow fluorescence was visible to the naked eye on UV irradiation (365 nm) of the tetraphenylethylene in the presence of Q[8]. DLS and TEM measurements on the polymers in water revealed the presence of aggregates of diameter *ca*. 60 nm.

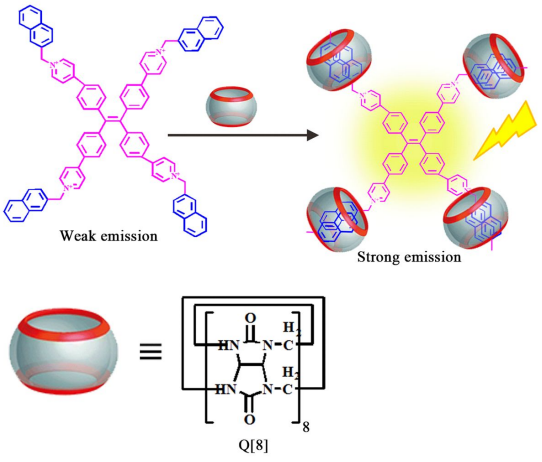

Figure 16. Supramolecular hyperbranched polymers from a naphthyl-substituted tetraphenylethylene with Q[8].

By employing a central 1,3,5-triphenylbenzene with 4,4′-bipyridin-1-ium groups connected to the *para* positions of the outer phenyl groups and introducing three bis(2-hydroxyethyl)carbamoyl groups at the other available positions on the central aromatic ring, it proved possible to a 2D supramolecular framework on reaction with 1.5 equivalents of Q[8] [57]. From DLS experiments, it was concluded that 350 hexagonal pores could be found in each 2D sheet. Use of more concentrated solutions afforded hydrogels (such systems are discussed in more details in section 13). Use of cryo-SEM revealed that the 2D sheets were actually curled, whilst AFM measurements revoked that the thickness of the layer was *ca*. 1.75 nm, *i.e*. the same as the diameter of one Q[8].

The three arm monomer 1,1′,1″-(benzene-1,3,5-triyltris(methylene))-tris(3-naphthalene-2-methyl)-1H-imidazol bromide and Q[8] employed at a liquid-solid interface, were found to form layer-by-layer films (figure 17) [58]. It proved possible to control the degree of supramolecular polymerization by controlling the degree of deposition of both Q[8] and the three arm monomer at each layer. AFM indicated that the films were 25 nm thick when using 20 layer pairs, and the degree of polymerization at the interface was found to be *ca*. 20. The driving force for the assembly, as evidenced by fluorescence spectroscopy, was the presence of the Q[8]-boosted π-π naphthalene interactions.

The films could be broken down by the addition of competing ions and the authors employed spermine, tyramine, dopamine and 1-amantadine, with the latter being most effective.

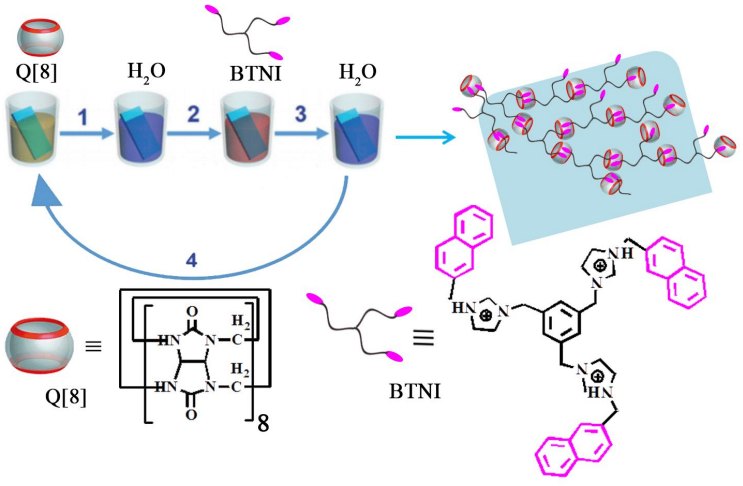

Figure 17. Layer-by-Layer films formed by host-enhanced π–π interaction as the driving force.

The layer-by-layer strategy was extended to systems involving a porphyrin bearing four naphthalene groups and its interaction with Q[8] [59]. The assembly process from solution to the interface was monitored by UV-Vis spectroscopy by measuring the absorption peak associated with the outer most layer, e.g either 444 nm (the porphyrin) or 438 nm (Q[8]). Furthermore, the intensity of absorptions increased as the layer-by-layer uptake of porphyrin and Q[8] increased. At 444 nm, a linear relation was noted for absorption *versus* number of layer pairs indicating a uniform deposition. AFM and SEM measurements indicated that the layers were fairly smooth and with five-layer pairs the thickness is 75 nm. The photocatalytic potential of such a layer-by-layer structure was investigated for the conversion of phenols to quinones. It was shown that oxidation was achievable for 1,5-dihydroxynaphthalene, hydroquinone, 1-naphthol, and 1,3,5-trihydroxybenzene, and multiple use of the system was possible without any reduction in $^1O_2$-generation efficiency.

Two separate well-ordered 2D supramolecular frameworks were constructed by Zhou *et al*. on employing two flexible oligoethylene glycols of differing lengths capped at each end with a 2,6-dihydroxynaphthalene to act as the linkers between more rigid nodes comprised of tetraphenylporphyrins, the latter possessing methyl viologens at the *para* position of each of the four phenyl groups [60]. The framework was held together by the ability of Q[8] to encapsulate and enhance the donor–acceptor interaction between the methyl viologen and 2,6-dihydroxynaphthalene motifs. ^{1}H NMR spectroscopic titration data was consistent with a 1:2:4 ratio for porphyrin:glycol:Q[8], whilst DOSY and DLS data suggested the formation of large aggregates. TEM, SEM and AFM images revealed these aggregates adopted corrugated films, with dimensions consistent with the adoption of a monolayer. The size of the pores were estimated by modelling to be 5.0 nm and 6.0 nm depending on the glycol employed.

Feng *et al*. employed both a tris(methoxynaphthyl)-substituted truxene spacer, prepared via the Suzuki coupling reaction of 6-methoxy-2-naphthaleneboronic acid with 2,7,12-tribromotruxene,

and a bis(methyl viologen) naphthalene diimide, obtained from the reaction of *N*,*N*-bis(2-bromoethyl)naphthalene diimide with 4,4′-bipyridine, and subsequent methylation with methyl iodide [61]. Combination of these two components with Q[8] furnished monolayers of two dimensional supramolecular organic frameworks. Given the solubilities of the species involved, it proved possible to assemble the layers at the toluene/water interface, although the time this took was problematic in terms of reproducibility. At certain concentrations and using a specially constructed container, it proved possible to reproducibly form monolayers at the toluene/water interface. AFM and TEM images confirmed the formation of a 1.8 nm thick monolayer. From grazing incidence wide-angle X-ray scattering results, it was concluded that a well-organized in-plane structure with a long-range order of molecules had formed.

6.5 Non-Covalent other systems

The mixing of 1,1′-(octane-1,8-diyl)bis(4- (ethoxycarbonyl)pyridin-1-ium) bromide with Q[6] was reported by Mei, Liu, Shi *et al*. to form a pseudorotaxane, which was subsequently reacted with uranyl nitrate in the presence of either sodium sulfate or oxalate at different pHs (1.09 to 5.67). This resulted in the formation of four coordination polymers, three of which were structurally characterized herein by X-ray crystallography. The structure of the other polymer has been previously reported [62]. It was found that very different structures were adopted including a kinked helical structure, a 2D interwoven structure and 1D chains. A number of factors influenced the structure formed including the mode of bonding of the carboxyl groups and the presence or not of monomeric uranyl centers chelated by oxalates [63].

Xia, Shi *et al*. employed Q[5], Q[6] and Q[8] as templates to assemble 2D uranyl/terephthalate acid networks under hydrothermal conditions in the presence of cations such as Na^+, K^+, Cs^+ or $H_2N(CH_3)_2^+$ [64]. The resulting ‘sandwich-like’ polymers adopted layered structures in which the size of the Q[*n*] employed dictates the distance between network layers. Moreover, as the size of the Q[*n*] increased, changes were seen in the make-up of the networks which resulted in a change from wavy to flat. The structure directing properties of the Q[*n*]s result from their extensive outer surface interactions (including hydrogen bonds, π–π and C–H···π interactions) with the uranyl terephthalate layers.

7. Copolymers

7.1 Covalent Q[6] systems

Ritter *et al* employed Click chemistry and microwave radiation to construct a cyclodextrin-Q[6] compound. By combining with *N*-isopropylacrylamide and an adamantane-containing methacrylate, a copolymer was formed in which the adamantane was thought to reside within the cyclodextrin (figure 18). Subsequent addition of *N,N*′-dimethyl-4,4′-bipyridinium resulted in an observed shrinkage (hydrodynamic volume reduced by 20 nm) as a result of the interaction with two 'capping' Q[6]s [65].

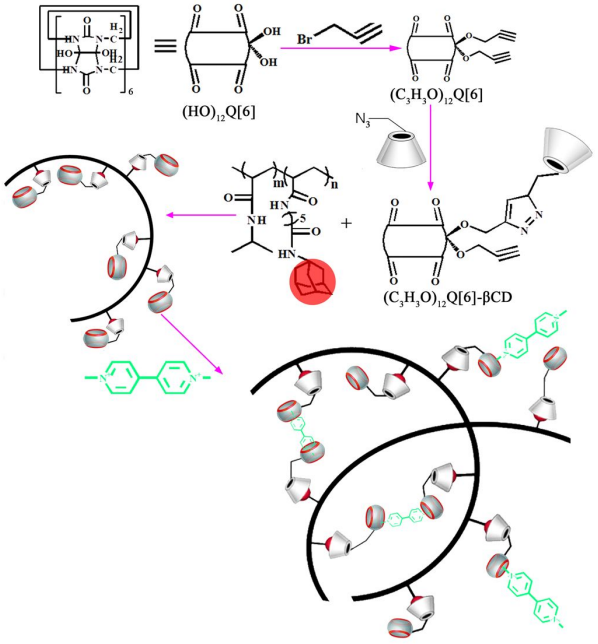

Figure 18. Use of Click chemistry to construct a cyclodextrin/Q[6] compound, and the addition of *N,N*′-dimethyl-4,4′-bipyridinium to a cyclodextrin-Q[6] methacrylate copolymer.

On combining *N*′-(4-vinylbenzyl)-1,4-diaminobutane dihydrochloride with Q[6], Tan *et al*. isolated a self-assembled pseudorotaxane, and then employed $K_2S_2O_8$ (KSP) as an initiator to conduct a free-radical polymerization with acrylamide (figure 19). The resulting copolymer was characterized by a variety of methods, and it was deduced that the Q[6] resided on the 1,4-diaminobutane parts of the side chains of the copolymer. Addition of Q[6] was found to enhance the thermal stability, whilst the hydrodynamic radius increased on increasing the copolymer concentration and also on increased pH. The increased pH (addition of NaOH) was thought to bring about dethreading of the Q[6] [66].

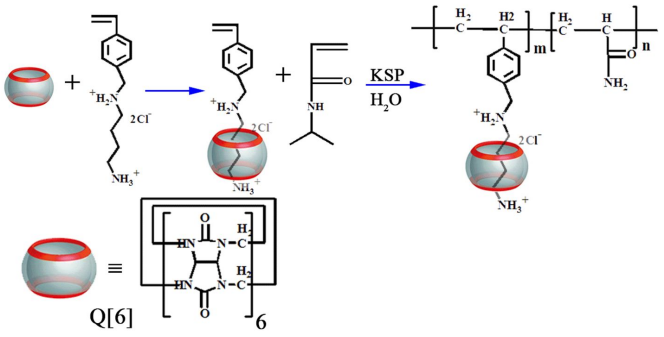

Figure 19. Copolymerization of *N'*-(4-vinylbenzyl)-1,4-diaminobutane dihydrochloride/Q[6] with acrylamide.

7.2 Covalent Q[7] systems

With an interest in rod-coil block copolymers, Li, Tan *et al*. targeted side-chain polypseudo-rotaxanes, for which the pseudo-rotaxane content was low (figure 20). The copolymer was synthesized via a redox-initiated polymerization involving *N*-isopropyacrylamide and *N*-adamantyl-*N*-(4-vinyl benzyl)-*N*,*N*-dimethylammonium chloride. Subsequent addition of Q[7] affords the copolymer incorporating the pseudo-rotaxane. The copolymer was described as containing two different types of sections, namely a rigid rod part associated with the pseudo-rotoxane, and soft coils which basically make up the remainder of the polymer chain. The lengths of these sections can be controlled by varying the pseudo-rotoxane content, and in this way the aggregation behavior can be controlled. Systems with very low pseudo-rotoxane content exhibited aggregation and thermal gelation [67].

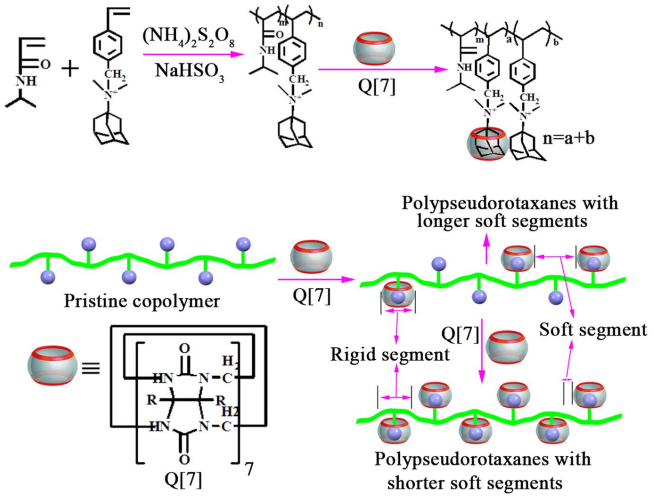

Figure 20. Copolymers derived from *N*-isopropyacrylamide and *N*-adamantyl-*N*-(4-vinylbenzyl)-*N*,*N*-dimethylammonium chloride and Q[7].

Tan *et al*. then employed free radical polymerization to access copolymers with side arms containing pendant Q[7]s. The method employed mono-OHQ[7] which was reacted with 4-vinylbenzyl chloride, and then in the presence of 3,3′-(octane-1,8-diyl)-bis-(1-ethyl-imidazolium) dibromide to aid solubility, was copolymerized with *N*-isopropylacrylamide (figure 21). The presence of 3,3′-(octane-1,8-diyl)-bis-(1-ethyl-imidazolium) dibromide can be problematic as it binds to the copolymer. The Q[7] moieties were still capable of guest recognition, for example high binding affinity (over $10^{12}M^{-1}$) was exhibited towards with amantadine hydrochloride [68].

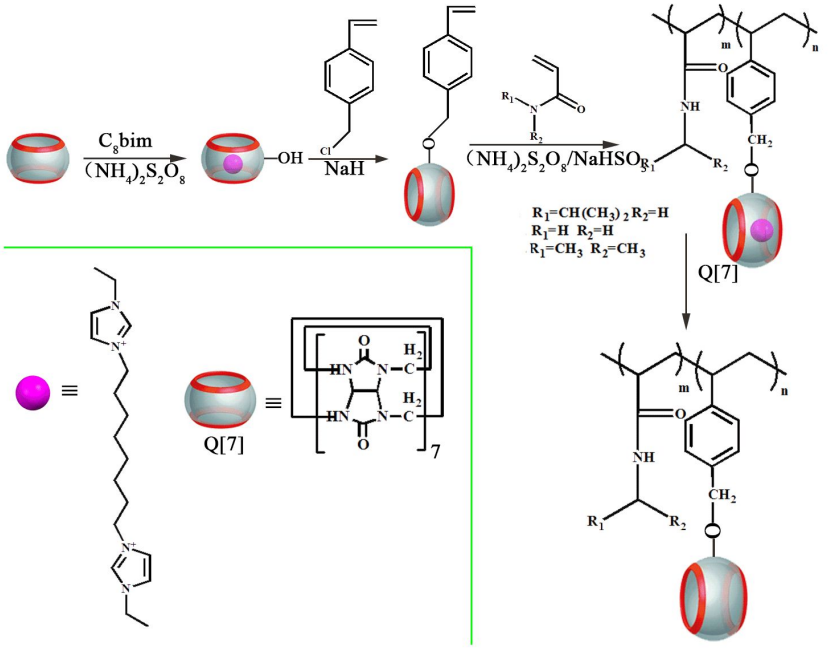

Figure 21. Reaction of mono-OHQ[7] with 4-vinylbenzyl chloride and copolymerization with *N*-isopropylacrylamide.

7.3 Non-Covalent Q[8] systems

ABA triblock copolymer formation was probed using diffusion NMR and solution viscometry by Robinson, Scherman *et al*. Experiments were conducted using a dimer (a triethylene glycol-spaced viologen), together with two polymers, one a naphthol-terminated PEG, the other a dibenzofuran-terminated poly(*N*-isopropylacrylamide) [69]. On addition of Q[8] to a solution containing an equimolar amount of the dimer and two equivalents of either of the polymers, 2:1:2 (Q[8]:monomer:polymer) tertiary 5-component complexes were formed (figure 22). The use of

in-situ NMR experiments allowed for the determination of molecular weights and solution mobility.

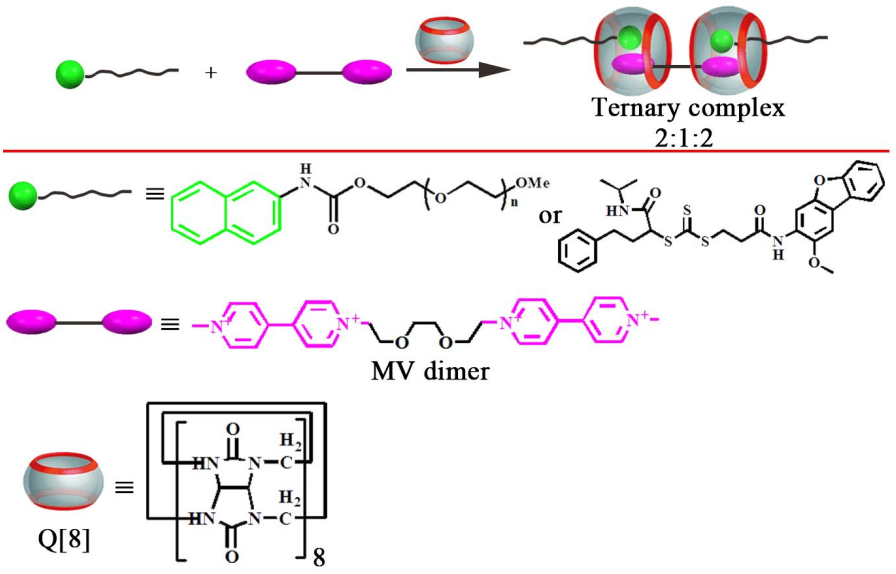

Figure 22. 5-component (2:1:2) complex formation.

8. Cyclic polymers

8.1 Covalent systems

8.1.1 Covalent Q[7] systems

Wang, Zhang *et al*. employed reversible conformational modulation and utilized a monomer in which a crown ether, namely bis(*m*-phenylene)-32-crown-10, is sandwiched between two ureidopyrimidinone groups. This monomer usually adopts a chair conformation, and can polymerize in solution to form a supramolecular structure. However, in the presence of bipyridinium salts, it folds and the resulting host-guest complexes have been coined '*taco*' complexes. Interestingly, this allows for control over the supramolecular process given that the presence of the *taco* structure depresses the supramolecular structure. Furthermore, by adding Q[7] to the system, the bipyridinium salt can be extracted by the Q[7], thereby disrupting the *taco* structure and the supramolecular polymer can reform. The result is control over the reversible transformation between linear polymer chains and cyclic species by host−guest competition [70].

8.1.2 Covalent Q[8] systems

Chen *et al*. have investigated the encapsulation of a naphthalene end-functionalized cationic PEG monomer of molecular weight 14,400 with Q[8]. At a 1:1 ratio, under high dilution conditions, this resulted in encapsulation of the naphthalene end groups and cyclization promoted by π-π stacking interactions (figure 23a). Higher concentrations favoured intramolecular polymerization. Although photo-irradiation of this system proved unsuccessful, the use of the related ligand with cationic anthracene end groups, prepared via Click chemistry using an azide-modified PEG, resulted in the formation of a covalently bonded (inside the Q[8] cavity, figure 23b) cyclic polymer as evidenced by GPC and NMR spectroscopy [71].

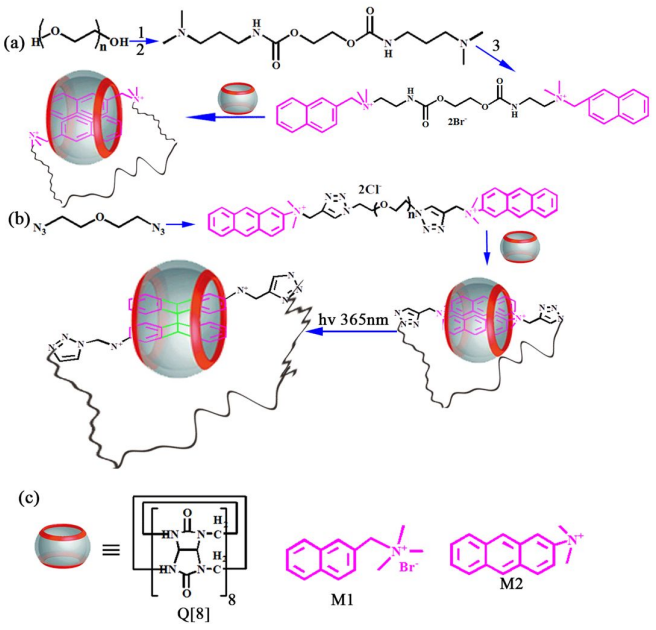

Figure 23. Formation of cyclic polymers via (a) π–π interactions or (b) covalent bonds; (c) Q[8] and the cationic end groups employed.

8.2 Non-Covalent Q[8] systems

By using poly(*N*-isopropylacrylamide) with naphthalene ends (M_n 6370 gmol^{-1}) and a viologen dimer possessing a central butane bridge, Chen *et al*. were able to form a cyclic polymer on combination with Q[8] (1:1:2) under high dilution conditions [72]. It was noted (using variable temperature ^{1}H NMR spectroscopy) that when heat was applied (36 ^{o}C) during this assembly process, dissociation of the tertiary complex occurred (figure 24). At the same time, the

poly(*N*-isopropylacrylamide)-based chains were dehydrated and formed particles thereby changing the environment from hydrophilic to hydrophobic in the vicinity of the tertiary complex. The result of this was the naphthalene groups were kicked out of the Q[8] cavity and a charged host-guest complex involving only the viologen dimer and Q[8] was released into solution. Further evidence of this release was provided by experiments employing naphthalene terminated poly(methyl methacrylate), and it was shown that the released Q[8]@viologen dimer could readily be captured.

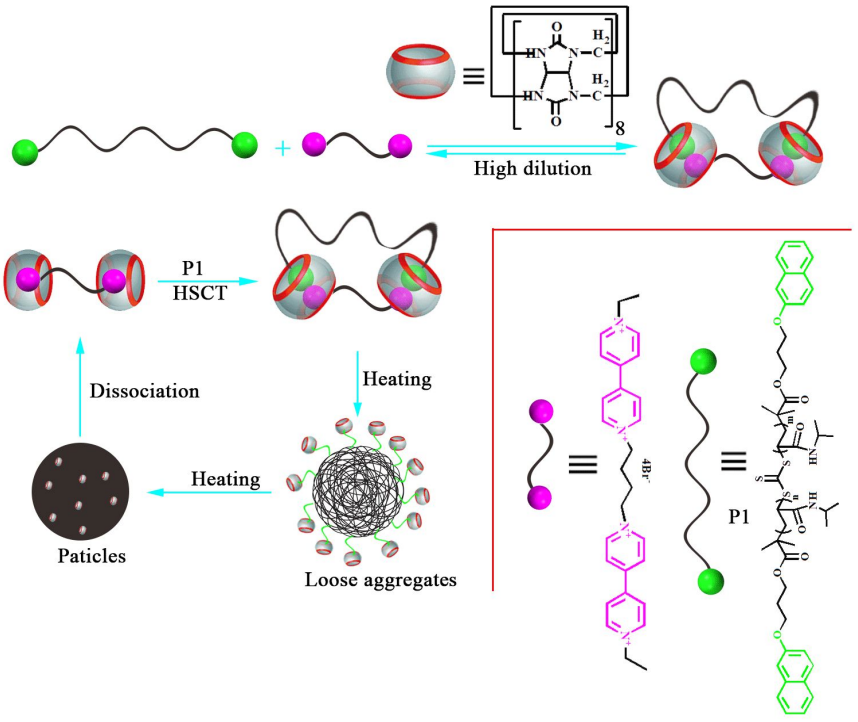

Figure 24. Heat driven dissociation during assembly of a cyclic polymer. HSCT = host-stabilized charge transfer.

9. Capsules, vesicles and alike

9.1 Covalent Q[6] systems

Building on preliminary work on Q[6](allyloxy)$_{12}$, where thiolene photopolymerization was employed to form polymer nanocapsules without the need for a template or alike [73], Kim *et al.* reported a more detailed study including mechanistic and theoretical discussions. From experimental observations, it was proposed that initially formed disk-shaped monomers utilize their surface functionality and under UV irradiation form thioether bridged dimers and trimers and subsequently 2D oligomeric patches (figure 25). Favourable energy profiles allow these

patches to bend and form loosely cross-linked hollow spheres, which are strengthened by the ability of allyl groups present to form additional thioether bridges. The result is a highly cross-linked polymer nanocapsule, which has disulfide loops, formed from the remaining allyl groups, protruding from its surface. The nanocapsule shell is only one or two monomers thick as evidenced by florescent tagging, HR- and cryo-TEM studies. Indeed, when prepared in chloroform, the nanocapsules are large enough to be observed by confocal scanning laser microscopy. This can be accomplished either by decorating the surface with a fluorescent dye or encapsulating the latter inside the capsule. Such behaviour established that it was possible to modify the capsule surface using non-covalent interactions whilst guests are held inside, and suggested such systems had many possible applications [74].

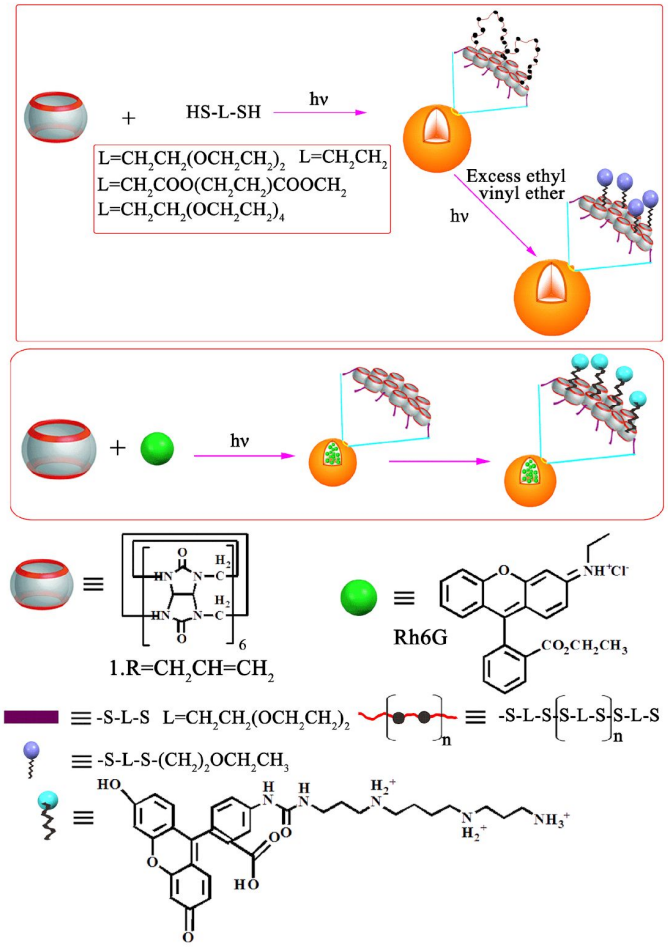

Figure 25. Nanocapsule formation from Q[6](allyloxy)$_{12}$, and decorating the surface with a fluorescent dye or encapsulating the latter inside the capsule.

9.2 Covalent Q[7] systems

Using a standard fluorometer, Hennig, Resch-Genger *et al*. were able to verify the number of functional groups that are available on a microsphere, typically poly(methylmethacrylate),

surface. The method involves adding Q[7] to a pre-reacted slurry of an adamantylmethylamine derivative and a carboxylic derivative of the microsphere, then after centrifugation there is an excess of Q[7] in solution. Use of the florescent dye acridine orange then allows for quantitative determination, *i.e.* the number of Q[7]s bound to the microsphere surface is the difference between the amount added and the amount remaining in solution (figure 26) [75].

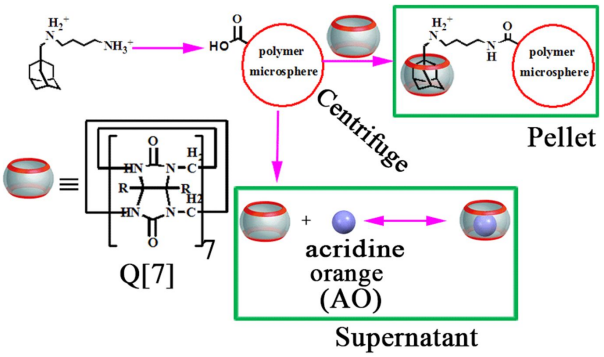

Figure 26. A new method for quantification of surface functionality of a microsphere surface.

Sherman *et al*. also employed Q[7] as an anchor and took advantage of its host-guest properties to construct polymeric nanocomposites. The methodology involved preparing, via the soap-free emulsion polymerisation of styrene and styrene methyl viologen, polymeric colloids of poly(styrene-co-styrene/methyl viologen) bearing methyl viologen. The polymeric nanocomposites were then prepared by an *in situ* reduction of metallic ions in an aqueous suspension of the poly(styreneco-styrene methyl-viologen). The metals reduced and conjugated with Q[7] included Pd, Au, Ag, and the former system was screened as a catalyst in the Suzuki coupling reaction between 4-iodophenol and benzyl boronic acid in water. A yield of 99% was achieved over 15 minutes with a catalyst loading of 0.15mol%, and even after six cycles, yields of 90% could be obtained [76].

9.3 Q[8]-based systems

Scherman *et al*. devised a route for the room temperature reversible functionalization of the shell of polymeric microspheres [77]. The key here was the use of Q[8], which can interact with the core scaffold, a viologen-containing microsphere, in the presence of a linear acylate polymer capped by a 2-naphthol end group and also functionalized with rhodamine-B units, to produce a

shell 21 nm thick. The Q[8] then has the ability to interact with another (competing) guest (e.g. 1-adamantaneamine) which leads to cleavage of the core-shell. Studies also showed that this resulted in an increase of cytotoxicity associated with the microspheres. As evidenced by TEM, similar use of Q[7] failed to produce such core shell microspheres.

Another hyper-branched polymer was reported by Ji *et al*. [78], who employed indole-terminated poly(*D*,*L*-lactide) and methyl viologen-containing hyperbranched polyphosphate. Initial interaction of Q[8] with the methyl viologen-containing hyperbranched polyphosphate was conducted in water, and the resulting host-guest complex was added to a DMSO solution of the indole-terminated poly(*D*,*L*-lactide). The formation of the tertiary complex can be followed by fluorescence spectra, and after dialyzing the complex with water, micelles were obtained. The micelles could be filled with coumarin 102, and when either adamantaneamine or $Na_2S_2O_4$ were added, controlled release of coumarin 102 was observed as evidenced by emission spectra.

Abell *et al*. then exploited electrostatic interactions between charged copolymers and charged surfactants to increase capsule formation at the droplet interface [79]. An aqueous emulsion of the droplets was generated in Fluorinert FC-40 perfluorinated oil containing fluorous surfactant. Dopants in the form of a carboxylate- or amine-terminated fluorocarbon ether polymers of polyhexafluoropropylene oxide were added to provide the charged interface. This then allowed for the selective partitioning of charged copolymers, which were either negatively charged polyacrylamide copolymers bearing either fluorescein and azobenzene or methyl viologen with styrene sulfonate, or positively charged polyvinylalcohol bearing rhodamine B and functionalized with either stilbene isocyanate or 6-(methyl viologen)hexamethylene isocyanate. The Q[8]-hosted cross-linking could then occur between one of these charged copolymers and its complementary charged surfactant. The process can be manipulated to deliver hollow, ultrathin capsules as well as solid microparticles from the one solution.

Using naphthol-bearing oligo(ethylene glycol)s and PEGs with 3 or, on average, 18, 111, or 464 ethylene glycol repeat units, Huskens *et al*. investigated the effect of these differing lengths on various properties of supramolecular nanoparticles [80]. The latter were formed by the combining

the aforementioned naphthol-PEGs with methyl viologen-poly(ethylene imine), naphthol-poly(amido amine) dendrimer and Q[8]. Use of tri(ethylene glycol) failed to produce supramolecular nanoparticles, whilst for the PEGs 18, 111, or 464 ethylene glycol repeat units, the supramolecular nanoparticles produced showed no distinct differences in size, although this was likely due to the broad nature of the data obtained via SEM. The last set of experiments reported in this study involved the use of a divalent naphthol-functionalized PEG, which was obtained via bromination (PBr_3) of naphthol$(PEG)_3$ followed by reaction with 3,5-dihydroxybenzonitrile hydrogenation in the presence of Raney Nickel and then reaction with methyl-poly(ethylene glycol) *N*-hydroxysuccinimide ester. The divalent guest, which had 113 PEGs, was capable of slowing down the supramolecular nanoparticles formation and when conducted at 40 ^{o}C over 12 hours, distinct sizes could be observed (as measured by SEM and DLS) when varying the amount of divalent and multivalent naphthol guests employed.

The formation of supramolecular microcapsules via the assembly of a amphiphilic block copolymer (azobenzene-functionalized poly(methyl methacrylate)-block-poly(acrylic acid)), which were of uniform size and were capable of dual-cargo loading was reported by Scherman, Abell *et al*. [81]. The process occurred via the intermediate formation of micelles in aqueous solution, which then as they assembled at a microdroplet interface were cross-linked via interaction with poly(*N*-vinylpyrrolidone)-co-poly(hydroxyethyl methacrylate)-co-poly(methylviologen-styrene) and Q[8].

In a microfluidic flow-focusing device, the components were also subjected to a perpendicular flow of perfluorinated oil to afford spherical microdroplets. Encapsulation of the hydrophobic dye, Nile Red within the micelles allowed the process to be monitored by fluorescence microscopy. Experiments showed how it was possible to encapsulate two guests at the same time, one in the core, one in the shell, namely fluorescein isothiocyanate-dextran (500 KDa) as well as Nile Red, respectively, with the former being added via an aqueous flow stream. After five cycles of dehydration and rehydration it was found that the cargo was still encapsulated. However, the size of the guest proved to be important, for example use of lower molecular weight fluorescein

isothiocyanate-dextran (70 KDa) led to loss of guest via diffusion. Both of the aforementioned guests can be released by addition of a competitive guest such as 1-adamantylamine. Use of photochemistry (*trans*/*cis* isomerization) was also shown to be useful in terms of guest release, and it proved possible to release for example 84% of fluorescein isothiocyanate-dextran (500 KDa) after irradiation for 18 minutes using UV light (λ_{max} 377 nm). In the absence of UV light, only 6% of fluorescein isothiocyanate-dextran (500 KDa) over the same period. The removal of Nile Red proved to be more problematic by the UV method, thus this system was capable of selected release of a guest.

The soap-free emulsion polymerisation of styrene and 1-methyl-1′-(4-vinylbenzyl)-[4,4′-bipyridine]-1,1′-diium chloride iodide, initiated by 2,2-azobis(2-methylpropionamide)dihydrochloride, was employed by Scherman, Abell *et al*. to afford colloidal particles [82]. These particles were then used as templates to afford methyl viologen bearing colloidal particles via polymerisation of *N*-isopropylacrylamide, *N*,*N*′-methylenebisacrylamide and 1-methyl-1′-(4-vinylbenzyl)-[4,4′-bipyridine]-1,1′-diium chloride iodide. The other guest component required for colloidal microcapsules formation, namely azobenzene-functionalised poly(vinyl alcohol), was prepared from the reaction of isocyanate-terminated azobenzene and poly(vinyl alcohol) using a tin catalyst. Using a microfluidic flow device, an aqueous flow of the binary complex comprised of the colloid particles described above and Q[8] was injected into the device at the same time as an aqueous flow of the azobenzene guest. The combined flows were then merged with a perfluorinated oil containing surfactant, which led to water-in-oil microdroplets. The microdroplets had a mean diameter of 62 μm, which decreased as the water was evaporated whereupon cross-linking was capable of forming a shell. Further loss of water led to ultimate destruction of the shell. SEM images showed the presence of folds and creases on the surface which undoubtedly contributed to the breakup on dehydration. In the microfluidic flow device, it also proved possible to load up the microcapsules with a cargo (figure 27), and to illustrate this fluorescein isothiocyanate-dextran was encapsulated whilst at the same time as a batch of Rhodamine B-labelled azobenzene guest

was added. Confocal laser scanning microscopy images showed red fluorescence (Rhodamine B) at the oil/water interface and green fluorescence (fluorescein isothiocyanate-dextran) spread inside the droplets. It was noted that on increasing the temperature, for example from 25 °C to 45 °C, larger pores were formed which resulted in an increase in guest (fluorescein isothiocyanate-dextran) release, in this case from 28 to 5% over 30 minutes. It also proved possible to use azobenzene photoisomerization as a trigger release.

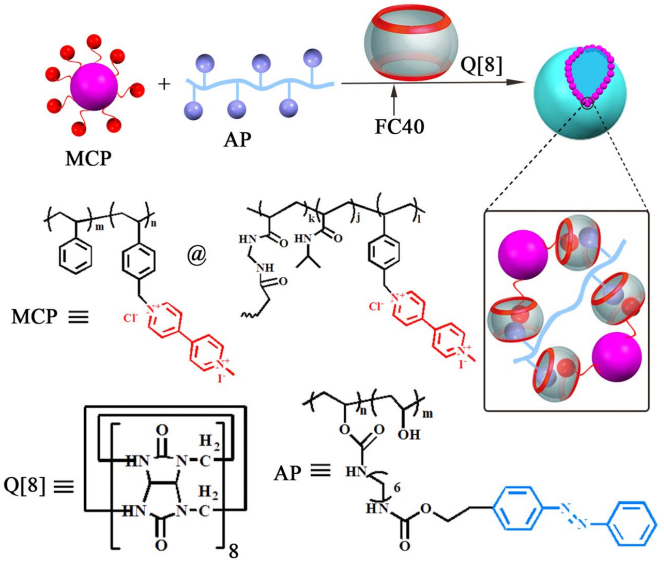

Figure 27. A microfluidic flow device to load up the microcapsules with a cargo.

Schmuck *et al*. investigated the use of a guest comprising a tetra cationic guanidiniocarbonyl pyrrole, which they had recently reported in a separate communication [83], with Q[8] at different pH (figure 28). Under acidic conditions (pH 4.1), the guest was fully protonated, which created favourable charge-dipole interactions, and a pair of the guanidiniocarbonyl pyrrole end groups were encapsulated by Q[8]. The result was an extended supramolecular network. The thickness of the network (from AFM mages) was equivalent to a Q[8] (< 2 nm). Under more neutral conditions (pH 6.8), AFM images revealed interconnected spherical particles forming vesicles of about 10 nm height. Under these conditions, the guest was only partially protonated and so the attraction to be encapsulated by Q[8] was lower. Moreover, because the charge is lower, there was less resistance to the formation of more closely packed aggregates and the result was the appearance of a globular vesicle-like shape [84].

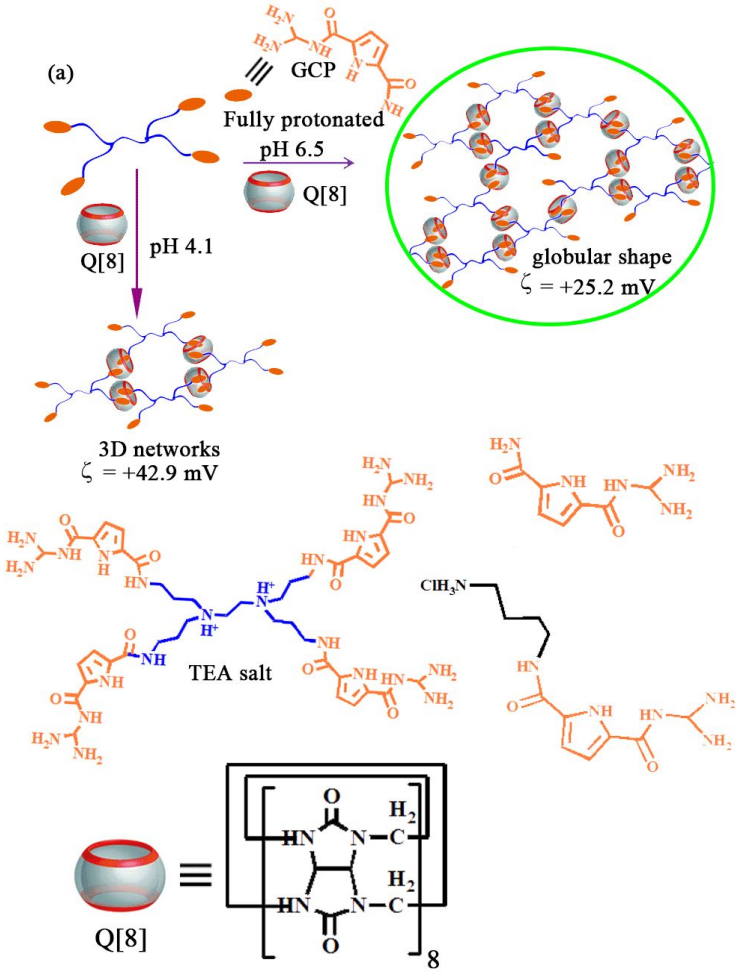

Figure 28. Use of a guanidiniocarbonyl pyrrole containing guest under different pH.

9.4. Others

The reaction between $(allyloxy)_{12}$Q[6] and 2-[2-(2-methoxyethoxy)ethoxy]ethanolthiol afforded an amphiphilic Q[6] derivative that in water can, following sonification, produce spherical vesicles with diameters between *ca*. 30 to 100 nm depending on the concentration of the Q[6] solution [85]. Treatment of the vesicles with fluorescein isothiocyanate spermine conjugate resulted in encapsulation of the spermine motif resulting in green fluorescence as observed by confocal microscopy. This showed that the vesicle could readily be decorated with a fluorescent tag. To probe this further, the interaction of sugar-coated vesicles with concanavalin A was investigated, and aggregation occurred immediately on mixing. Surface plasmon resonance measurements indicated that the binding constant was *ca*. 3x 10^4 M^{-1}, far higher than just the free ligand alone.

A 2D polymer was prepared by the photopolymerization of perallyloxyQ[6] with 1,2-ethanedithiol, and was deposited evenly in multi-layer fashion, with a thickness of *ca*. 100

nm, on polytetrafluoroethylene [86]. The dyes methylene blue, rhodamine 6G, naphthalene sulfonate and calcein were used to probe the permeability of the membrane. Whilst methylene blue and naphthalene sulfonate passed through the system, rhodamine 6G and calcein did not, and the system was capable of repeating this for at least three filtration cycles. It proved possible to further improve the selectivity of membrane by utilizing the attraction of Q[6] for spermine derivatives. For example, use of a positively charged spermine created a cationic surface and so the permeation of the likes of positively changed methylene blue became unfavourable. In the same way, use of a negatively charged spermine reduced the permeation of negatively charged species such as naphthalene sulfonate. Treating the membrane with a pH 12.0 buffer helped to avoid seepage of naphthalene sulfonate by neutralizing the effect of any spermine ammonium groups. If the system was deposited on a porous anodic aluminium oxide, then hydrophobic dependent permeability proved possible.

10. **Azo and related photo active systems**

10.1 Covalent Q[8] systems

The host-guest capabilities of Q[8] can be combined with the photochemical properties of an azastilbene to control multi-colour emissions, and results have been compared against the use of Q[7] by Wang, Zhang *et al*. In the case of Q[8], because of the large size of the cavity, two azastilbene groups were encapsulated, and via host-guest interactions, supramolecular polymers were formed which emitted orange light. After UV irradiation, the azastilbene groups underwent a [2+2] cycloaddition within the cavity, and this process can be observed by ^{1}H NMR spectroscopy, *i.e.* the disappearance of the HC=CH signals and downfield shifts associated with the azastilbene groups. The result is a supramolecular polymer which emits blue light. In the case of Q[7], only one azastilbene was encapsulated, and this system emitted dark purple light. Following UV irradiation, the stilbene bond changed from *trans* to *cis*, and thereafter emitted green light. Thus, multicolour emissions are exhibited by these host-guest systems and their photochemical products [87].

A three-arm photosensitive monomer prepared in good yield from 1,3,5-tris(4-bromobutoxy)benzene (formed from *m*-trihydroxybenzene, 1,4-dibromobutane and K_2CO_3), 1,2-di(4-pyridyl)ethylene and HBr was reported by Zhang *et al*. On addition of Q[8] (in a 3:2 ratio), a supramolecular photosensitive hyperbranched polymer was formed (the inclusion complex was 37 times the size of Q[8]), see figure 29, which was characterized by ^{1}H NMR spectroscopy and DOSY. Data were consistent with the azastilbene encapsulated within the Q[8] cavity. UV irradiation at 365 nm for 3 hours afforded covalently attached hyperbranched polymers via [2+2] cycloaddition. Monitoring this process by fluorescence spectroscopy indicated that the emission decreased at 580 nm and increased at 440 nm, which corresponds to a colour change from light orange to light blue [88].

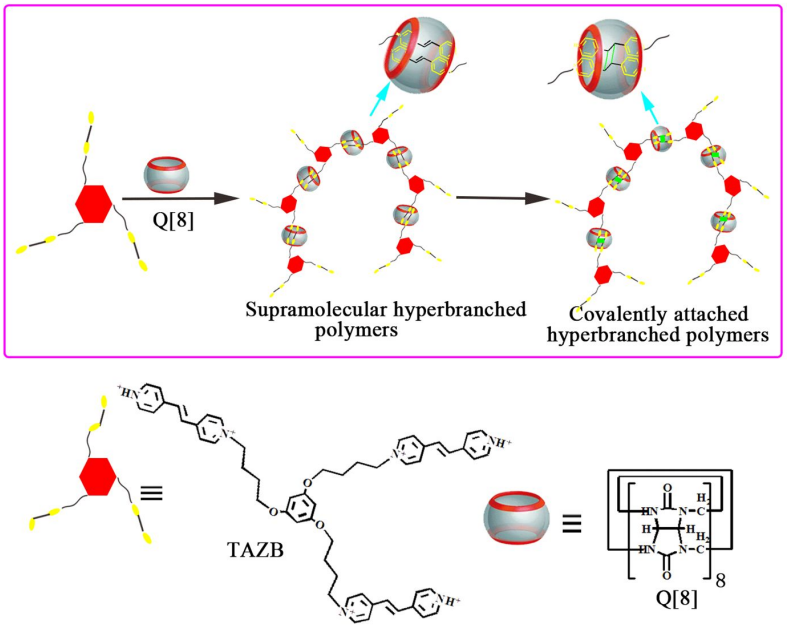

Figure 29. Encapsulation of a three-arm photosensitive monomer.

Kang, Zhang *et al*. reacted Q[8] with the monomer merocyanine-propyl-merocyanine, and the resulting homo-ternary host–guest complex was subjected to UV irradiation. This resulted in photo-dimerized products, however given the cavity exhibits smaller affinity for these new species, they are replaced by unreacted end groups of the monomer, and in this way the photodimerization continues. In other words, Q[8] appears to move along the polymer chain as it is irradiated, and 10 mol% is sufficient to effectively catalyse the polymerisation. Diffusion coefficients suggested the products were of high molecular weight, for example after 4 hours, the molecular weight was *ca*. 5004 Da, but this number increased on further cycles [89].

10.2 Non-Covalent Q[8] systems

Using Q[8] as an example, Scherman *et al*. showed how it was possible to exploit both redox and light-responsive guests to effect reversible orthogonal control [90]. The photochemical switching exploited the *cis*/*trans* photoisomerization available to azobenzene. To demonstrate this, it was first shown that the host-guest complex between Q[8] and methyl viologen dication exhibited a preference for *trans*-4,4′-azobis(phenol) when forming the 1:1:1 ternary complex. It was shown that by applying UV radiation, photoisomerization occurred; it was necessary for solubility reasons to employ an asymmetric triethylene glycol azo derivative. Visible light was found to be capable of reversing the process and the isomerization rate was 0.080 s^{-1}, which was somewhat slower than that of the parent azo compound. The electrochemical switching was provided via the use of viologens. From CV and spectroelectrochemical experiments, it was clear that electrochemical reduction and oxidation was reversible, and that the homoternary complex $(MethylViologen^{+\bullet})_2$@Q[8] formed on one electron reduction of the heteroternary complex $(MethylViologen^{2+}\bullet$(triethylene glycol azo))@Q[8] was readily reoxidized. It was then shown that it was possible to reversible apply either of the external stimuli without impacting on the ability for the other to operate reversibly. Moreover, it also proved possible to use these findings to influence macroscopic properties, and this was demonstrated for surface wettability.

By using monomers containing the azobenzene functionality, for example 1-[*p*-(phenylazo)benzyl)]pyridinium chloride, it proved possible to form Q[8]-based supramolecular polymers, whose photochemical properties could be controlled via *E*-*Z* isomerization at the azobenzene [91]. The X-ray crystal structure of Q[8] with the *Z*-azobenzene moiety held within the cavity was determined. A larger guest molecule containing two azobenzene motifs was found to form a supramolecular *E*,*E*-polymer, however upon irradiation, depolymerization occurred and the *Z*,*Z*-tertiary host guest complex was formed.

Scherman *et al*. initially prepared a tertiary complex involving methyl viologen, 4-hydroxyazobenzene (*trans* isomer) and Q[8], and found that upon irradiation with UV light (350 nm), the structure was broken down and free *cis*-azo isomer released [92]. Interestingly though, it

proved possible to reverse this step by using visible light irradiation (420 nm). Extending this methodology to 4-hydroxyazobenzene-functionalized silica microspheres and combining with methylviologen functionalized polymeric nanoparticles@Q[8], it proved possible to form hybrid raspberry-like colloids. By analogy with the initial 4-hydroxyazobenzene@Q[8] system above, it proved possible to reversibly break down and reform these colloids under different types of irradiation. Using TEM, it was discovered that reformed colloids possessed slightly less methylviologen functionalized polymeric nanoparticles at the core.

A number of azo-containing species were also employed by Huskens *et al*. to assemble dual responsive supramolecular nanoparticles [93]. This involved the use of an azo-terminated poly(amidoamine) dendrimer, Azo_8-PAMAM, an azo-functionalized poly(ethylene glycol) of M_w 5000 $gmol^{-1}$, and a methyl viologen-substituted poly(ethyleneimine), MV-PEI, the latter containing about 4.5 methyl viologens per polymer chain. These ingredient's interact with Q[8] in aqueous/DMSO solution to form a supramolecular nanoparticle (figure 30). By varying the amounts of the respective ingredients, it proved possible to control the size of these self-assembled nanoparticles. Particle size could be doubled (to 110 nm) by increasing the amount of azo-terminated poly(amidoamine) dendrimer present *versus* the amount of azo-functionalized poly(ethylene glycol). The increase in size was linear up to about a 30% increase in the amount of azo-terminated poly(amidoamine) dendrimer, but thereafter further increases led to uncontrolled large aggregate formation. Similar use of Q[7] failed to afford any particles. Using the tertiary complex resulting from Q[8], methyl viologen, and Azo-PEG, it was observed that upon irradiation with UV light (<400 nm), 80 to 90% of the *trans*-poly(ethylene glycol) had been converted into the *cis* form within 1 minute. The process could be reversed in natural light over 20 minutes. Exposing the supramolecular nanoparticles to UV irradiation for 14 hours, led to their disintegration, and as for the tertiary complex, reassembly was possible under visible light. Particle degradation was also possible using the reducing agent $Na_2S_2O_4$, however is was not possible to reverse the process with visible light.

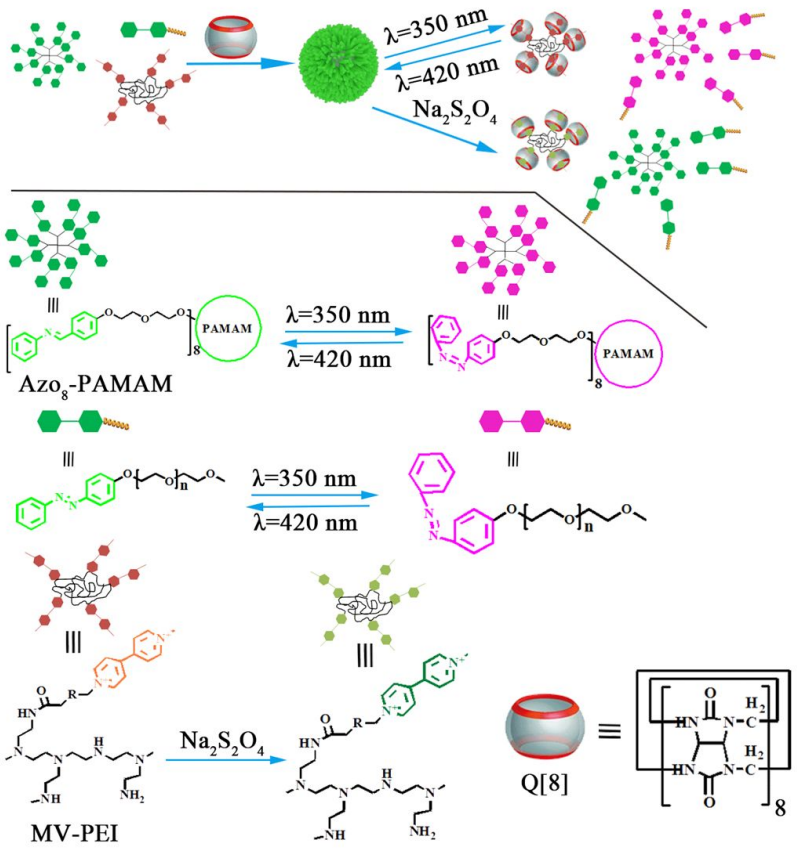

Figure 30. Use of azo-containing species to assemble dual responsive supramolecular nanoparticles.

The same group then extended their work to include zwitterionic supramolecular nanoparticles [94]. Using the previous ingredients azo-terminated poly(amidoamine) and a methyl viologen-substituted poly(ethyleneimine), in combination with a zwitterionic azo-carboxybetaine acting as a monovalent capping ligand to control uncontrolled growth of the core. Despite the absence of long PEGs, the system exhibited stabilization under a number of biologically relevant conditions and nanoparticle aggregation was observed over the pH range 6.2 to 6.8. The size of the particles could be tuned by adjusting the amount of azo-terminated poly(amidoamine) *versus* azo-carboxybetaine. As in the previous system, reversibility could be achieved via photo-isomerization of the azo moiety using either UV or visible light.

The guest molecule Phe-Gly-Gly with an azobenzene end group has been reacted with Q[8] in a 2:1 molar ratio in aqueous solution [95]. The resulting tertiary complex possessed an azobenzene function at each end. These monomers could then be converted into supramolecular polymers by the addition of an equimolar amount of bis-β-cyclodextrin, whereupon the latter encapsulated the azo groups. Data from single molecule force spectroscopy and asymmetric flow field flow

fractionation experiments was consistent with the formation of these supramolecular polymers. The calculated polymer molecular weight was reported as 5.4 x 10^4 $gmol^{-1}$ (PDI 1.4).

Wang, Ma *et al*. utilized a guest comprising an azobenzene capped with viologens and reacted it with Q[8] to afford a linear polymer via head-to-tail inclusion of two 4,4′-bipyridin-1-ium units from two separate guests [96]. Upon irradiation (254 nm), the system underwent slow *trans-cis* photoisomerization (compared to the free azo monomer) and a coiled/curved polymer formed. The reverse process was also possible at 365 nm albeit sluggishly.

Abell *et al*. then exploited electrostatic interactions between charged copolymers and charged surfactants to increase capsule formation at the droplet interface [97]. An aqueous emulsion of the droplets was generated in Fluorinert FC-40 perfluorinated oil containing fluorous surfactant. Dopants in the form of carboxylate- or amine-terminated fluorocarbon ether polymers of polyhexafluoropropylene oxide were added to provide the charged interface. This then allowed for the selective partitioning of charged copolymers, which were either negatively charged polyacrylamide copolymers bearing either fluorescein and azobenzene or methyl viologen with styrene sulfonate, or positively charged polyvinylalcohol bearing rhodamine B and functionalized with either stilbene isocyanate or 6-(methyl viologen)hexamethylene isocyanate. The Q[8]-hosted cross-linking could then occur between one of these charged copolymers and its complementary charged surfactant. The process can be manipulated to deliver hollow, ultrathin capsules as well as solid microparticles from the one solution.

An ABBA type monomer, namely DIAV-4 (1′,1‴-(butane-1,4-diyl)bis(1-(4-(phenyldiazenyl)benzyl)-[4,4′-bipyridine]-1,1′-diium)) has been combined with differing amounts of Q[8] to from a supramolecular polymer [98]. The process was controllable and the products formed varied with the amount of Q[8] *versus* monomer added. Given the presence of the azo functionality, it also proved possible to induce *cis-trans* isomerization by exposing to light (365 and 420 nm). Monitoring the systems when exposed to these light sources revealed differing degrees of isomerization and that the *trans* form was more

favourable for supramolecular polymer formation, whilst the *cis* isomer has the ability to bend and fully occupy the Q[8] cavity, *i.e*. prevents the inclusion of viologens and polymer formation.

By using naphthyl-functionalised hydroxyethyl cellulose, a viologen-bearing polymer, 1-[*p*-(phenylazo)benzyl)]imidazolium and Q[8], del Barrio, Scherman *et al*. were able to access photo-rheological fluids [99]. Model studies were conducted first using methyl viologen and a PEG of 5000 Da bearing a naphthyl group. Combining the viologen and naphthyl species with Q[8] in an aqueous solution also containing 1-[*p*-(phenylazo)benzyl)]imidazolium led predominantly to the formation of a tertiary complex involving Q[8] with the viologen and naphthyl species. However, upon UV irradiation (360 nm) of the solution, azo isomerization takes place and the resulting *Z*-isomer was able to displace the other guests in the Q[8] cavity. It even proved possible to obtained a crystal structure of this *Z*-isomer which showed the encapsulated *cis*-azobenzene and also the proximity of a ureido portal to the imidazolium function. Given the results using these model guests, the methodology was extended to the use of the polymers mentioned at the start of this section, ensuring that low concentrations were employed. The result was a viscoelastic polymer network. If 1-[*p*-(phenylazo)benzyl)]imidazolium was also presented, then upon exposure to UV irradiation (360 nm, 5 minutes), a fast gel-to-sol transformation was observed, which was the result of reduced polymer entanglement following photoisomerization. Use of a neutral azo guest (*i.e*. with no charge) failed to produce such a transformation. Attempts to reverse the transformation using visible light, although successful revealed a somewhat sluggish process. The networks also proved to be self-healing such that following deformation, mechanical properties recovered rapidly.

Supramolecular hyperbranched-like polymers have been accessed by employing a bis(methyl viologen) linked by a short central glycol chain, and a tritopic monomer in the presence of Q[8] [100]. The tritopic monomer had azobenzenes at the end of each of the three arms linked to the central benzene 1,3,5-tricarboxamide core via imidazolium salts. The Q[8] and the bis(methyl viologen) formed a 2:1 complex, and when this was added to a solution of the tritopic monomer (0.5 molar equiv.) a product of composition 1.5:1:3 (bis(methyl viologen: tritopic monomer:Q[8])

was obtained. ^{1}H NMR spectroscopic data were consistent with the formation of a supramolecular polymer. Upon exposure to UV light (λ_{max} 360 nm), discoloration occurred and a binary complex involving Q[8] and *Z*-tritopic monomer precipitated. This could be reversed by applying blue light (λ_{max} 450 nm) or by heating to 80 ºC. Disassembly was also possible via the use of competing guests such as adamantylamine hydrochloride. In this work, it also proved possible to use droplets as templates which enable the assembly to gel, and the system exhibited self-healing characteristics.

Cyclic oligomers have been formed from a bifunctional guest comprising a central dimethylphenylene linkage flanked by stilbazolium groups on interaction with Q[8] [101]. In these oligomers, the azo groups were encapsulated in the Q[8] cavity. Upon irradiation with UV light, [2+2] photodimerization occurred resulting in high-molecular-weight supramolecular polymers. The length of the polymer could be controlled by the length of the irradiation time until all the reactive components for [2+2] photodimerization had reacted. As an example, over 60 minutes irradiation (365 nm), polymers with weight average molecular weight 265 Da were obtained.

Park *et al*. utilized a cyanostilbene, namely (*Z*)-4,4′-((1-cyanoethene-1,2-diyl)bis(4,1-phenylene))bis(1-methylpyridin-1-ium) chloride, to access a supramolecular polymer exhibiting *J*-type stacking [102]. This monomer possesses a fluorescence quantum yield of <1%, *i.e*. is weakly emissive, however on combination with Q[8] a supramolecular polymer was formed and absorption/emission spectra experienced red shifts, whilst the quantum yield increased to 91 %, *i.e*. strongly emissive (appearing green in colour). The encapsulation of the guests resulted in a *J*-type π-stacked structure. This contrasts with the use of the related stilbene monomer for which the cyano group has been removed, namely (*E*)-4,4′-(ethene-1,2-diylbis(4,1-phenylene))bis(1-methylpyridin-1-ium) chloride. In this case, fluorescent quenching occurred as a result of cyclic (2:2) rather than polymer species being formed. In the cyano case, ITC data and a Jobs plot confirmed a 1:1 stoichiometry with Q[8], and

dynamic light scattering measurements revealed the formation of particles of diameter *ca*. 1 μm. TEM measurements revealed rectangular entities of length *ca*. 1 μm. If Q[7] was employed instead, which can only accommodate one guest, then a complex with a 1:2 (cyano:Q[7]) stoichiometry was formed, for which the quantum yield is *ca*. 7%. The Q[8]cyano polymer structure described above was utilized as a tryptophan sensor, and was found to have a limit of detection of 6.3 nm.

The potential of a Q[8]-based system to act as a scaffold for transporting proteins in aqueous environments (figure 31) was investigated by Wang, Feng *et al*. [103]. The method involved the use of a core comprised of methyl viologen functionalized nanoparticle surrounded by an anti-inflammatory antagonist called interleukin-1 receptor antagonist, a number of which were held in place as part of modified azobenzenes. The azobenzenes were involved in Q[8]-mediated host-guest interactions with the viologens on the nanoparticle surface. It was demonstrated that this system could be exploited for therapeutic applications, for example it was capable of inhibiting IL-1 mediated signaling. Furthermore, the nanoparticles bearing the antagonist exhibited improved *in-vivo* imaging and immunostaining by virtue of prolonged retention as demonstrated for rat joints using the near infrared dye Cy7.

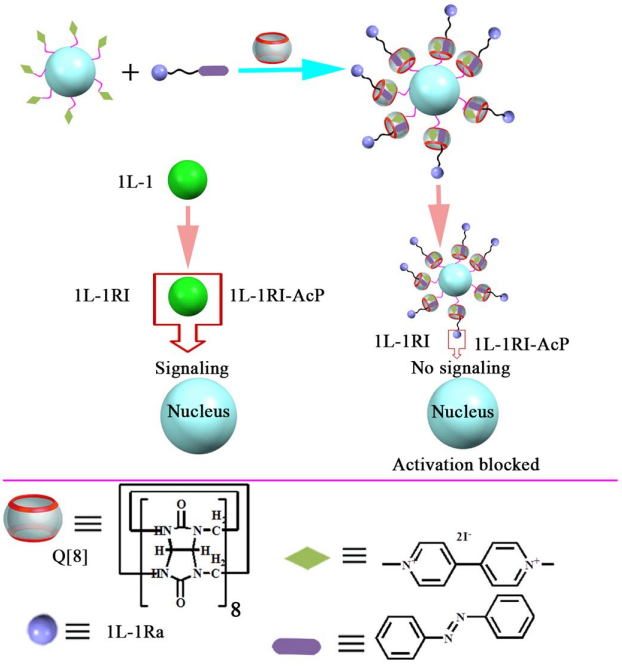

Figure 31. A Q[8]-based transporter for proteins.

Park, Gierschner *et al*. used polarized fluorescent spectroscopy to investigate supramolecular polymers based on a cyanostilbene monomer with a view to understanding the influence of such structures on the photoluminescence properties [104]. The emission properties of the 1:1 1D supramolecular strands formed on interaction with Q[8] were studied, and the radiative rate was discussed in terms of H- and J-aggregates. The crystal structure of the cyanostilbene guest was determined, which revealed extensive H type interactions, and these results were discussed alongside the features in the crystal photoluminescence spectrum. AFM images of the 1:1 complex revealed brittle fibres of diameter < 0.5 μm and lengths > 10 μm, possessing kinks and defects. The work then went on to further discuss the photoluminescence in light of non-homogenous nature of the particles.

The use of a fluorinated azobenzene monomer who structure comprised a central flexible butyl linkage which connected viologen/fluorinated azobenzene motifs was investigated by Zhan, Liu, Zhang *et al.* [105]. On interaction of this monomer (as the *E*-isomer) with Q[8], both viologen and fluorinated azobenzene were encapsulated in head-to-tail fashion such that a supramolecular polymer was formed. If this ternary complex was irradiation with visible light (λ > 500 nm) for 90 minutes, photoisomerization of the guest to the *Z*-isomer took place and resulted in the viologen been kicked out of the cavity which are then only occupied by the *Z*-isomer. The result of this irradiation is therefore depolymerization and formation of a ternary complex.

A number of coumarin derivatives were investigated as guests by Zou *et al*. [106]. In particular, one guest possessed a central flexible hexyl flanked by viologen/coumarin motifs, whilst a second guest possessed a central 4,4′-azodiphenol-derived core flanked by two flexible butyl chains connected to viologen/coumarin motifs. Combining the first guest with two equivalents of Q[8] led to the formation of a supramolecular polymer of high molecular weight (hydrodynamic radius *ca*. 1.9 μm by DLS). By contrast, use of the second guest led ultimately to the formation of dendritic polymers. NMR titration experiments indicated that that this was a multiple step process with initial encapsulation of pairs of viologen/coumarin motifs and viologen/azobenzene motifs.

On addition of more Q[8] (2 equivalents), a dendritic morphology appears (TEM) and the hydrodynamic radius (DLS) increased from 120 to 180 nm. Under these conditions, the central azobenzene underwent *cis* to *trans* isomerization, and as a consequence when subjected to UV light, did not undergo any further change.

Wang *et al*. employed the interaction of *trans*-4,4′-(bisaminomethyl)azobenzene dihydrochloride with Q[5] to construct a supramolecular polymer (1:1) promoted by the association of the ammonium groups with the Q[5] portals [107]. TEM images of the *trans*-azo product (rod-like crystals) revealed a length of *ca*. 120 nm. The *cis*/*trans* photoisomerization of the azobenzene allowed for reversibility between linear and folded polymeric structures (figure 32). Irradiating with UV light (365 nm) for 15 minutes partially converted *trans*-azo to *cis*-azo, which could be reversed by exposure to 254 nm light. The photoisomerization in this case does not lead to polymer breakdown, however the morphology changes to a curved structure.

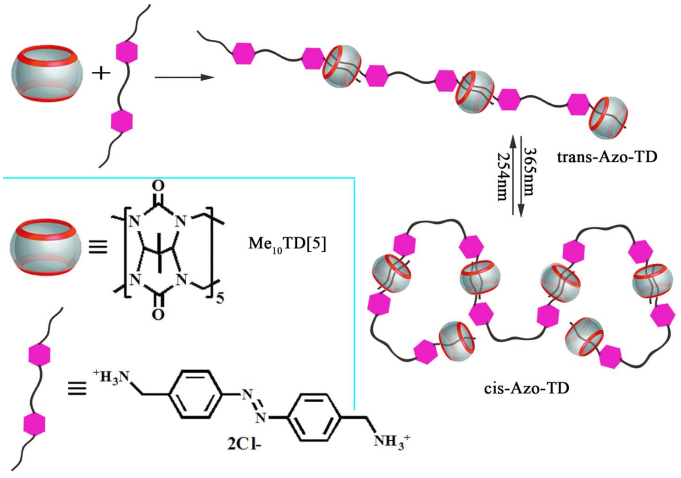

Figure 32. A photo-responsive Q[5]-based polymer.

A number of azo functional gold systems have also been studies and these are discussed in section 12 (gold surfaces).

11. Viologen containing systems

11.1 Covalent systems

11.1.1 Covalent Q[6] systems

Kim and coworkers have extended their studies to the use of a polyviologen, in which around 10 bipyridinium groups were present separated by decamethylene spaces (figure 33). It proved

possible to control the degree of threading in this system, with the amount of Q[6] per repeat unit varying between 0.1 and 1.0, and this was achieved simply by changing the amount of Q[6] added. ^{1}H NMR studies, including 2D NOSY and COSY, indicated that the Q[6]s resided in the middle of the decamethylene units. Changes in the spin lattice relaxation times also indicated that the polymer backbone became more rigid once the Q[6] was present, and at the same time, the size (measured by diffusion NMR spectroscopy) of the polymer increased from 56±1 to 62±1 Å. The expanded structure of the polymer also resulted in a higher intrinsic viscosity and smaller shape dependent constant (Huggins) *versus* the parent polymer. Notably, the decomposition temperature also increased with increasing amounts of added (threaded) Q[6] [108].

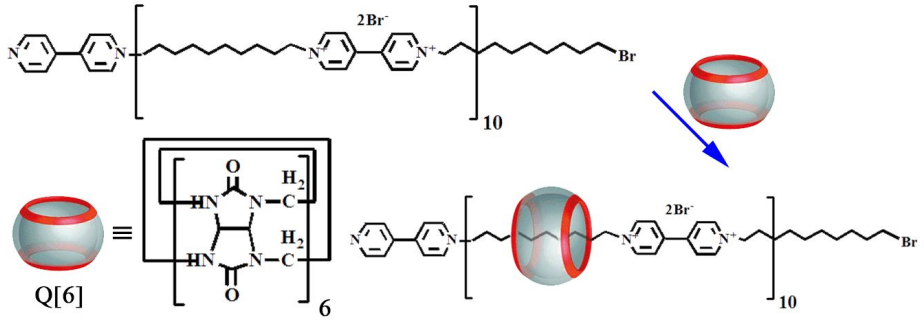

Figure 33. Formation of a polyviologen pseudopolyrotaxane.

Side chains can be added to the main polymer chain, for example Q[6] can be readily threaded onto a backbone containing pendant protonated diaminobutane groups. The result is higher conformational rigidity and thermal stability, but probably the most fascinating features of these systems is that the threading/dethreading can be reversibly controlled simply by adjusting the pH of the solution [109].

Hou *et al*. employed the viologen *N*-*n*-butyl-*N*′-(p-vinylbenzyl)-4,4′-bipyridinium bromide chloride, which bears a terminal alkenyl group. Interaction with Q[6] in water at room temperature afforded a 1:1 pseudo-rotaxane, in which the Q[6] beads reside at the terminal aliphatic chain. Studies revealed that the thermal stability and the rigidity of this pseudo-rotaxane was greater than that of the parent viologen, whereas it exhibited lower crystallizable capability [110].

11.1.2 Covalent Q[7] systems:

A study by Tan *et al*. also reported side chain polypseudo-rotaxanes, which were prepared from poly-*N*-*n*-butyl-*N*′-(4-vinylbenzyl)-4,4′-bipyridinium bromide chloride and Q[7] (figure 34). It was shown by ^{1}H NMR and IR spectroscopies, XRD (powder) and UV–vis studies that the Q[7] resided on the viologens, with 0 to 0.3 Q[7]s present depending on the amount of Q[7] added. The more Q[7] added the more stable is the system as evidenced by TGA data. The average hydrodynamic radius of the aggregates also increased on adding more Q[7] [111].

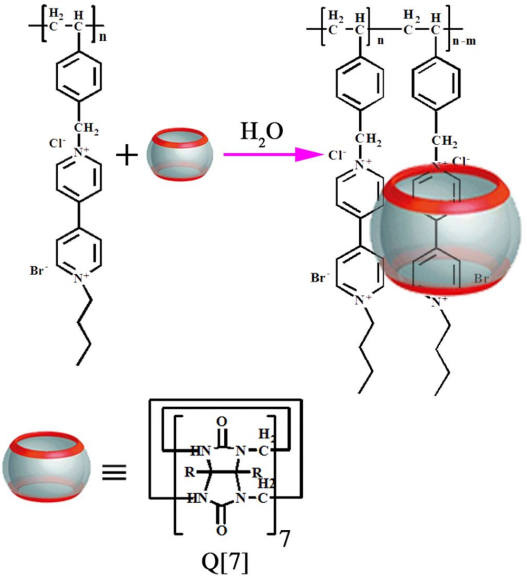

Figure 34. Side chain polypseudo-rotaxanes derived from poly-*N*-*n*-butyl-*N*′-(4-vinylbenzyl)-4,4'-bipyridinium bromide chloride.

By combining 4-(pyridin-4-yl)-1-(6-(pyridinium-1-yl)hexyl)pyridinium dibromide with 4-vinybenzyl chlorine, Tan *et al*. isolated the monomer 1-(6-(pyridinium-1-yl) hexyl)-10-(4-vinylbenzyl)-4,40-bipyridine-1 and 10-diium dibromide chloride. This monomer could be combined with Q[7] to afford a side chain polypseudo-rotaxane, and by varying the ratio of monomer to Q[7], the position occupy by the Q[7] could be altered (figure 35). For example, on increasing the Q[7]:monomer ratio from 1:1 to 2:1, the Q[7] moves from the hexyl groups to the benzyl and part of the viologen of the side chains, as monitored by ^{1}H NMR spectroscopy. In electrochemical studies, current levels significantly decreased on increasing the ratio of Q[7]:monomer [112].

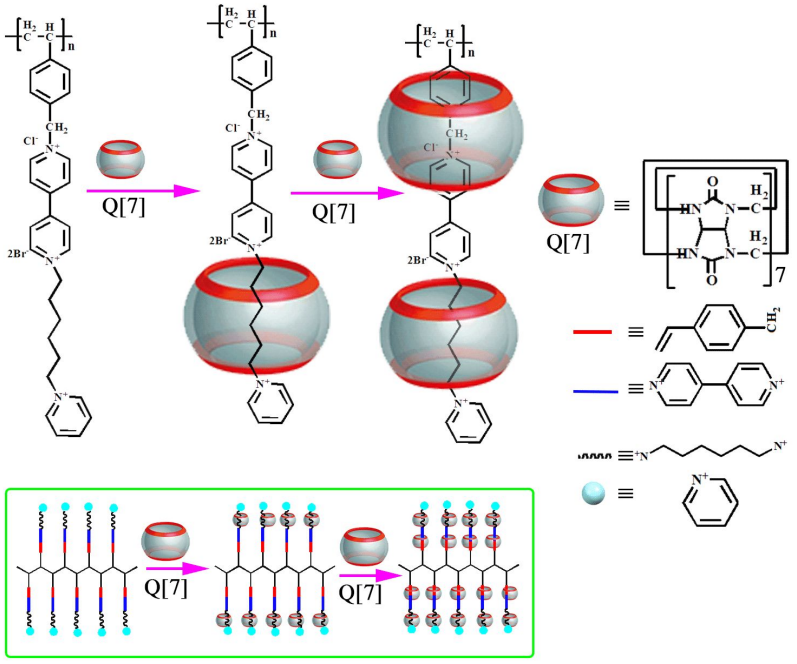

Figure 35. A side chain polypseudo-rotaxane derived from 1-(6-(pyridinium-1-yl) hexyl)-10-(4-vinylbenzyl)-4,40-bipyridine-1 and 10-diium dibromide chloride in the presence of Q[7].

11.1.3 Covalent other systems

A dibutyl tin dilaurate catalyzed coupling reaction was used to appended methyl viologen to poly(*N*-hydroxyethylacrylamide) polymers [113]. This was then combined with solid *nor*-*seco*-Q[10], and at concentrations of 0.1 mg/ml of polymer in solution, intramolecular collapse of the polymer chains occurred with concomitant particle formation. Dynamic light scattering indicated that the polymers present possessed monomodal distributions, whereas at higher concentrations, the species present were of multi-modal distribution (multi-chain aggregates). Through various experiments, it was noted that particle sizes were readily tuned via either polymer molecular weight or the degree of cross-linking.

11.2**Non-Covalent Q[8] systems**

The reaction of Q[8] with methylviologen-terminated poly(ethylene glycol)$_n$ monomethyl ether (molecular weight 5000 gmol^{-1}) and 2-naphthol has been investigated, and was found to result in the formation of a 1:1:1 tertiary complex [114]. Similar species could be obtained using polymeric (molecular weight 5000 gmol^{-1}) 2-naphthoxy-terminated poly(ethylene glycol)$_n$ monomethyl ether. In fact, by adding this second monomer to solutions that contain Q[8] and the aforementioned methylviologen-terminated polymeric monomer, it proved possible to

encapsulate both polymer end groups and their change transfer interaction was evident in UV/Vis absorption spectra. In this way, the length of the polymer chain had been significantly increased. Such tertiary complexes can be a good way of increasing the solubility of a compound. For example, octadecyl methyl viologen, which is sparingly soluble in water, is far more soluble when combined with Q[8] and 2-naphthoxy-terminated poly(ethylene glycol)$_n$ monomethyl ether. Diblock copolymers were also accessible using this methodology. For example, by combining methylviologen-terminated poly(ethylene glycol)$_n$ monomethyl ether (molecular weight 5000 gmol^{-1}), 2-naphthoxy-terminated *cis*-1,4-poly(isoprene) (molecular weight 10,500 gmol^{-1}) and Q[8], a charge transfer 1:1:1 ternary complex was formed after a couple or so hours.

Following interaction of a viologen possessing an α-mannoside end group with Q[8], which resulted in the viologen motif being embedded in the cavity, Scherman *et al*. added a linear 2-naphthol appended methacrylate copolymer on which the 2-naphthol groups were randomly distributed along the methacrylate backbone [115]. The copolymer also possessed about one fluorescent rhodamine B motif per chain. This resulted in a multivalent ternary 1:1:1 complex glycopolymer in which all of the naphthol were encapsulated by Q[8]s, and which exhibited yellow-green fluorescence. Reversibility was demonstrated on addition of sodium dithionite to the supramolecular glycopolymer, resulting in precipitation of the copolymer from the now purple solution. The recognition properties of the supramolecular glycopolymer towards lectin were investigated. Extensive cross-linking ensued on addition to the tetrameric lectin Concanavalin A, a process which could be monitored via absorbance spectra.

It has been shown that it is possible to convert cyclic oligomers into linear polymers using a tertiary complex derived from bis(*p*-sulfonatocalix[4]arene), *N*′,*N*″-hexamethylenebis(1-methyl-4,4′-bipyridinium) and Q[8] [116]. Bis(*p*-sulfonatocalix[4]arene), *N*′,*N*″-hexamethylenebis(1-methyl-4,4′-bipyridinium) cannot form a polymeric structure, and instead prefer to form a cyclic oligomer. However, on addition of Q[8], ^{1}H NMR spectra indicate that the 1-methyl-4,4′-bipyridinium could be found in the

calixarene cavities, whilst the hexamethylene fragment was encapsulated by the Q[8]. TGA analysis confirmed a Q[8]@ *N*′,*N*″-hexamethylenebis(1-methyl-4,4′-bipyridinium) to bis(calixarene) ratio of 2:1. The addition of hydrazine to the tertiary system resulted in two electron reduction of the viologen, and kicked out the bis(calixarene) whilst the topology of the Q[8]@viologen reverted to a molecular loop.

A range of high molecular weight poly(*N*-hydroxyethylacrylamide) polymers functionalized with both napthyl and viologen-containing side-arms, introduced via the use of isocyanates in the presence of a tin catalyst, have been employed by Scherman *et al*. [117]. The resulting single polymer chains, when treated with Q[8] in water, were broken down into smaller particles via intramolecular cross-linking. The particle sizes could be controlled by controlling the degree of cross-linking through Q[8] addition. AFM images clearly showed that on addition of Q[8], polymeric nanoparticles were present. If the order of addition is changed then multi-chain aggregates are formed, whilst the use of Q[7] did not result in any cross-linking as its cavity is too small.

Chen *et al*. investigated the use of a ditopic viologen in combination with an equimolar amount of a short hydrophilic polymer with two Np ends in the presence of two equivalents of Q[8] [118]. The result was polymeric chain extension as a result of host-stabilized charged transfer. Viscosity measurements indicated that maximum viscosity was achieved at equal molar ratios of Q[8], naphthalene end group and viologen. The results also indicated the supramolecular polymer had a degree of polymerization of 300 *versus* 52 for the parent short hydrophilic polymer. By employing a slightly different backbone in the parent polymer, it proved possible to prepare temperature sensitive supramolecular polymers. A surprisingly significant change (32 ^{o}C to 16 ^{o}C) in the lower critical solution temperature was reported, which was tentatively attributed to the aggregation characteristics of Q[8].

A triangular rigid backbone possessing viologen end groups, that had been reduced to radical cations using sodium dithionite, has been used to produce a self-assembled 2D honeycomb network (figure 36) [119]. On interaction with Q[8], further stabilization was achieved by stacking of radical cation dimers within the Q[8] cavities and the integrity of the planar aggregate

was maintained. Given that the triangular rigid backbone also contained three amide arms, any possible 1D stacking was suppressed.

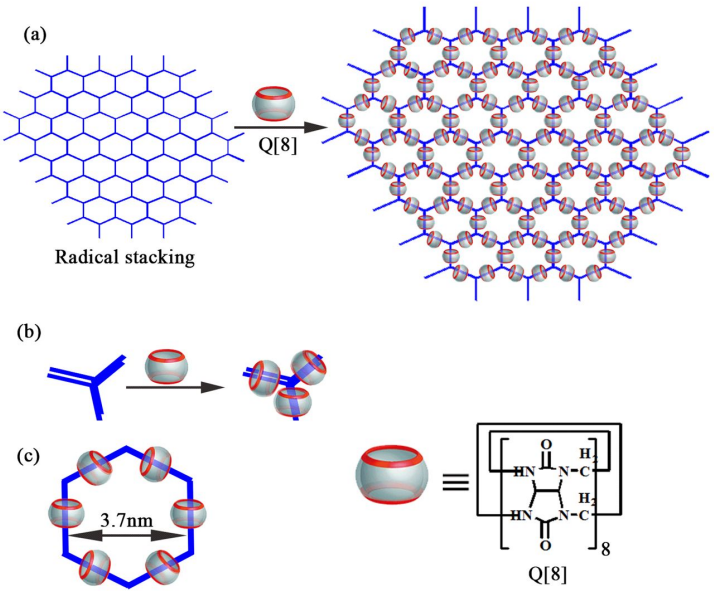

Figure 36. (a) 2D honeycombed networks formed by either reduced viologens or Q[8]/viologens; (b) the triangular rigid backbone and (c) hexagonal motif formed via the Q[8]s.

Liu *et al*. reported a cross-linked supramolecular polymer possessing aggregation induced emission (AIE) [120]. The polymer was assembled from a heteroternary complex of a flexible oligoethylene glycol capped at each end with an azobenzene grouping, Q[8] and 1,1-dimethyl-4,4-bipyridinium dications at the end of four arms extending out of a tetraphenylethylene core (figure 37). DOSY NMR data was consistent with the formation of an extended high molecular weight polymer in aqueous solution, and in SEM images of highly concentrated solutions, fibres were evident. On irradiation using UV light (365 nm) over 10 minutes, small sphere rather than fibres were formed. Specific viscosity changes were evident upon exposure to light, such that use of UV light led to a decrease, tentatively assigned to *trans* to *cis* isomerization, whilst exposure to visible light led to increased viscosity and re-assembly. The fluorescence intensity of the system increased as more Q[8] was added, and this was attributed to AIE. Observations on films indicated that AIE was also in operation in the solid state.

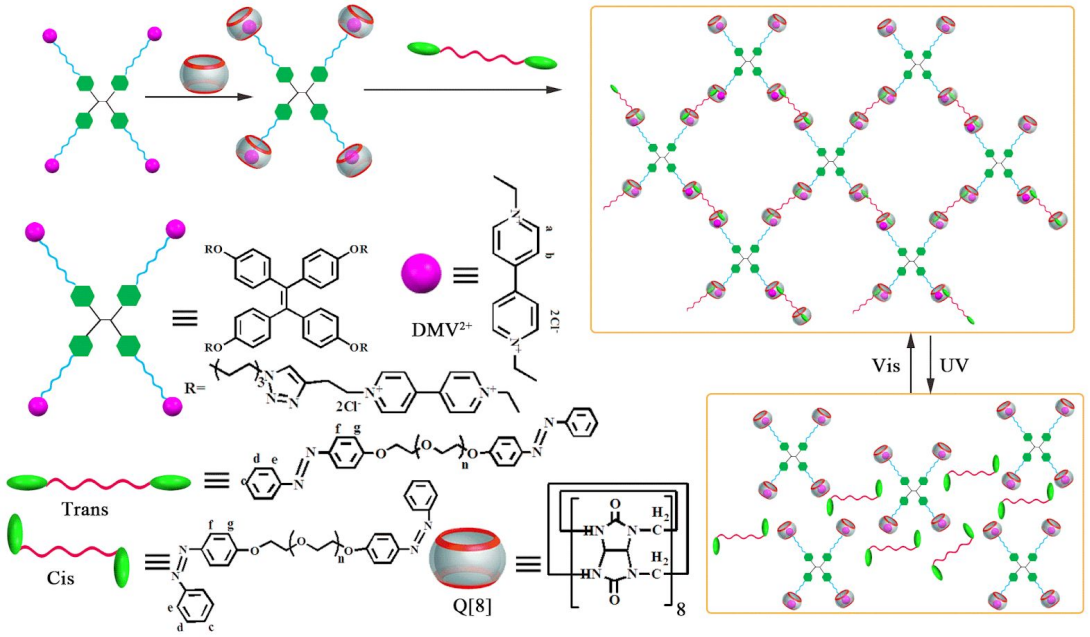

Figure 37. A cross-linked supramolecular polymer exhibiting AIE.

An alternating copolymer, which by manipulation of its redox chemistry, could be converted into a homopolymer has been reported [121]. The guests involved in the construction of this system were a bis-tryptophan with a central hexyl linker, a bis(methyl viologen) linked by a short central glycol chain and Q[8]. This bis(methyl viologen), as one might expect, interacts with two Q[8]s whereupon the viologen motifs are encapsulated. Further addition of a molar equivalent of the bis-tryptophan results in a heteroternary complex where the tryptophans are also encapsulated. DLS, FESEM, AFM and diffusion data were all supportive of the formation of a polymeric material which appeared as micro-globules of various sizes (150 to 250 nm). The addition of a competing guest such as 2,6-dihydroxynaphthalene or 1-adamantylamine broke up the polymer by either displacing the tryptophans from the cavity as in the former case or both guests as in the latter case. Treatment with hydrazine resulted in reduction to viologen radical cations, which were capable of forming dimers within the Q[8] cavities, and this led to release of the bis-tryptophan and the formation of a homopolymer (figure 38) that appeared as micro-globules of size 900–1000 nm. The dimerization process was evident from bathochromic shifts in the absorption spectra. This process proved to be reversible by the addition of H_2O_2 whereupon smaller (*ca*. 150 nm) micro-globules formed. An electrochemical study on the bis(methyl viologen) guest separately and that of the hydrazine-reduced solution mentioned above revealed

waves for reduction to dications and then neutral species and matched CVs previously reported for reductions within a Q[8] cavity.

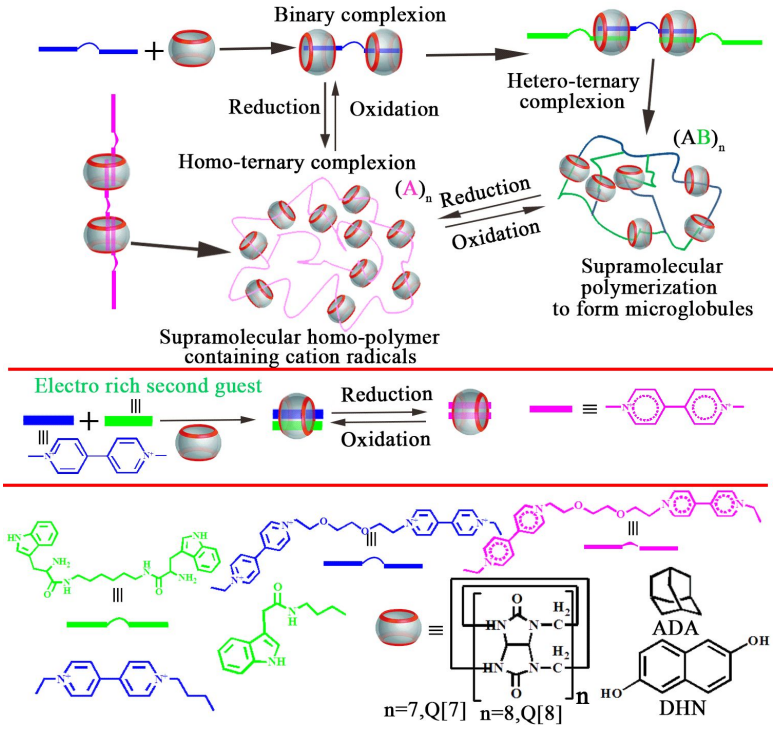

Figure 38. Converting an alternating copolymer into a homopolymer.

The use of naphthyl-viologen-naphthyl and viologen-naphthyl-viologen in which the various motifs are separated by flexible butyl chains has been investigated [122]. In the case of the naphthyl-viologen-naphthyl guest, from the ^{1}H NMR spectroscopic shifts, addition of one equivalent of Q[8] led to a back-folding and π-π stacking of a naphthyl-viologen within a Q[8] cavity. Addition of a further 0.5 equivalents of Q[8] resulted in the encapsulation of the other naphthyl group. Further addition of Q[8] led to poorly resolved spectra suggesting the formation of polymeric species. Use of the viologen-naphthyl-viologen guest with one equivalent of Q[8] resulted in backfolding of the viologen onto the naphthalene so that π-π stacking could occur within the Q[8] cavity. Addition of a further 0.5 equiv. of Q[8] resulted in encapsulation of the other viologen. During the same study, an ethyl-terminated trimeric viologen was also used as a guest. When three equivalents of Q[8] was added, the bipyridinium groups were encapsulated. Further addition of an equivalent of naphthyl-viologen-naphthyl led to π-π stacking between a

naphthyl and a viologen in one of the Q[8] cavities. Colour changes accompanied the above encapsulation processes which were evident in the UV-vis spectra. TEM measurements gave some insights into the morphologies adopted by the three systems with antler-shaped, spherical assemblies and dendritic type morphologies being observed, respectively.

11.3 **Non-Covalent other systems**

Zhang, Liu, Li *et al*. synthesized three oligo(ethyleneglycol) containing pyridinium monomers which were prepared from bis(hydrazone)s and a dicationic viologen capped at both ends with a benzaldehyde group [123]. Another monomer was prepared by reacting the dialdehyde with hydrazine for 48 hours. These four monomers were then subject to reduction using excess sodium dithionite, which reduced the dicationic pyridinium to a radical cation. Analysis of the UV-vis spectra revealed the presence of dimerized radical cation, *i.e*. $(\text{viologen}^{+\bullet})_2$. For the shorter monomers, this was thought to occur intermolecularly, whilst for the longer monomers, their increased flexibility would allow for this to take place intramolecularly. This would result in stacking and the likely formation of pleated sheets. If 2.5 equivalents of Q[7] was added to these reduced systems, then the absorption band associated with the $(\text{viologen}^{\bullet+})_2$ disappeared, as the Q[7] encapsulates the $\text{viologen}^{\bullet+}$ during pseudorotoxane formation. The process could be reversed rapidly by adding the competing guest 1-adamantane ammonium chloride. In separate experiments, the longer of the two polymers was exposed to increasing amounts of Q[8], and at a ratio of Q[8]/viologen of 0.5, a maximum was noted for the absorption band, whereupon it diminished on addition of further Q[8]. This suggested the adoption of doubly pleated sheets of $(\text{viologen}^{+\bullet})_2$ dimers via the formation of ternary complex of the type $(\text{viologen}^{+\bullet})_2$@Q[8]. Under the same conditions, similar use of Q[10] resulted in maximum absorption at a ratio of Q[10]/viologen 0.33, and suggested that the larger cavity here allowed for the encapsulation of three stacked units, and three triply pleated sheets resulted. The processes observed when using Q[8] or Q[10] could be reversed by the addition of competing guests, and to demonstrate this, hexamethylenetetramine and Q[5] respectively, were employed.

12 **Au surfaces**

12.1 Non-Covalent Q[8] systems

A method has been devised by which it proved possible to grow a polypseudorotaxane on a gold surface [124]. This involved the use of a guest molecule comprised of a central xylylene motif to which was bound at the 1,4-positions (*i.e*. *para*) 2-hydroxynaphthalene and 4,4′-bipyridinium groups. Combining this monomer with Q[8] in aqueous solution resulted in a 3:2 mixture of a 2:2 complex and oligomeric species. To the gold surface was attached a thiol which had at the other end of a pentyl chain a dipyridiniumethylene unit. At same time as exposing the gold substrate to this thiol, Q[8] was added and after 60 hours, a monolayer had formed. This monolayer was then further exposed to the xylylene-containing guest and a further batch of Q[8]. The resulting polymerization was monitored by IR spectroscopy and after 24 hours this revealed a degree of polymerization of *ca*. 4; the repeat units are linked by charge transfer interactions. The polymerization growth on the surface could be controlled by both the immersion time and the monomer concentration. Plunging the grown surface polymer into water resulted in depolymerization showing that the process was reversible.

Scherman *et al*. also studied gold surfaces and their interaction with Q[8] in water. The approach here involve first attaching ligands to a gold nanoparticle to form a monolayer and then subsequently form tertiary complexes with Q[8]. The ligands employed were tri(ethyleneglycol)-1-butanethiol and 1-methyl-4,40-bipyridinium-dodecanethiol bisbromide in a ratio of 92:8. The functionalized nanoparticle was further treated with the copolymer poly(2-hydroxyethyl acrylamide)-co-(naphtholtriazole acrylamide) which contains a pendant naphthol substituent on the side arms (figure 39). Following addition of Q[8] and then centrifuging, aggregation and precipitation was observed. The same could not be said if a gold nanoparticle minus the viologen was employed. Use of an ultracentrifuge with the Q[8] and viologen-containing gold nanoparticle led to the formation of pellets. When a similar system involving Q[7] was tested, no pellets were formed, *i.e.* the aggregation observed was driven by the presence of the Q[8]-based tertiary complex [125].

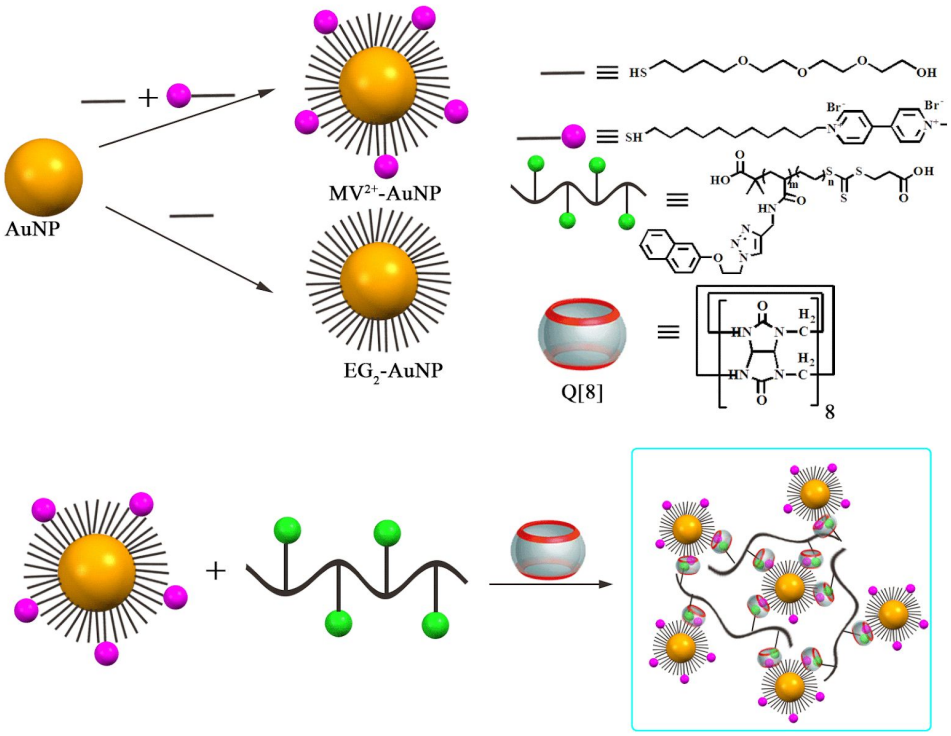

Figure 39. Aggregation of gold nanoparticles driven Q[8]-based tertiary complex.

The work was then extended to the development of porous microcapsules, which was accomplished in one step using microfluidic droplets. At the liquid-liquid interface the 'glue' was made up of tertiary complexes comprising Q[8], methyl viologen, gold nanoparticles and the copolymer poly(2-hydroxyethylacrylamide)-co-(naphtholtriazole acrylamide) which contains a pendant naphthol substituent. Once formed, the microcapsules could be dehydrated and quickly (minutes) isolated, and were found to be hollow. Importantly, the administration of a second aqueous supply containing a water-soluble cargo, e.g. fluorescein isothiocyanate–labeled dextran allows for complete encapsulation as evidenced by florescent studies. Cargo can also be released on demand by administering a one electron reduction of the methyl viologen moiety. It proved possible to probe the interior using surface enhanced Raman spectroscopy [126].

An intriguing method whereby loaded micelles could be immobilized onto a gold surface (figure 40) and then by way of exposing to a solvent change, in this case the addition of THF, chloroform or toluene, the micelle structure is rapidly destroyed and the payload released has been described [127]. The system was comprised of a diblock copolymer (M_n 19KDa) containing

poly(methyl methacrylate), *N*-hydroxyethyl acrylamide and 2-(2-(2-(naphthalen-2-yloxy)ethoxy)ethoxy)-ethyl acrylate, with a ratio of naphthol:MMA of 0.06:1. The self-assembled micelles, which had an average hydrodynamic diameter of 375 nm, can then interact with a modified gold surface functionalized with rotaxane and are immobilized within 30 seconds. The spherical micelles were densely packed on the gold surface as a monolayer, and this structure was only maintained in water due to favourable hydrophilic and hydrophobic interactions. The addition of the second solvent upsets this balance and the structure crumbles. The successful storage and rapid release ability of the micelle was readily demonstrated by loading them with Nile Red.

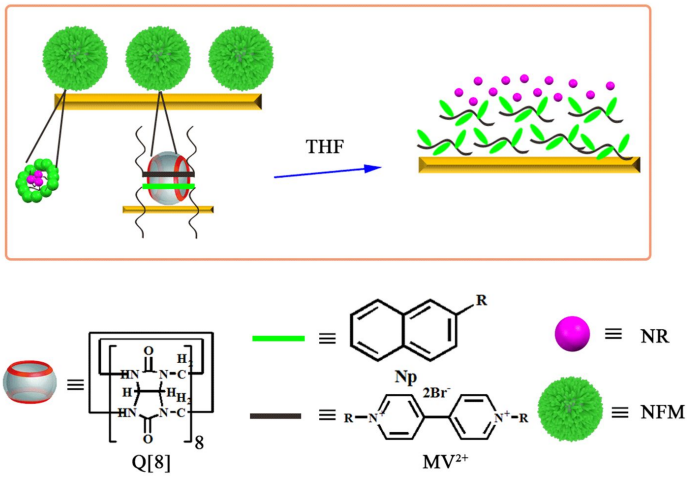

Figure 40. Loading and unloading of micelles on a gold surface.

A PEG bearing a single naphthol group (M_n 5170 gmol^{-1}) was prepared by Scherman *et al*. and was used to prepare a polymer brush by dipping a Q[8] rotaxane functionalized Au surface into a solution of the PEG monomer for 30 minutes [128]. Contact angles measurements were consistent with the formation of a more hydrophobic surface. SEM and AFM data revealed a dotted pattern of wide strips for these brushes. The behaviour of the brushes in solvents such as water, acetonitrile and toluene was investigated, and it was found that in water, the PEG chains extend to give a smoother surface. In 50:50 acetonitrile/toluene, the brushes were coarse and globules had appeared, whilst in solely toluene a more pronounced collapse of other polymer brushes was observed. It proved possible to modify (reduce) the brush density by adding a second

small guest molecule, and the brush height *versus* time was measured on addition of the guest naphthol. After 8 hours, complete removal of the brush from the surface was observed. The study was then extended to include a PEG monomer with a *trans* azo end group. Both approaches proved to be reversible by employing redox control in the form of $Na_2S_2O_4$, however the azo-containing brushes also exhibited reversibility via *cis*-*trans* photoisomerization by employing either UV or visible light. It also proved possible to prepare 'mixed' brushes containing both azo and naphthol polymers and these could be disassembled in two steps using external stimuli.

The same group then extended their work to a monolayer colloidal crystal templated route in order to access nanopatterned polymer brushes [129]. This involved a four step process whereby initially a dip coating technique was employed to coat a Q[8]-rotaxane gold surface with a *trans*-azo Si colloidal crystal monolayer. SEM and AFM revealed a hexagonal arrangement of azo-Si on the surface. In the second step, a tertiary complex was formed by dipping (for 30 minutes) the above assembly into an aqueous solution of a naphthol-containing PEG (M_n 2170 $gmol^{-1}$), *i.e.* the formation of brushes, and the hexagonal ordering was preserved. Thirdly, UV irradiation was employed to induce *trans*/*cis* isomerization, which resulted in release of the azo-Si colloids from the surface. AFM images revealed the presence of cavities of diameter 333 nm and height 10 nm, which occurred at regular intervals. These cavities were then filled, dipping as before, into an aqueous solution of a poly(ethylene glycol) polymer (M_n 5223 $gmol^{-1}$) bearing a terminal azobenzene group. This resulted in the formation of a dual polymer brushes on the surface as evidenced by SEM and AFM images, with the azo-containing brushes appearing *ca*. 3 times as long as the naphthol-derived brushes. The stability associated with the PEG brushes in this system was thought to arise from the ability to form extensive H-bonding with water present.

12.2 Non-Covalent other systems

The possibility of immobilizing a protein on a solid (gold) surface using non-covalent interactions via the use of Q[7] has been explored [130]. Immobilization was achieved by employing Grubbs Second generation catalyst in conjunction with (allyloxy)Q[7] and an

alkanethiolate self-assembled monolayer on the gold. Then separately, ferrocene methylammonium (*ca*. 19 units) was attached to glucose oxidase via 1-ethyl-3-(3-dimethylaminopropyl)carbodiimide coupling, and a buffer solution of this was prepared. The Q[7] functionalized gold surface was then immersed in this solution for 24 hours, and the immobilization was monitored by IR spectroscopy and surface plasmon resonance and the surface density of the ferrocene methylammonium glucose oxidase was calculated to be 1.1 x 10^{-12} mol cm^{-2}. Electrochemistry conducted in the presence of glucose revealed that the catalytic current increased with increasing glucose concentration (up to 30 mM), which suggested the possibility of using this system as a sensor for glucose (figure 41).

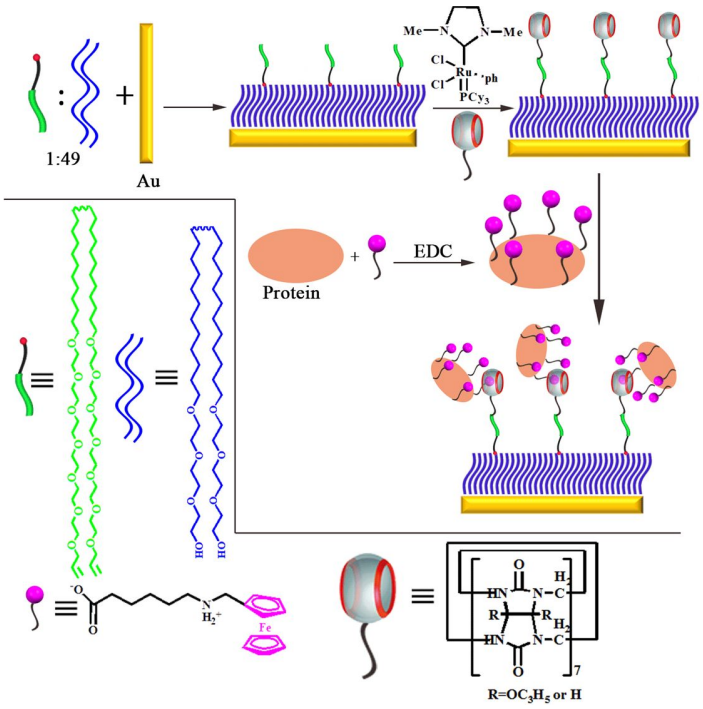

Figure 41. A potential glucose sensor based on Q[7].

Jonkheijm, Hecht, Huskens *et al*. prepared an azopyridine containing guest which also possessed a tetra(ethylene glycol) chain. This monomer was then used to access both di- and trimeric guests via ring opening of succinic anhydride and reaction with either *N*-Boc-serinol or Boc-protected aminotris(hydroxymethyl)methane followed by deprotection with trifluoroacetic acid. Fluorescein derivatives of these three azopyridines were then prepared. Heteroternary host-guest complexes involving Q[8] as the anchor were prepared both in solution and on various surfaces. On gold surfaces, it proved possible to determine binding enhancements when using

multi-valency as opposed to monovalent guests. This then made it possible to deposit and replace specific guests at designated positions on the surface, *i.e*. replaced mono with multivalent guests, and thereby tuning the surface properties. Furthermore, the presence of the azo function allows such surfaces to exhibit light responsive properties [131].

13. Hydrogels

13.1 Covalent systems

13.1.1 Covalent Q[7] systems

The control of gelation kinetics by studying copolymers (*N,N*-dimethyl acrylamide based) with either pendant Q[7] or adamantane groups (figure 42) was investigated by Li, Tan *et al*. [132]. This was achieved by pre-occupying the Q[7] cavity with competing guest molecules, and it proved possible to significantly reduce gelation times down from hours to seconds. Moreover, the mechanical properties and stability of the hydrogels were not compromised, and they proved suitable for potential injection and printing applications.

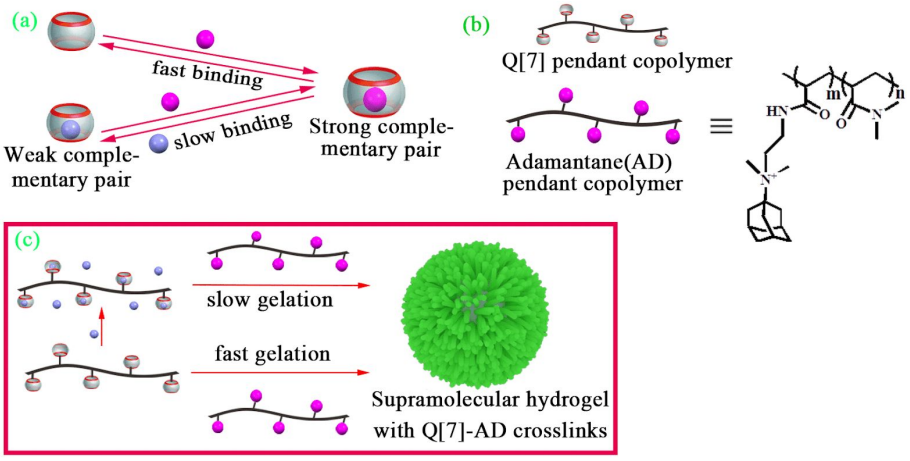

Figure 42. Control the gelation kinetics.

13.1.2 Covalent Q[8] systems

Host-guest complexes of Q[8] with hyaluronic acid and hydroxyethyl cellulose functionalized with coumarin have been prepared [133]. The polymer products formed were self-assembled, photo-tunable hydrogels, and contained two coumarin motifs with each Q[8] cavity. Subsequent photodimerization resulted in cross-linking and formation of covalent gels. In the hydroxyethyl cellulose case, the addition of Q[8] resulted in a slight stiffness and a 3-fold increase in complex modulus. On irradiating with light (>310 nm), major stiffening occurred as a result of coumarin

cross-linking. Further irradiation at 254 nm failed to re-dimerize the system back to the covalent state, and there was a reduction in stiffness. This was thought to be due to polysaccharide matrix photo-degradation rather than decoupling of the coumarin cross-linking. For the hyaluronic acid derivative, there was again a stiffening on addition of Q[8], and upon irradiation (>310 nm) stiffened yet further and there was a significant increase in the storage modulus. It proved possible to revert the system to its physical state and then to cross-link again for at least two cycles on irradiation for 1.5 hours. However, on prolonged exposure (6 hours) to UV light (<310 nm), the stiffness struggled to fully recover. Thus, the two systems differed in their behaviour with one system (hydroxyethyl cellulose) showing that it could be photo-cured but not reversibly, whilst the other system (hyaluronic acid) displayed properties that were potential more useful, namely it was photo- and shear-reversible. Indeed, for the latter system, degradation only took place following systematic energy saturation.

13.2 Non-Covalent systems

Scherman *et al* expanded work on Q[8]-containing tertiary complexes to cross-linking of multivalent copolymers and the formation of hydrogels [134]. This was accomplished by first employing radical polymerization to access polymers bearing side chains containing either viologen or 2-naphthoxy groups. The resultant polymers were then shown to be capable of forming 1:1:1 tertiary complexes with Q[8]. Due to the nature of the guests, reversible cross-linking ensued with substantial changes in viscosity. It proved possible to control hydrogel properties by adjusting the amounts of Q[8] present, *i.e.* via control over the amount of cross linking.

It also proved possible to form hydrogels with impressive water content (≤ 99.5%) via the interaction of cellulose-based polymer bearing pendant naphthyl groups, a viologen-functional poly(vinylalcohol)polymer and their interaction with Q[8] [135]. The hydrogel was orange in colour, which was the result of change transfer occurring within the Q[8] cavity between the polymer side chain end groups, *viz* naphthyl and viologen. Use of Q[7] here failed to afford a hydrogel. In terms of practical applications, the ability to control both the mechanical and viscosity properties of the system by simply adjusting the amount of one of the component

present or the concentrations involved, should prove beneficial. The lack of cytotoxicity displayed by the polymers employed here is similarly beneficial. Protein loaded gels could also be prepared, and in this work, systems employing Bovine Serum Albumen and lysozyme were prepared. Protein release was found to be affected by both protein molecular weight and the size of the loading (wt%).

The same group then reported even high water content (≤99.7wt%) by employing a system based on naphthyl-functionalized cellulose, the viologen-functional poly(vinylalcohol) polymer used in the previous study and Q[8] (figure 43) [136]. This one-step procedure again resulted in a light orange coloured hydrogel. The hydrogel exhibited a self-healing property in that if it was broken up, it reformed when the pieces were again united. Addition of an excess of a competing guest such as toluene can impact greatly on the structure and behaviour of the system, leading to loss of the bulk properties such as the colour. However, on removal of the toluene, the hydrogel structure returned.

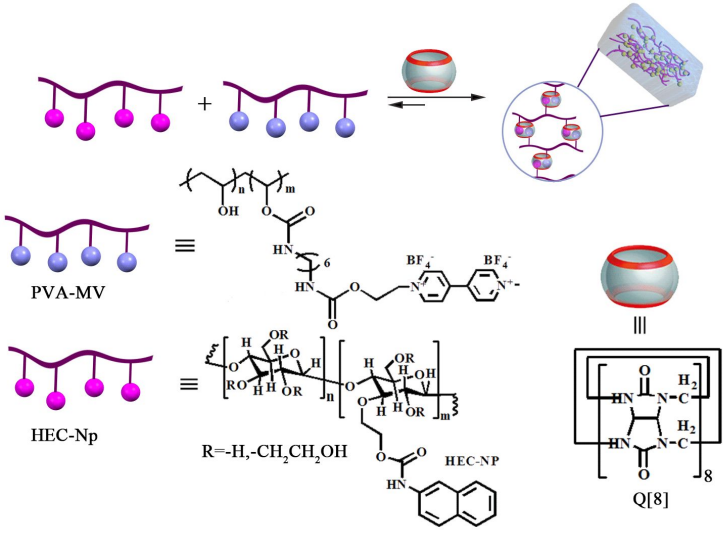

Figure 43. Route to a hydrogel exhibiting a self-healing property.

Poly(*N*-(4-vinylbenzyl)-4,49-bipyridinium dichloride-co-acrylamide), P4VBAM, and Q[8] were utilized by Tan *et al*. to form hydrogels (figure 44) by manipulation of the pH of the aqueous solution (addition of NaOH) [137]. In alkaline solution, the structure was that of a 3D network and the gelation to the hydrogel only occurred when the NaOH was present. However, the addition of HCl revealed that the process was reversible, and the cycle was possible until the

amount of undesirable sodium salts became problematic, typically four cycles. These hydrogels are thermally sensitive and their flow rate increased on increasing the temperature.

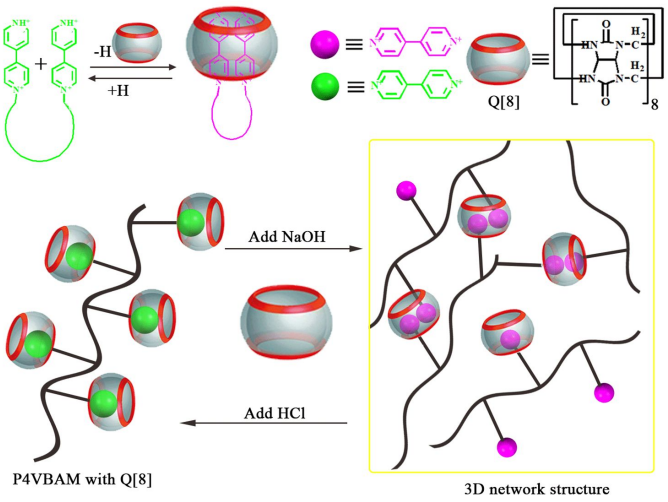

Figure 44. pH dependent formation of hydrogels.

pH sensitive gels, reported by Li *et al*, could be utilized as a transporter of a drug-controlled release system, and are discussed in the medical section of this review [138].

Hydrogels that were accessible from systems derived from amino acid containing rigid polymers and Q[8] have been reported [139]. In particular, the combination of cationic styrenic amino acid random copolymers, where the amino acids were phenylalanine and tryptophan, with ≥0.5 equivalents of Q[8] resulted in greatly increased viscosity. The hydrogen formation was associated with the 2:1 interaction of the two charged amino acid residues within the Q[8] cavity. It was deduced that in terms of hydrogel formation, the phenylalanine motif performed better than did the tryptophan.

By employing a central 1,3,5-triphenylbenzene with 4,4′-bipyridin-1-ium groups connected to the *para* positions of the outer phenyl groups and introducing three bis(2-hydroxyethyl)carbamoyl groups at the other available positions on the central aromatic ring, it proved possible to a 2D supramolecular framework on reaction with 1.5 equivalents of Q[8] [140]. From DLS experiments, it was concluded that 350 hexagonal pores could be found in each 2D sheet. Use of more concentrated solutions afforded hydrogels. Use of cryo-SEM revealed that the 2D sheets were actually curled, whilst AFM measurements revoked that the thickness of the layer was *ca*. 1.75 nm, *i.e*. the same as the diameter of one Q[8].

Scherman, Ikkala *et al*. employed the viologen-functional poly(vinylalcohol)polymer that had used earlier to good effect to form hydrogels derived from cellulose-based polymers [141] and extended that work here by using it combination with a second guest comprising random copolymer grafts of dimethylaminoethyl- and napththyl-functionalized methacrylate blocks (figure 45) [142]. Under acidic conditions (pH 0.5), the second guest was added to a preformed solution of Q[8]@viologen, which resulted in a red precipitate and following subsequent treatment by centrifuge, a rubbery material. When near equal amounts of napththyl and viologen were employed in the synthesis, the resulting product displayed the highest zero-stress storage modulus ($G' = 14.3$ kPa). Electron microscopy revealed the guest was comprised of random copolymer grafts of dimethylaminoethyl- and napththyl-functionalized methacrylate blocks and existed as homogeneously dispersed rod-like entities in the hydrogels and this was the case for all compositions. The hydrogels possessed a self-healing property and showed that after experiencing serve strain and rupture of cross-linking, they were quickly (in seconds) able to recover. This self-healing property was even evident on a macro scale for both fresh or aged samples, such that two separated pieces could be brought together and then the newly formed materials when subject to further strain was found to break in a completely different place.

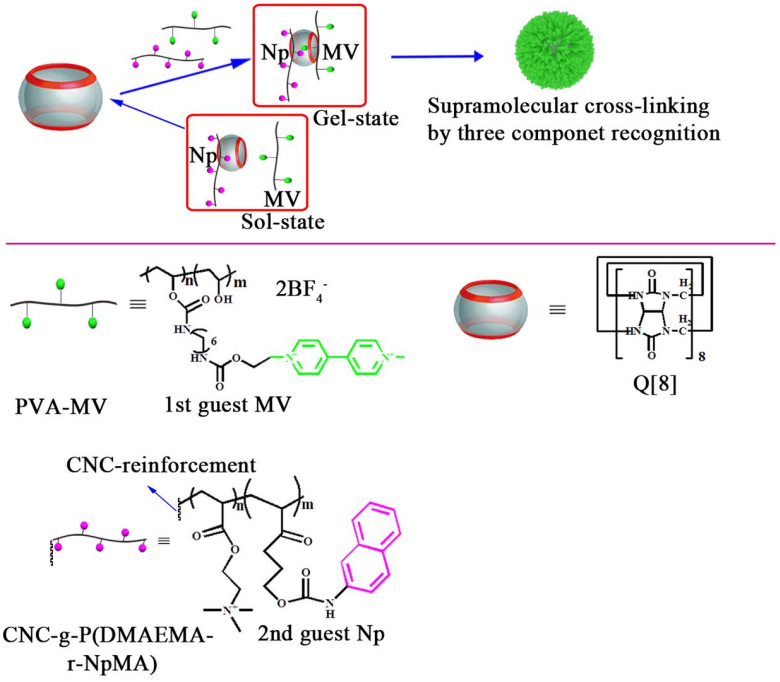

Figure 45. Formation of self-healing hydrogels.

Stopped-flow spectrofluorometry was employed to investigate the kinetics associated with the addition of a second guest to Q[8]@viologen, and used the information gleaned to gain some insight into hydrogel structures [143]. Copolymers containing pyrenyl, dibenzofuranyl, and 2-naphthyl motifs were used in the study; as many factors as possible, such as copolymer molecular weights, were kept constant throughout. The first guests employed were either a methyl viologen containing poly-(vinyl alcohol) or a copolymer derived from a styrenic monomer bearing an MV moiety. The study revealed that energetic barriers to both dissociation and association of guest molecules are pivotal in controlling the mechanical strength and self-healing capacity of a hydrogel, respectively.

Scherman, Abell *et al*. demonstrated that it was possible to form hydrogel microcapsules in microfluidic droplets [144]. This was achieved by employing a homotertiary complex comprised of Q[8] and anthracene-functionalized hydroxyethyl cellulose. Within the Q[8], there was head-to-tail encapsulation of anthracene moieties, and this allowed adjacent polymers to cross-linking in non-covalent fashion, and thereby form the skin of the hydrogel at the water-in-oil interface for individual droplets. Encapsulated species could then be released by adding a competitive guest. The ability of the capsules to perform storage and release was demonstrated by encapsulating fluorescein isothiocyanate-dextrans and monitoring the process by fluorescence microscopy. The release rates were found to depend on the molecular weight of the encapsulated fluorescein isothiocyanate-dextrans, with the larger ones being released somewhat slower, *i.e*. a diffusion-controlled process. Exposing the system to UV radiation resulted in [4+4] photodimerization and a covalently linked structure. This produces a more robust storage structure whose molecular permeability could be controlled by the length of exposure of the system to UV light with an upper limit of 60 seconds or so. Beyond this time, no further improvement in cargo loss was observed presumably because the cross-linking was near complete.

Microdroplets have been employed as templates and it was observed that it was possible to form supramolecular hydrogel beads [145]. The system utilized a methyl viologen-containing

poly((vinylbenzyl)trimethylammonium chloride) copolymer and a 2-naphthyl-modified poly(hydroxyethyl cellulose) copolymer in combination with Q[8]. These ingredients were mixed in a low-focusing microfluidic device, where after the microdroplets formed were collected and allowed to evaporate affording hydrogels. Monodisperse hydrogel beads could then be accessed upon rehydration. These beads were capable of triggered cargo (e.g. fluorescein isothiocyanate–dextran) release by addition of the competing guest 1-adamantylamine.

Self-healing hydrogels based on the interaction between poly(*N*1,*N*1,*N*2,*N*2-tetramethyl-*N*1-(naphthalen-2-ylmethyl)-*N*2-(4-vinylbenzyl)ethane-1,2-diaminium-co-*N,N*-dimethylacrylamide) and Q[8] have been reported [146]. The formation and self-healing of the hydrogels was driven by π-π interactions between naphthaline groups and Q[8] as well as dipole-dipole interaction between the quaternary ammonium cation and Q[8]. Investigation of the self-healing properties revealed that it is reliant of the Q[8] to naphthaline molar ratio, and the results suggested that the availability of guest or host molecules at the surface of a cut were capable of 're-complexation', thereby leading to the observed self-healing.

Tan *et al*. employed a *N*-isopropylacrylamide-based copolymer bearing naphthyl groups on its side chains in combination with methyl viologen and Q[8] to afford a red solution [147]. ^{1}H NMR spectra indicated that viologen and naphthyl groups were encapsulated within the Q[8] cavities. Heating the red solution above 32 ^{o}C, led to formation of a stable hydrogel. By modifying the make-up of the copolymer or varying the amounts of Q[8] and/or viologen present, the gelation temperature could be varied over the range 26.4 ^{o}C to 34.6 ^{o}C. If competing guests such as 1-adamantanamine hydrochloride or 1,6-hexanediamine dihydrochloride were added, then the red solution turned pink and then became colourless as increasing amounts were added, and on heating gelation failed to occur.

It has been shown that it is possible to increase the strength of hydrogels by incorporation of inorganic ($CePO_4$) nanowires into the supramolecular structure [148]. The hydrogel investigated was that derived from naphthyl-functionalized cellulose and viologen-functionalized

poly(vinylalcohol), which in the presence of Q[8]readily form a dynamic hydrogel. The process involved adding small amounts (0.001 to 0.030 wt%) of $CePO_4$ nanowires, whereupon increases of up to 48% in the storage moduli were observed. SEM images showed how the nanowires extended across the structure of the hydrogel, and it was proposed that the polymer chains present were able to H-bond the length of the nanowires and thereby provide enhanced cross-linking and reinforce the structure. The presence of too many nanowires leads to aggregation and a weakening of the hydrogel structure.

14. Medical applications

14.1 Covalent Q[6] systems

Kim et al established that it was possible to modify the surface of a nanocapsule using non-covalent interactions whilst guests are held inside, see section 9.1. [74] This suggested such a system had potential application in targeted drug delivery, and with this in mind, stimuli-responsive polymer nano-capsules were reported [149]. The principal involved creating reductively labile polymer capsules that can under specific circumstances open-up and release their payload. Disulfide bridges were employed as they are known to readily cleave under reducing environments (e.g. in the presence of dithiothreitol) to thiols, and were used in conjunction Q[6] linked with amide bonds via polymerization (figure 46). The collapse of the capsules was monitored using SEM and HRTEM studies, which revealed that after 30 min., most of the capsules had broken down. Comparative experiments using CH_2-CH_2 linkages rather than disulfide showed that the presence of -S-S- is a pre-requisite for cleavage and collapse. The fluorescent dye carboxyfluorescein was encapsulated (about 700 molecules in a capsule of diameter 90 nm) and SEM and HRTEM studies revealed that the spherical nature of the capsule was retained. Dispersion of this carboxyfluorescein-containing capsule in a buffer solution revealed little change in emission intensity over 3 hours, however on addition of dithiothreitol, there was a sudden increase in emission intensity that leveled off after 3 hours. Control experiments confirmed that the dye had been released via collapse of the capsule brought about by the presence of the reducing agent. To verify the potential of such a system as a drug delivery agent, the carboxyfluorescein-containing capsule was treated with a galactose-spermidine

conjugate in order to target HepG2 hepatocellular carcinoma cells. Following incubation, confocal microscopy was employed to visualize the increase in the intracellular fluorescence as a result of bisulfide bridge rupture and dye release; the analogous CH_2-CH_2 linked system did not exhibit any increased intracellular fluorescence as the CH_2-CH_2 links were not cleaved and therefore the dye was not released.

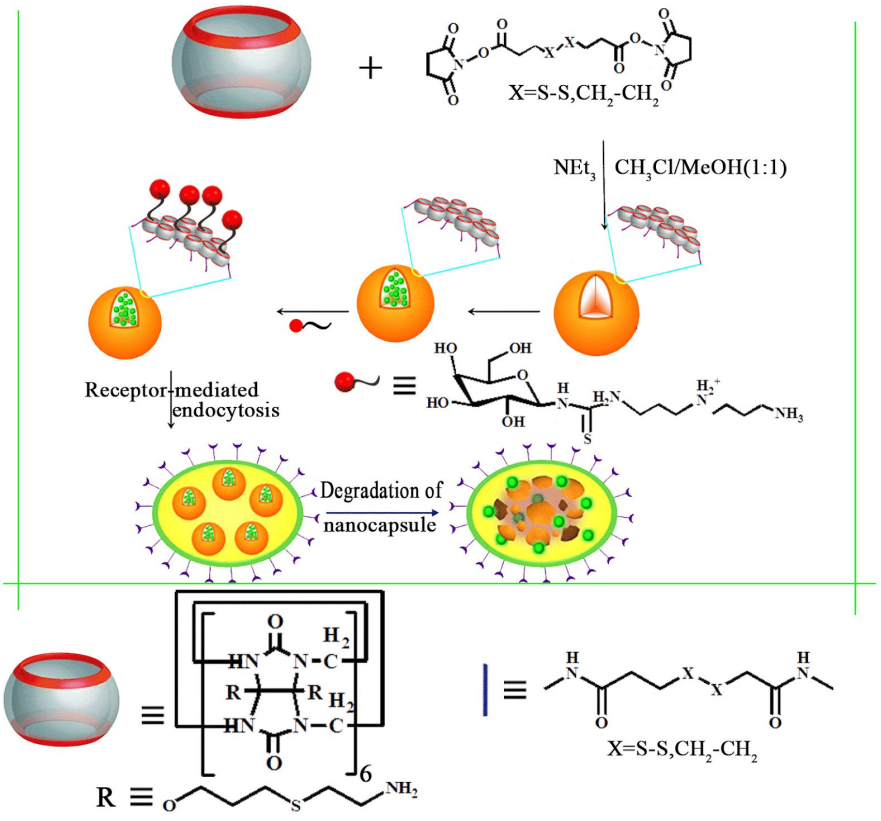

Figure 46. Preparation of stimuli-responsive polymer nano-capsules, and stimuli-responsive polymer nano-capsules with a galactose-spermidine conjugate; targeting of HepG2 hepatocellular carcinoma cells.

Another example of a drug delivery system was reported by Ghosh *et al*. They utilized a bottom-up approach to target a tubulin using Q[6]; we note here that α- and β-tubulins polymerize into microtubules, which are a major component of the eukaryotic cytoskeleton. The methodology involved capping Q[6] with gold nanoparticles and then appending a peptide to the nanoparticle. The specific peptide chosen allowed for the delivery (and release) of curcumin to cancel cells which overexpress the receptor Nrp-1-rich. This resulted in self-assembly and the Q[6]/gold nanoparticle/peptide formed a nanocapsule which buried the curcumin. The presence of the Q[6] interfered with the polymerization of tubulin, whilst the loaded nanocapsule was

found to exhibit little toxicity toward human lung fibroblasts cells. Furthermore, the loaded nanocapsule significantly inhibited the growth of *in vivo* mice melanoma tumours [150].

Nanocapsules for targeted photodynamic therapy were reported by Wang *et al*. The approach here started with perhydroxyQ[6], which was alkylated with 1,4-dibromobut-2-ene using NaH in DMSO to afford self-assembled nanocapsules (figure 47). It proved possible to encapsulate the photosensitive therapeutic payload Chlorin e6, and by exploiting the interactions between the antifolate drug sulfadoxine/pyrimethamine (SP) and Q[6], it proved possible to modify the nanocapsules so that they could target cancer cells with overexpressed FA receptors [151].

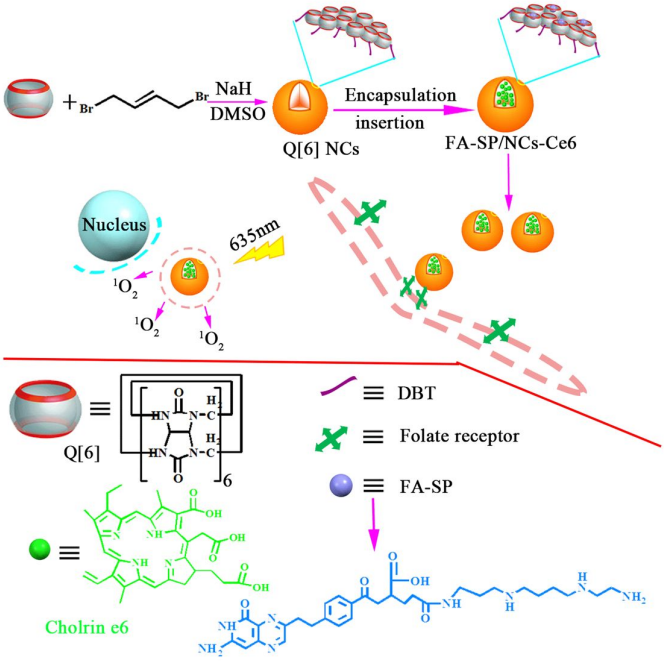

Figure 47. Photodynamic therapy using Q[6]-based nanocapsules.

14.2 Q[7]-based systems

We note here that Ghosh and Nau have reviewed Q[*n*]s, as well as (cyclodextrins and sulfonatocalixarene) and how their ability to encapsulate drugs can impact on pKa values and enhance the bioavailability of drugs (figure 48). However, it was noted that these pKa changes are not predictable, whilst anion receptors are in short supply. The authors thought that Q[*n*]s offered the best opportunities going forward of the macrocycles discussed [152].

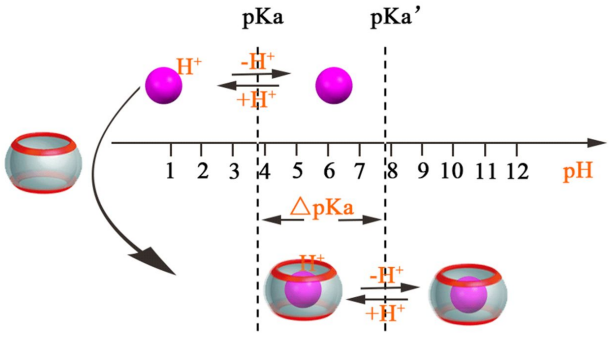

Figure 48. pKa values change upon encapsulation.

Polypseudo-rotaxanes have been prepared based on ε-poly-*L*-lysine hydrochloride with a view to studying its antibacterial activity upon *Escherichia coli* (*E. coli*). ^{1}H NMR spectroscopy and ITC were employed to study the polypseudo-rotaxane formation using Q[7], and the degree polymerization was found to be *ca*. 30 (M_w 4.96 x 10^3 g/mol). The Q[7] encapsulated 1 in 3 of the lysine fragments with two other 'uncomplexed' lysines acting as spacers in each of the repeating unit. Quantitative studies of the antibacterial activity revealed that it could be controlled and was aligned with the number of repeating units. Twelve repeating units of lysine was calculated to be the minimum required for high (>90% efficiency) antibacterial activity [153].

Lv, Wang *et al*. investigated the impact of Q[7] on the ability of the cationic poly(fluorene-co-phenylene) derivative (PFP-NMe_3^+) to bind to pathogen membranes. The Q[7] encapsulated the alkyl chain side arms, however on subsequent addition of amantadine, a more stable Q[7]/amantadine was formed and the PFP-NMe_3^+ was released. The fluorescent intensity changes associated with this process could be monitored, and this allowed for the *in-situ* identification of multiple pathogens within a sample given that PFP-NMe_3^+ interacted differently with cell surfaces. Indeed, the system even possessed the ability to discriminate between different strains of the same species. The benefits of this system are that it requires only 2 hours to classify pathogen types nor are specific biomarkers or cell labeling required [154].

14.3 Q[8]-based systems

The interaction of the 1-ethyl-10-arylmethyl-4,40-bipyridinium viologens, where the aryl is phenyl, 2-naphthyl, 2-anthracenyl or 1-pyrenyl, with DNA has been studied, with and without

Q[8] present, in Tris-HCl buffer. The inclusion compounds were characterized by ^{1}H NMR and UV-vis spectroscopic studies as well as by ESI-MS. Similar binding modes were proposed for all four derivatives, with the aryl end group and most of a pyridinium ring encapsulated by the Q[8]. Electrochemical studies indicated that the electron reduction ability and intramolecular electron transfer was more facile for the bipyridinium derivatives in the presence of Q[8]. The DNA photocleavage efficiency was probed in the presence of various radical scavengers such as *L*-histidine, NaN_3, KI, DMSO, isobutyl alcohol, HCOONa, mannitol and superoxide dismutase. In the absence of light, no cleavage took place. For the 2-anthracenyl and phenyl derivatives, it was concluded that $^1O_2$ and ▪OH were the reactive species responsible for DNA cleavage. In general, it was found that the presence of Q[8] increased the efficiency of DNA cleavage [155].

Given that the use of host-guest chemistry is a possible route for enhanced drug delivery, Tao, Wei *et al*. studied inclusion complexes formed by gefitinib, which is used as a drug for lung cancer in patients who have previously received chemotherapy, with both Q[7] and Q[8] [156]. Two forms of gefitinib were studied, namely the diprotonated and the neutral form. It was found that both Q[7]and Q[8] influenced the acid-base character by similar degrees, with shifts in the gefitinib pKa of 1.4 and 0.7, respectively. Determined thermodynamic parameters indicated that the inclusion process was enthalpy controlled, with hydrophobic and van der Waals interactions the main driving forces. ^{1}H NMR spectroscopic studies on the systems revealed that fast dynamic equilibria were in operation. In the case of Q[7], this involved encapsulation of the quinazolin, the morpholin ring and the alkyl chain moieties of gefitinib in the cavity. For Q[8], the quinazolin ring and phenyl moiety of the guest gefitinib were entrapped in the cavity. Taking into account these observations, it was noted that the Q[7]-based system had the greater potential to enhance the solubility and dissolution rate of gefitinib in aqueous solution.

Given the presence of two imidazolium moieties as well as numerous other potentially beneficial properties, Urbach, Bielawski, Scherman and coworkers decided to probe the use of benzobis(imidazolium) salts in Q[8] chemistry [157]. In particular, tetramethyl benzobis(imidazolium) was combined with Q[8] and found to form a 1:1 host-guest complex.

Interestingly, unlike for methyl viologen, there was a large preference for Q[8] *versus* Q[7]. One of the benefits of employing benzobis(imidazolium) salts is their intrinsic fluorescence, and upon encapsulation by Q[8], this was maintained though bathochromically shifted (by *ca*. 13 nm). However, when a second guest was introduced, this fluorescence was quenched. This was illustrated by adding 4-iodophenol, and control experiments revealed that in the absence of Q[8] the quenching of the benzobis(imidazolium) salt fluorescence was far less marked. These observations then led to wider sensing applications of this tetramethyl benzobis(imidazolium)@Q[8] system, such as the sequence-selective recognition of peptides and controlled disassembly of polymer aggregates.

A copolymer comprised of blocks of poly(*N*-isopropylacrylamide) and poly(dimethylaminoethylmethacrylate) was assembled via its interaction with Q[8] [158]. The driving force behind this work was to access a stimuli-responsive chemotherapeutic drug delivery system, and hence the constituents of the copolymer were selected for their ability to act as temperature-responsive and pH-responsive blocks, respectively, both with molecular weights below 10000 g/mol. The formation of a tertiary complex in the presence of Q[8] was confirmed by ^{1}H NMR and UV-vis spectroscopic studies as well as by ITC measurements. Observing the system using dynamic light scattering and increasing the temperature above 4 ^{o}C revealed the formation of supramolecular micelles. Use of competitive guests (e.g. adamantaneamine) or changes in pH changed the size of the particles present. It proved possible to load the micelles with the drug doxorubicin via solvent exchange and dialysis. Subsequent drug release and IC_{50} values could be controlled by a number of factors including temperature, pH and addition of a competing guest; drug release was enhanced by a factor of 3.

N-(4-diethylaminobenzyl) chitosan, prepared via the reduction ($NaBH_4$) of a mixture of chitosan and 4-(diethylamino)benzaldehyde, was combined with Q[8] at 25 ^{o}C to afford a gel (figure 49) [159]. Increasing the temperature to 50 ^{o}C led to a yellow solution that reverted to the gel again on cooling. SEM revealed the presence of a cross-linked network with pore size 5 – 10 μm. Gel formation was favoured by acidic conditions, which allowed for protonation of the diethylamino

groups and subsequent electrostatic interactions with the Q[8] portals. Use of higher pH (6.8) made the protonation less favourable. ^{1}H NMR spectroscopic studies indicated that aromatic groups on the *N*-(4-diethylaminobenzyl) chitosan were encapsulated by Q[8] cavities. Release profiles of the cancer drug 5-fluorouracil were pH sensitive, raising the prospect that such a gel system could be utilized as a transporter of a drug-controlled release system.

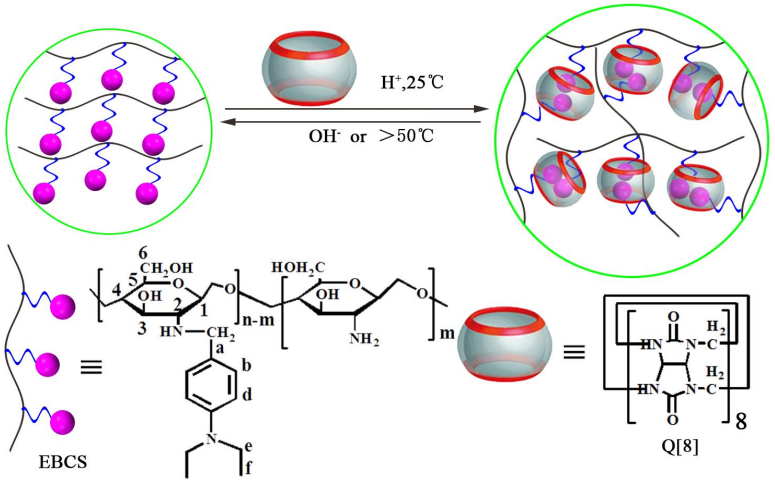

Figure 49. pH sensitive gels based on *N*-(4-diethylaminobenzyl) chitosan (EBCS) and Q[8].

Insulin releasing micelles that could be triggered in three ways, namely by adding a competing guest (e.g. adamantane amine), a change of temperature (37 to 15 ºC) or by a change in the concentration of glucose present have been reported [160]. The system demonstrated on demand release as ON and OFF states were readily accessible when using as one of the three triggers. The Q[8] tertiary complex system used for the assembly of the micelles was comprised of some quite complicated guests. One was a block copolymer containing poly(*N*-isopropylacrylamide) and poly(acrylamidophenyl boronic acid) segments, and the second poly(dimethylacrylamide). At physiological temperature, the tertiary complex self-assembled into micelles, and these were able to encapsulate insulin by pH adjustment (2 to 6) and heating (to 37 ºC), and the subsequent release profile was determined by dialysis. Light scattering techniques were employed to study the interaction of the micelles by two of the three factors capable of triggering insulin release. Results revealed that addition of adamantane amine resulted in a size reduction of *ca*. 30 nm, whilst treatment with glucose increased particle size by around 300 nm. The tertiary complexes and its constituents revealed no cytotoxicity against MTT assays.

Wang, Zhang *et al*. isolated a porphyrin-containing hyperbranched supramolecular polymer by employing a porphyrin bearing four naphthyl-substituted arms with a -CH_2- bridge separating them from the porphyrin, and combining it with Q[8] [161]. ITC measurements were consistent with a 1:2 ratio (porphyrin:Q[8]), and ^{1}H NMR spectroscopic studies indicated that naphthyl groups were encapsulated by Q[8]s; no end groups were evident. Diffusion coefficient determined via DOSY were consistent with the formation of large hyperbranched polymeric structures. EPR spectroscopic studies, conducted in the presence of 2,2,6,6-tetramethylpiperidine, indicated that the systems exhibited improved $^1O_2$ generation efficiency.

A supramolecular peptide–polymer conjugate was accessible via the interaction of an imidazolium containing pyrene functionalized peptide with a poly(*N*-isopropylacrylamide) bearing a methyl viologen end group when in the presence of Q[8] [162]. The formation of this tertiary complex was accompanied by a loss of fluorescence. If the temperature of the system was then raised from ambient to 37 ºC, double layered vesicles were formed. TEM micrographs of the vesicles stained with uranyl acetate revealed diameters of *ca*. 180 nm. Using these vesicles, it proved possible to encapsulate the mitogenic cytokine protein basic fibroblast growth factor. Moreover, after 5 days, the immunoreactivity of the protein was some 3 times higher than a sample of the same protein treated in the same way but not encapsulated. Treatment of a 3T3 cell proliferation assay revealed a 30% enhancement in cell growth over 4 days for encapsulated *versus* free protein.

14.4 Non-Covalent other systems

Disulfide linkages have been introduced at a thiolated mesoporous silica surface of spherical nanoparticles by reaction with 2-carboxyethyl 2-pyridyl disulfide, and then in a two-step process introduced amine terminated poly(glycidyl methacrylate) type chains [163]. It then proved possible to load the anticancer drug doxorubicin hydrochloride into the pores of the construct (loading 1.4 wt%), and finally addition of Q[7] allowed for host-guest complexation with the protonated amines and increasing loading (6.3 wt%). The presence of the Q[7] promoted the formation of supramolecular polymers by linking two adjacent polymer chains, and the flexible

nature of this assembly means that it is subject to change by external forces. With this in mind, the release of the anticancer drug was then investigated under different conditions of pH (7.4 to 2.0) and levels of glutathione (0, 2, 5, 10, 20 mM at pH 5.0) present. At pH 7.4, there was only very limited drug release as a result of the tightly linked network, whilst on lowering the pH the network began to crumble as Q[7] preferred to bind with hydronium ions. By the time the pH reached 4.0, drug release reached 28.6%. In terms of glutathione addition, the ability to cleave the disulfide bonds present also led to drug release at certain pH values. Importantly, this did not occur under normal physiological conditions which suggested drugs could be delivered to specific sites, where pH values and glutathione levels differ, without premature loss and thus minimize potential unwanted side effects. The potential of these systems was further demonstrated by the ability to inhibit *in vitro* cell growth.

Using a thiol-end Click reaction between (allyloxy)Q[7] and thiol-terminated polylactic acid (PLA) which also required UV irradiation (254 nm), Wang *et al*. synthesized a Q[7] bearing a PLA chain of relatively low molecular weight [164]. Nanoparticles of size suitable for the proposed medical applications were obtained by blending with poly(lactic-co-glycolic acid) in DMSO/water followed by sonification. By altering the composition, nanoparticles with sizes in the range 200 to 322 nm were accessible. The surface of the nanoparticles could be readily functionalized via non-covalent interactions by making use of the host-guest properties of the Q[7] present. In this way, it proved possible to access folate-amantadine, fluorescein isothiocyanate-amantadine as well as PEG-amantadine modified nanoparticles. The possibility of synergic treatments for cancer also moved a step nearer when it was shown that this system was capable of binding a second drug molecule (e.g. oxaliplatin) in the Q[7] cavity in addition to drug bound by the PLA/ poly(lactic-co-glycolic acid) nanoparticle, *i.e*. one in the core, one on the surface.

15. **Other potential uses**

15.1 **Sorption properties**

The portal size associated with Q[5] is relatively small and because of this its host-guest chemistry has been somewhat limited. However, despite this, there are some interesting reports

on Q[5]-based systems. For example, Tao *et al* applied a one-pot free radical polymerization strategy, using ammonium persulfate as the initiator and acrylic acid as the monomer, to synthesize polyacrylic acid chains grafted onto Q[5], see figure 50 [165]. The process was well-controlled, and it was observed that the feed mass of the acrylic acid as well as the concentration of initiator employed were crucial factors in dictating the type of structure formed. Indeed, when the initiator to Q[5] ratio was 46 or 72 to 1, polymer nanocapsule structures were observed, which exhibited different shapes/morphologies, as evidenced by TEM/SEM, depending on the initiator:Q[5] ratio employed. The sorption properties of the Q[5]-anchored polyacrylic acid aggregates was studied, and several volatiles solvents including methanol (20 wt%), acetonitrile (3wt%), ethanol (8wt%), acetone (5.3wt%) and carbon tetrachloride (5.18wt%) were measured. The high values observed for both methanol and ethanol were attributed to the presence of hydrogen bonding between the Q[5] carbonyl portals and the alcoholic guests.

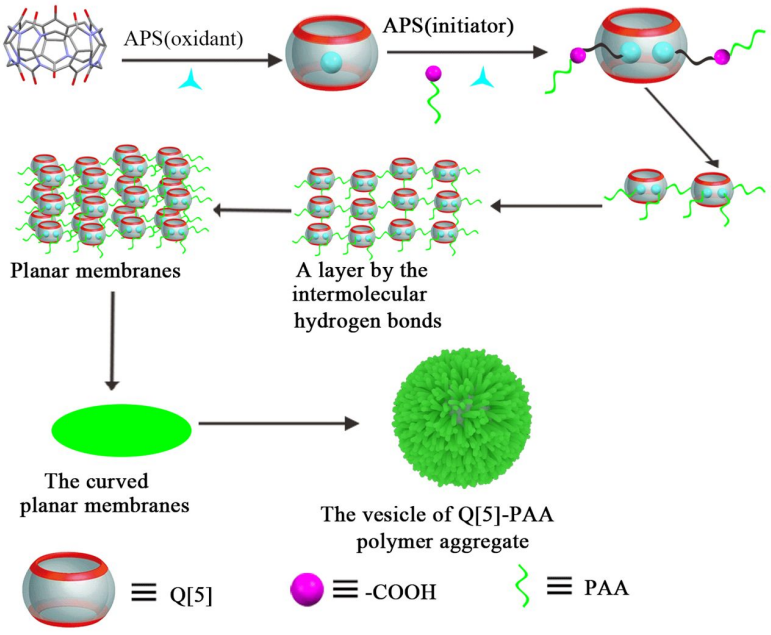

Figure 50. Formation of Q[5] anchored polyacrylic acid aggregates.

15.2 Detection of explosives

With a view to exploiting Q[6]-based systems for polymer monolithic microextraction for trace analysis of nitroaromatics, Jia *et al.* constructed poly(glycidyl methacrylate-co-ethylene dimethacrylate)-based capillary columns inside pre-conditioned fused silica capillaries, and pumped sample solutions through at a rate of 0.1 mL min^{-1}. The rotaxane employed was synthesized (in 76% yield) by treating Q[6] with concentrated HCl in the presence of

1,6-hexanediamine, followed by the addition of hydroxyl benzoyl chloride and LiOH. This rotaxane was then reacted in a ring opening reaction with glycidyl methacrylate, and then polymerization with ethylenediamine tetra acetic acid was conducted in dodecanol and toluene. When samples were tested, it was found that the presence of the rotaxane was beneficial for nitroaromatic extraction, boosting the column efficiency by as much as 35.5-fold. This enhancement was thought to arise due to favourable interactions between the rotaxane and the nitroaromatics, namely hydrophobic interactions, electrostatic interactions, hydrogen bonds and π- π interactions. For the determination of nitroaromatics in water and blood samples, recoveries of 83.2–107.9% and 88.2–112.5%, respectively were achieved; standard deviations were 4.1–11.2% and 2.1–9.6%, respectively [166].

15.3 Polymers for the oil industry

In order to meet the demands of the oil exploitation industry, new polymers with desirable properties such as salt tolerance, heat resistance and improved surfactant interaction, have been sought. With this in mind, Zou *et al*. have investigated the introduction of a Q[7] into a hydrophobically associating acrylamide polymer. In order to ensure the requisite properties were incorporated, an acrylic acid cucurbit[7]uril ester was employed which provided the temperature resistance and salt tolerance, together with hexadecyl dimethyl allyl ammonium chloride which is a hydrophobic monomer. Aqueous free-radical polymerization was employed to synthesize the polymer, which was characterized by FRIP and ^{1}H NMR spectroscopy [167].

An ‘intelligent’ polymer composed on an acrylamide monomer, an acrylic cucurbit[7]uril ester and 2-acrylamido-2-methylpropanesulfonic acid has been reported [168]. The acrylic cucurbit[7]uril ester was prepared by treating Q[7](OH)$_2$ with acrylic acid in the presence of sulfuric acid to afford Q[7](OH)(OCOCHCH$_2$). The polymer was then prepared by mixing the Q[7](OH)(OCOCHCH$_2$) with acrylamide and 2-acrylamido-2-methylpropanesulfonic acid $(NH_4)_2S_2O_8$-$NaHSO_3$ as an initiator. The driving force for this work was to improve the efficiency and accessible of restrictive reservoirs of the likes of oil and natural gas. One possible avenue to do so is to improve acidity and thereby permeability via controlling of acid-rock reaction rate. Use of a thickening reagent allows control over the diffusion rate of active acid and

this can be used to improve production. Thus, the response of the polymer prepared from the acrylic cucurbit[7]uril ester to H^+ was studied. On increasing the acid concentration, the apparent viscosities ranged between 19 and 32 mPas, and followed a trend such that they initially decreased, then increased and then decreased again. Other measurements of the thickening process indicated that the properties of this Q[7]-based containing polymer met with the expectations of the oil industry for unconventional reservoir recovery.

15.4 Control of lower critical solution (CD based systems)

15.4.1Covalent Q[7] systems

Side chain polypseudo-rotaxanes were successfully synthesized by Ogoshi, Nakamoto and coworkers using cyclodextrins (R-CD, γ-CD or Q[7]. In the presence of the side chains R-CD or Q[7], the lower critical solution temperature was found to increase, whereas the opposite was found for γ-CD (figure 51). Indeed, the lower critical solution temperature could be controlled by judicious choice of side arm substituents [169].

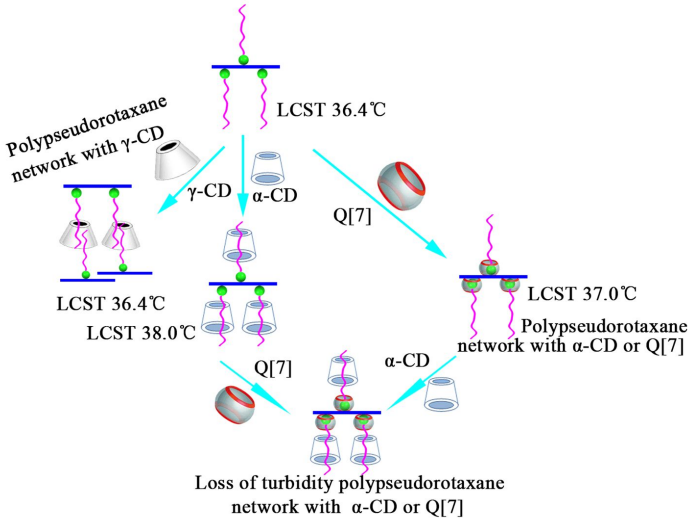

Figure 51. Control of lower critical solution temperature using side arms.

15.4.2 Non-Covalent Q[8] systems

A dibenzofuran-capped poly(*N*-isopropylacrylamide) has been combined with the host-guest complex derived from Q[8] and methyl viologen (figure 52) [170]. The lower critical solution temperature of the dibenzofuran-capped poly(*N*-isopropylacrylamide) was elevated by more the 5

°C upon complexation, and was associated with the change in the nature of the end group (hydrophobic to charged). Decomplexation was possible via the addition of 1-aminoadamantane.

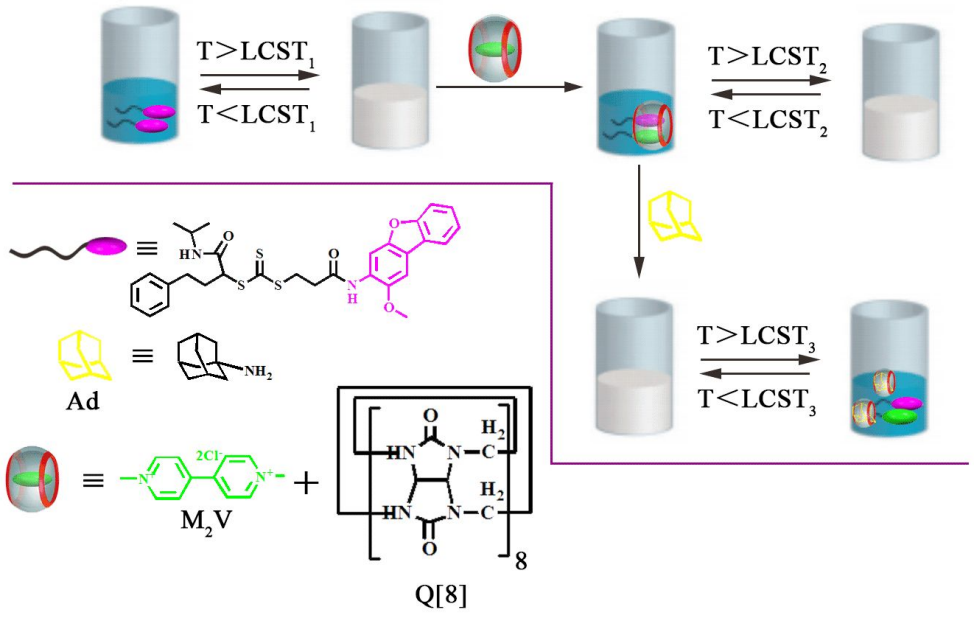

Figure 52. Lowering of critical solution temperature by change of end group.

15.5 Emitters

15.5.1 Covalent Q[7] systems

Tuncel *et al*. targeted fluorene–thiophene polyrotaxanes based on the hexyl derivative poly(9,9′-bis(6″-(*N*,*N*,*N*-trimethylammonium)-hexyl)fluorene-*alt*-co-thiophenelene) or the propyl derivative poly(9,9′-bis(6″-(*N*,*N*,*N*-trimethylammonium)-propyl)fluorene-*alt*-co-thiophenelene) and Q[7], see figure 53. Interestingly, the threading efficiency differed significantly between the two derivatives, with the hexyl (50%) > propyl (15%). The resulting polyrotaxanes exhibited improved thermal and optical properties with enhancements observed, up to 4-fold in the case of the hexyl derivative, in their fluorescent quantum yields *versus* the parent polymers. Longer fluorescence lifetimes *versus* the parent polymers in solution and the solid state were also observed. Given the attractive properties associated with the hexyl derivative, an OLED device was fabricated for it and was compared to one made from the parent polymer. The device employing the polyrotaxanes exhibited superior higher electroluminescence colour purity and lower turn-on voltages *versus* that derived from the polymer alone [171].

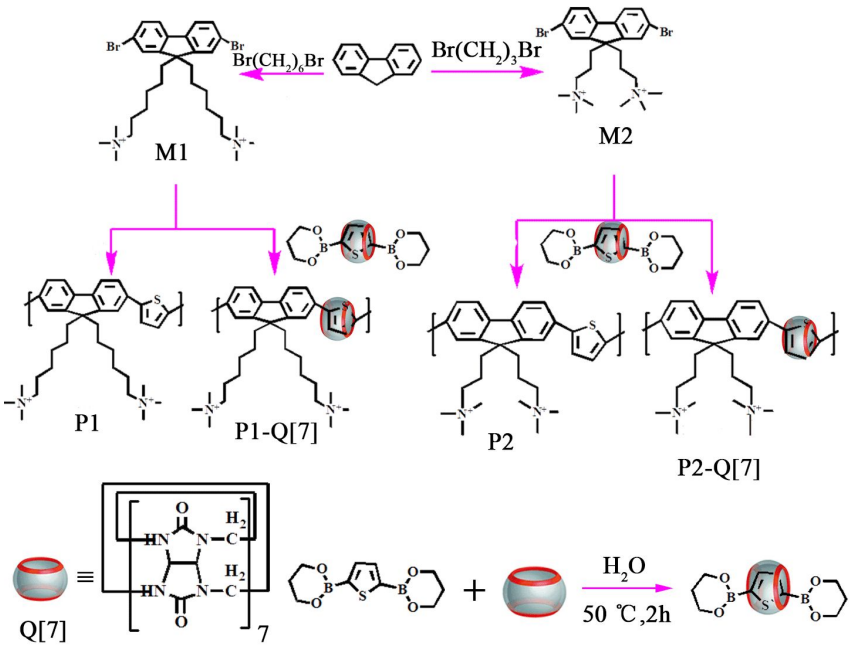

Figure 53. Hexyl and propyl derivatives of the fluorene–thiophene polyrotaxanes and their parent polymers.

The backbone of poly(9,9′-bis(6″-(*N*,*N*,*N*-trimethylammonium)hexyl)fluorene-*alt*-*co*-thiophenelene) has been threaded with Q[7], and incorporated the polypseudo-rotaxane into various hosts including NaCl, sucrose, and trehalose [172]. In the organic matrices, quantum yields of the light emitting powders were ≤52.4%, which was higher than observed in the absence of the matrices (22.8%). Pellets were prepared from co-crystallization of polyrotaxanes with sucrose and were used as part of a device (UV-LED emitting at 400 nm). The LED revealed green emission with luminous efficiencies values >6.5 lm/Welect.

15.5.2 Covalent Q[8] systems

A study of the behavior of the non-ionic polymer poly[9,9-bis{6(*N*,*N*-dimethylamino)hexyl}fluoreneco-2,5-thienylene on addition of Q[8] in aqueous solution was reported by Tuncel *et al*. On addition of Q[8], dissolution occurred and the product, as characterized by ^{1}H and selective 1D-NOESY NMR spectroscopy, was assigned a structure in which part of the aromatic backbone of the polymer was encapsulated by Q[8] and where side chain NMe_2 groups were close enough to the Q[8] to be likely protonated by coordination with the Q[8] carbonyls. The effect of Q[8] on the optical properties of the polymer

and the protonated version thereof were also explored in methanol and water. Only minor changes in emission wavelengths were noted, however the quantum yields were significantly different, *viz* 8% for the protonated polymer in water, 35% for the polymer@Q[8] in water and 45% for the polymer in methanol. Dynamic light scattering of the aqueous solutions of polymer@Q[8] indicated the presence of aggregates which under atomic force microscopy appeared spherical in nature with diameters of between 50 nm and 1 μm. Further studies using TEM and SEM confirmed the formation of vesicles, the fluorescence micrograph of which revealed green emission. Interestingly, these Q[8] induced changes were not observed when employing either Q[6] or Q[7] [173].

15.6 Extraction or encapsulation

15.6.1 Covalent Q[7] systems

Zhu, Tao *et al*. also used free radical copolymerization to construct water soluble polyacrylic acid microspheres anchored on Q[7]. This was achieved by polymerizing acrylic acid in the presence of ammonium persulfate salt and Q[7], *i.e.* a one-pot synthesis. It was found that in general, increasing the amount of ammonium persulfate salt present, which acted as both an initiator and oxidant, the average molecular weight of the copolymer increased. The study was extended to esterification with 2-naphthol, the products from which were water insoluble. It was noted that such species could interact with dye molecules e.g. acridine orange: thionine, proflavine, neutral red, basic yellow, thiazole orange, and it was noted that in general the absorbance associated with these dyes would decrease on addition of esterified product. Of particular note was the ability to capture neutral red from a neutral medium, and then release it upon washing (using ethanol) [174].

15.6.2 Covalent other systems

The reaction of the hexa-methyl-substituted HMeQ[6] with a number of alkyldiammonium guests, specifically $(H_3N(CH_2)nNH_3)^{2+}$, where n = 4, 6, 8, 10, 12 in both aqueous solution and DMSO has been reported [175]. The solvent played a pivotal role in the observed behaviour. For

example, in water, the alkyldiammonium guests were encapsulated within the hydrophobic cavity of HMeQ[6] cavity, driven by the release of water from the cavity and the attraction between the portal carbonyls and the ammonium ions. By contrast, in DMSO, the NH_3^+ groups are preferentially encapsulated and for n = 4 – 8, the whole guest is encapsulated. For n = 10 and 12, 'head' inclusion complexes are formed, whereby only the NH_3^+ group is inside the cavity. The 'head' inclusion complexes, by applying heat, could be switched back to supramolecular polymers.

Xiao, Jiang *et al*. probed the potential of the four-arm guest 5,10,15,20-tetrakis(*N*-butyl-4-pyridinium)porphyrin tetrabromide, and combined it with the twisted cucurbituril Q[14] in aqueous solution (figure 54). ^{1}H NMR spectroscopic studies and ITC measurements were consistent with a 2:1 ratio (Q[14]:guest). Competition experiments using KCl revealed that it was possible to displace the 'four-arm' guest and form a new inclusion complex between Q[14] and KCl [176].

del Barrio, Scherman *et al*. employed naphthalene-containing imidoazolium salts in reactions with Q[8] to access intermediate semiflexible polymer chains and crystalline nanostructures (figure 54a). The first guest studied was comprised of a central imidoazolium motif sandwiched between two naphthalene groups. Data collected on a 1:1 mixture of this guest with Q[8] was consistent with the presence of Q[8]n▪(guest)n species in the form of semiflexible polymer chains and rod-like structures. The second guest investigated contained a central phenylene moiety flanked either side by imidoazolium/naphthalene motifs. The behavior of this guest was similar to the first, and using AFM and TEM, there was evidence of the presence of elongated fibres (thickness 1.8 nm by AFM), and it was proposed that these resulted from aggregation of the initially formed host-guest species, i.e. an incubation period was necessary. Images of the first guest revealed shorter platelets. Cryo-TEM maps (figure 54b) suggested the fibres were composed of a single layer of host-guest complexes. Further analysis of the fibres revealed that they exhibited both viscoelastic and lyotropic properties [177].

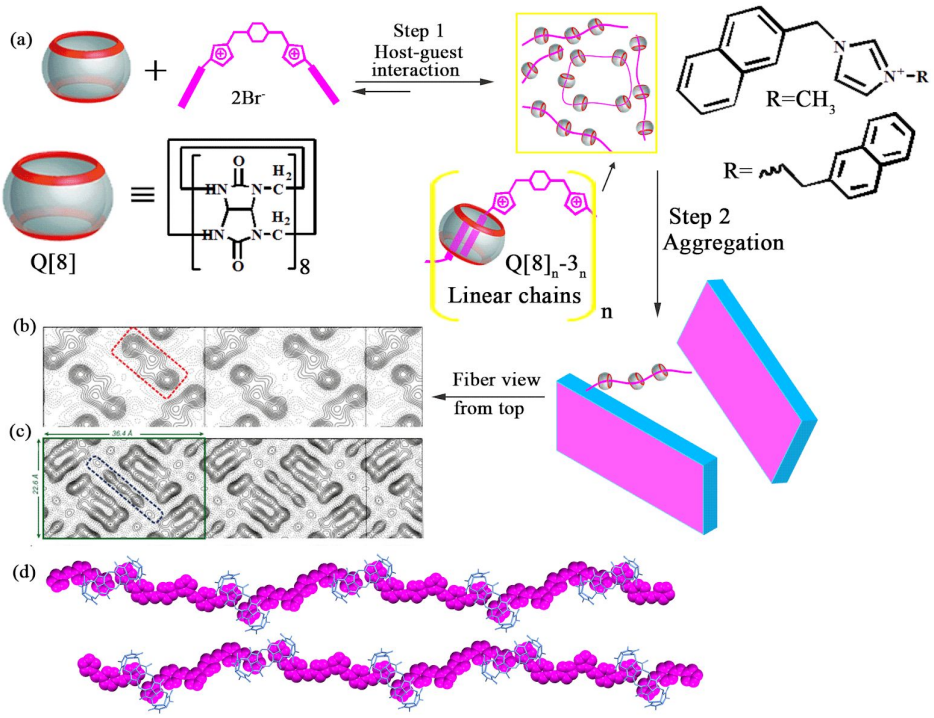

Figure 54. (a) Step-wise self-assembly using Q[8] naphthalene-containing imidoazolium salts; (b) cryo-TEM maps at a resolution of 5 (b) and (c) 4 Å; (d) a packing model for the Q[8] imidoazolium salt fibers.

15.6.3 Non-Covalent Q[8] systems

Thiazole orange dyes have been combined with Q[8] and the absorption and fluorescence changes monitored [178]. The monomer absorption was blue shifted (H-dimer aggregate formation), whilst an increase in fluorescence was observed. A Jobs plot and mass spectral data was consistent with the formation of a 2:2 host-guest complex, and molecular modelling revealed the Q[8] cavity was capable of accommodating the H-dimer. The presence of J-aggregates was also suggested from UV-vis data, and so the proposed structure included both the dimer and linear supramolecular polymers of different sizes (40 to 200 nm from AFM studies). Polymerization was not observed when Q[7] was similarly employed. Addition of 1-amantadine hydrochloride to either the Q[7] or Q[8] systems led to release of the dye.

16. **Concluding remarks**

An overview of cucurbit[*n*]uril (Q[*n*], n = 5 to 14) self-assembly into polymeric species via Q[*n*]-mediated supramolecular system is provided herein. It is clear from the amount of work described in this review that the field of Q[*n*]-based polymers is developing rapidly. The ability to utilize both covalent and non-covalent interactions to form extended structures as well as

variable size of the cavity available allows for much varied host-guest chemistry and adds to the ability to control structural dimensionality. Indeed, the structural types identified to-date are truly impressive and the likes of polymers, dendrimers, microcapsules, hydrogels, micelles, vesicles and colloids can readily be accessed. This is turn is opening up many varied applications based on Q[*n*]s, which currently range from the detection of explosives to photodynamic therapy and the delivery of anti-cancer agents. Indeed, Q[*n*]s are quickly becoming the macrocycles of choice for many applications, given their many favorable attributes. One drawback is their limited solubility which has restricted direct functionalization, however with the current level of interest in the field, we believe challenges such as this will be resolved in the near future leading to yet more exciting Q[*n*]-based chemistry.

17. **List of abbreviations**

AFM = Atomic force microscopy

AIE = Aggregation induced emission

Boc = *tert*-butoxycarbonyl

CV = Cyclic voltametry

DLS = Dynamic light scattering

DOSY = Diffusion order spectroscopy

EPR = Electron paramagnetic resonance

Gly = Glycine

ITC = Isothermal titration calorimetry

Leu = Leucine

Lys = Lysine

MALDI-ToF = Matrix assisted laser desorption/ionization-time of flight

Naph = Naphthyl

NIR = Near infrared

NMR = Nuclear magnetic resonance

PEG =Polyethyleneglycol

Phe = Phenylalanine

Phen = Phenantholine

SEM = Scanning electron microscopy

TEM = Transmission electron microscopy

XPS = X-ray photoelectron spectroscopy

Declaration of Competing Interest

The authors declare that they have no known competing financial interests or personal relationships that could have appeared to influence the work reported in this paper.

Acknowledgements

This work was supported by the National Natural Science Foundation of China (No. 21861011, 21871064), the Innovation Program for High-level Talents of Guizhou Province (No. 2016-5657), the Major Program for Creative Research Groups of Guizhou Provincial Education Department (2017-028), the Science and Technology Fund of Guizhou Province (No. 2018-5781). CR thanks the EPSRC for financial support (EP/S025537/1 and EP/R023816/1).

References

[1] R. Behrend, E. Meyer, F. Rusche, Justus Liebigs Ann. Chem. 339 (1905) 1.

[2] W. A. Freeman, W. L. Mock, N. Y. Shih, J. Am. Chem. Soc.103 (1981) 7367–7368.

[3] J. Kim, I. S. Jung, S. Y. Kim, E. Lee, J. K. Kang, S. Sakamoto, K. Yamaguchi, K. Kim, J. Am. Chem. Soc. 122 (2000) 540–541.

[4] A. I. Day, R. J. Blanch, A. P. Arnold, S. Lorenzo, G. R. Lewis, I. Dance, Angew. Chem., Int. Ed. 41 (2002) 275–277.

[5] X. J. Cheng, L. L. Liang, K. Chen, N. N. Ji, X. Xiao, J. X. Zhang, Y. Q. Zhang, S. F. Xue, Q. J. Zhu, X. L. Ni, Z. Tao, Angew. Chem., Int. Ed. 52 (2013) 7252–7255.

[6] K. Kim. Chem. Soc. Rev. 31 (2002) 96–107.

[7] Y. Yu, J. Rebek, Acc. Chem. Res. 51 (2008) 3031−3040.

[8] K. Kim, N. Selvapalam, Y. H. Ko, K. M. Park, D. Kim, J. Kim, Chem. Soc. Rev. 36 (2007) 267–279.

[9] K. I. Assaf, W. M. Nau, Chem. Soc. Rev. 44 (2015) 394–418.

[10] W. Liu, S. K. Samanta, B. D. Smith, L. Isaacs, Chem. Soc. Rev. 46 (2017) 2391-2403.

[11] A. E. Kaifer, Acc. Chem. Res.47 (2014) 2160.

[12] R. Pinalli, A. Pedrini, E. Dalcanale, Chem. Soc. Rev. 47 (2018) 7006-7026.
[13] J. Murray, K. Kim, T. Ogoshi, W. Yao, B. C. Gibb, Chem. Soc. Rev. 46 (2017) 2479-2496.
[14] J. Lü, J. X. Lin, M. N. Cao, R. Cao, Coord. Chem. Rev. 257 (2013) 1334–1356.
[15] X. L. Ni, X. Xiao, H. Cong, L. L. Liang, K. Chen, X. J. Cheng, N. N. Ji, Q. J. Zhu, S. F. Xue, Z. Tao, Chem. Soc. Rev. 42 (2013) 9480–9508.
[16] Y. Liu, H. Yang, Z. Wang, X. Zhang, Chem. Asian J. 8 (2013) 1626.
[17] J. Tian, L. Zhang, H. Wang, D. -W. Zhang, Z.-T. Li, Supramol. Chem. 28 (2016) 769–783.
[18] H. Zou, J. Liu, X. Li, X. Wang, Small 14 (2018) 1802234.
[19] S. Gürbüz, M. Idris, D. Tuncel, Org. Biomol. Chem.13 (2015) 330–347.
[20] A. Koc, D. Tuncel, *Isr. J. Chem*. 58 (2018) 334–342.
[21] J. Liu, C. S. Y. Tan, Y. Lan, O. A. Scgerman, Macromol. Chem. Phys. 217 (2016) 319−332.
[22] F. Biedermann, U. Rauwald, J. M. Zayed, O. A. Scherman, Chem. Sci. 2 (2011) 279–286.
[23] M. Cziferszky, F. Biedermann, M. Kalberer, O. A. Scherman, Org. Biomol. Chem. 10 (2012) 2447–2452.
[24] E. Cavatorta, P. Jonkheijm, J. Huskens, Chem. Eur. J. 23 (2017) 4046-4050.
[25] O. J. G. M. Goor, R. P. G. Bosmans, L. Brunsveld, P. Y. W. Dankers, J. Polym. Sci. Polym. Chem. 55 (2017) 3607–3616.
[26] J. B. Wittenberg, L. Isaacs, Supramol. Chem., 26 (2014) 157-167.
[27] X. Tan, L. Yang, Y. Liu, Z. Huang, H. Yang, Z. Wang, X. Zhang, Polym. Chem. 4 (2013) 5378–5381.
[28] R. Nally, L. Isaacs, Tetrahedron 65 (2009) 7249–7258.
[29] F. Lin, T. -G. Zhan, T. -Y. Zhou, K. -D. Zhang, J. Wu, X, Zhao, Chem. Commun. 50 (2014) 7982-7985.
[30] Z.-J. Yin, Z.-Q. Wu, F. Lin, Q.-Y. Qi, X.-N. Xu, X. Zhao, Chinese Chem. Lett. 28 (2017) 1167–1171.
[31] Wu, H. Hua, Q. Wang, New J. Chem. 42 (2018) 8320-8324.
[32] D. Whang, Y.-M. Jeon, J. Heo, K. Kim, J. Am. Chem. Soc. 118 (1996) 11333-11334.
[33] H. Wang, Y. Zhu, X. Ren, M. Wang, Y. Tan, Iran Polym. *J*. 21 (2012) 783–792.
[34] Z.-Y. Hua, C. Chen, F.-H. Zhou, H. Zhang, Z. Q. Zhu, W.-W. Ge, K. Chen, *Inorg. Chmica Acta*, 499 (2020) 119183.
[35] Y. Liu, J. Shi, Y. Chen, C.-F. Ke, Angew. Chem. Int. Ed. 47 (2008) 7293 –7296.
[36] Z. Huang, L. Yang, Y. Liu, Z. Wang, O. A. Scherman, X. Zhang, Angew. Chem. Int. Ed. 53 (2014) 5351–5355.
[37] L. Chen, Z. Huang, J.-F. Xu, Z. Wang, X. Zhang, Polym. Chem. 7 (2016) 1397-1404.
[38] Z. Huang, Y. Fang, Q. Luo, S. Liu, G. An, C. Hou, C. Lang, J. Xu, Z. Dong, J. Liu, Chem. Commun. 52 (2016) 2083-2086.

[39] R. Nally, O. A. Scherman, L. Isaacs, Supramol. Chem. 22 (2010) 683–690.
[40] Y. Liu, K. Liu, Z. Wang, X. Zhang, Chem. Eur. J. 17 (2011) 9930 – 9935.
[41] Y. Liu, R. Fang, X. Tan, Z. Wang, X. Zhang, Chem. Eur. J. 18 (2012) 15650 – 15654.
[42] Q. Wang, Y. Chen, Y. Liu, Polym. Chem. 4 (2013) 4192–4198.
[43] L. Yang, X. Liu, X. Tan, H. Yang, Z. Wang, X. Zhang, Polym. Chem. 5 (2014) 323–326.
[44] F. Lin, T.-G. Zhan, T.-Y. Zhou, K.-D. Zhang, G.-Y. Li, J. Wu, X. Zhao, Chem. Commun., 50 (2014) 7982-7985.
[45] Q. Song, F. Li, L. Yang, Z. Wang, X. Zhang, Polym. Chem. 6 (2015) 369–372.
[46] J.-F. Yin, Y. Hu, D.-G. Wang, L. Yang, Z. Jin, Y. Zhang, G.-C. Kuang, ACS Macro Lett. 6 (2017) 139 −143.
[47] Q. Song, J. Yang, J. Y. Rho, S. Perrier, Chem. Commun. 55 (2019) 5291-5294.
[48] Sohail, M. A. Alnaqbi, N. Saleh, Macromolecules 52 (2019) 9023-9031.
[49] Y. Yang, X.-L. Ni, J.-F. Xu, X. Zhang, Chem. Commun. 55 (2019) 13836-13839.
[50] M.-H. Xiang, Q.-Y. Qi, X. Zheng, X. Zhao, Tetrahedron Letters 60 (2019) 1727–1731.
[51] Y. Zhang, S. Panjikar, K. Chen, I. Karatchevtseva, Z. Tao, G. Wei, Inorg. Chem. 58 (2019) 506−515.
[52] D. Whang, K. Kim, J. Am. Chem. Soc. 119 (1997) 451-452.
[53] X. Hou, C. Ke, Y. Zhou, Z. Xie, A. Alngadh, D. T. Keane, M. S. Nassar, Y. Y. Botros, C. A. Mirkin, J. F. Stoddart, Chem. Eur. J. 22 (2016) 12301-12306.
[54] Z. Gao, J. Zhang, N. Sun, Y. Huang, Z. Tao, X. Xiao, J. Jiang, Org. Chem. Front. 3 (2016) 1144–1148.
[55] R. Fang, Y. Liu, Z. Wang, X. Zhang, Polym. Chem. 4 (2013) 900–903.
[56] F. Qiao, Z. Yuan, Z. Lian, C.-Y. Yan, S. Zhuo, Z.-Y. Zhou, L.-B. Xing, Dyes and Pigments 146 (2017) 392-397.
[57] K.-D. Zhang, J. Tian, D. Hanifi, Y. Zhang, A. C.-H. Sue, T.-Y. Zhou, L. Zhang, X. Zhao, Y. Liu, Z.-T. Li, J. Am. Chem. Soc. 135 (2013) 17913−17918.
[58] H. Yang, Z. Ma, B. Yuan, Z. Wang, X. Zhang, Chem. Commun. 50 (2014) 11173-11176.
[59] B. Yuan, H. Yang, Z. Wang, X. Zhang, Langmuir 30 (2014) 15462−15467.
[60] X. Zhang, C.-B. Nie, T.-Y. Zhou, Q.-Y. Qi, J. Fu, X.-Z. Wang, L. Dai, Y. Chena, X. Zhao, Polym. Chem. 6 (2015) 1923–1927.
[61] M. Pfeffermann, R. Dong, R. Graf, W. Zajaczkowski, T. Gorelik, W. Pisula, A. Narita, K. Mullen, X. Feng, J. Am. Chem. Soc. 137 (2015) 14525−14532.
[62] F.-z. Li, L. Mei, K.-q. Hu, J.-p. Yu, S.-w. An, K. Liu, Z.-f. Chai, N. Liu, W.-q, Shi, Inorg. Chem. 57 (2018) 13513−13523.
[63] F.-z. Li, L. Mei, S.-w. An, K.-q. Hu, Z.-f. Chai, N. Liu and W.-q. Shi, Inorg. Chem. 59 (2020) 4058−4067.

[64] S.-w. An, L. Mei, K.-q. Hu, Z.-h. Zhang, C.-q. Xia, Z.-f. Chai, W.-q. Shi, Inorg. Chem. 59 (2020) 943-955.

[65] M. Munteanu, SooWhan Choi, H. Ritter. Macromolecules 42 (2009) 3887–3891.

[66] Q. Ma, H. Yang, J. Hao, Y. Tan, J. Dispersion Sci. & Tech. 33 (2012) 639–646.

[67] H. Chen, H. Ma, Y. Y. Chieng, S. Hou, X. Li, Y. Tan, RSC Adv. 5 (2015) 20684–20690.

[68] H. Chen, H. Ma, Y. Tan, *J. Polym. Sci. A,* Polym. Chem. 53 (2015) 1748–1752.

[69] S. Deroo, U. Rauwald, C. V. Robinson, O. A. Scherman, Chem. Commun. (2009) 644–646.

[70] J.-F. Xu, Z. Huang, L. Chen, B. Qin, Q. Song, Z. Wang, X. Zhang, ACS Macro Lett. 4 (2015) 1410−1414.

[71] Z. Ji, Y. Li, Y. Ding, G. Chen, M. Jiang, Polym. Chem. 6 (2015) 6880–6884.

[72] Z. Ji, J. Li, G. Chen, M. Jiang, ACS Macro Lett. 5 (2016) 588−592.

[73] D. Kim, E. Kim, J. Kim, K. M. Park, K. Baek, M. Jung, Y. H. Ko, W. Sung, H. S. Kim, J. H. Suh, C. G. Park, O. S. Na, D.-k. Lee, K. E. Lee, S. S. Han, K. Kim, Angew Chemie Int. Ed. 46 (2007) 3471-3474.

[74] D. Kim, E. Kim, J. Lee, S. Hong, W. Sung, N. Lim, C. G. Park, and K. Kim, J. Am. Chem. Soc. 132 (2010) 9908–9919.

[75] A. Hennig, A. Hoffmann, H. Borcherding, T. Thiele, U. Schedlerb and U. Resch-Genger, Chem. Commun. 47 (2011) 7842-7844.

[76] Y. Wu, Y. Lan, J. Liu and O. A. Scherman, Nanoscale 7 (2015) 13416–13419.

[77] Y. Lan, X. J. Loh, J. Geng, Z. Walsh, O. A. Scherman, Chem. Commun. 48 (2012) 8757–8759.

[78] C.-J. Chen, D.-D. Li, H.-B. Wang, J. Zhao, J. Ji, Polym. Chem. 4 (2013) 242-245.

[79] R. M. Parker, J. Zhang, Y. Zheng, R. J. Coulston, C. A. Smith, A. R. Salmon, Ziyi Yu, O. A. Scherman, C. Abell, Adv. Funct. Mater. 25 (2015) 4091–4100.

[80] C. Stoffelen, E. Staltari-Ferraro, J. Huskens, J. Mater. Chem. B 3 (2015) 6945-6952.

[81] Z. Yu, Y. Zheng, R. M. Parker, Y. Lan, Y. Wu, R. J. Coulston, J. Zhang, O. A. Scherman, C. Abell, ACS Appl. Mater. Interfaces 8 (2016) 8811−8820.

[82] Z. Yu, Y. Lan, R. M. Parker, W. Zhang, X. Deng, O. A. Scherman, C. Abell, Polym. Chem. 7 (2016) 5996–6002.

[83] K. Samanta, C. Schmuck, Chem Commun. 51 (2015) 16065-16067.

[84] M. K. Samanta, W. Sicking, C. Schmuck, Eur. J. Org. Chem. (2018) 6515–6518.

[85] H.-K. Lee, K. M. Park, Y. J. Jeon, D. Kim, D. H. Oh, H. S. Kim, C. K. Park, K. Kim, J. Am. Chem. Soc. 127 (2005) 5006-5007.

[86] K. Baek, D. Xu, J. Murray, S. Kim, K. Kim, Chem. Commun. 52 (2016) 9676-9678.

[87] H. Yang, Y. Liu, K. Liu, L. Yang, Z. Wang and X. Zhang, Langmuir 29 (2013) 42, 12909-12914.
[88] H. Yang, Z. Ma, Z. Wang and X. Zhang, Polym. Chem. 5 (2014) 1471–1476.
[89] X. Tang, Z. Huang, H. Chen, Y. Kang, J.-F. Xu and X. Zhang, Angew. Chem. Int. Ed. 57 (2018) 8545 –8549.
[90] F. Tian, D. Jiao, F. Biedermann, O. A. Scherman, Nat. Commun. 3 (2012) 1207.
[91] J. del Barrio, P. N. Horton, D. Lairez, G. O. Lloyd, C. Toprakcioglu, O. A. Scherman, J. Am. Chem. Soc. 135 (2013) 11760−11763.
[92] Y. Lan, Y. Wu, A. Karas, O. A. Scherman, Angew. Chem. Int. Ed. 53 (2014) 2166 –2169.
[93] C. Stoffelen, J. Voskuhl, P. Jonkheijm, J. Huskens, Angew. Chem. Int. Ed. 53 (2014) 3400 –3404.
[94] C. Stoffelen, J. Huskens, Nanoscale 7 (2013) 7915-7919.
[95] Q. Song, F. Li, X. Tan, L. Yang, Z. Wang, X. Zhang, Polym. Chem. 5 (2014) 5895–5899.
[96] T.-T. Cao, X.-Y. Yao, J. Zhang, Q.-C. Wang, X. Ma, Chin. Chem. Lett. 26 (2015) 867-871.
[97] R. M. Parker, J. Zhang, Y. Zheng, R. J. Coulston, C. A. Smith, A. R. Salmon, Ziyi Yu, O. A. Scherman, C. Abell, Adv. Funct. Mater. 25 (2015) 4091–4100.
[98] L. Yang, Y. Bai, X. Tan, Z. Wang, X. Zhang, ACS Macro Lett. 4 (2015) 611−615.
[99] C. S. Y. Tan, J. del Barrio, J. Liua, O. A. Scherman, Polym. Chem. 6 (2015) 7652–7657.
[100] A.S. Groombridge, A. Palma, R. M. Parker, C. Abell, O. A. Scherman, Chem. Sci. 8 (2017) 1350–1355.
[101] Y. Kang, Z. Cai, Z. Huang, X. Tang, J.-F. Xu, X. Zhang, ACS Macro Lett. 5 (2016) 1397-1401.
[102] H.-J. Kim, D. R. Whang, J. Gierschner, S. Y. Park, Angew. Chem. 128 (2016) 16147 -16151.
[103] T. Wang, Y. Tang, X. He, J. Yan, C. Wang, X. Feng, ACS Appl. Mater. Interfaces 9 (2017) 6902-6907.
[104] P. C. Nandajan, H.-J. Kim, S. Casado, S. Y. Park, J. Gierschner, J. Phys. Chem. Lett. 9 (2018) 3870−3877.
[105] T.-T. Jin, X.-H. Zhou, Y.-F. Yin, T.-G. Zhan, J. Cui, L.-J. Liu, L.-C. Kong, K.-D. Zhang, Chem. Asian J. 13 (2018) 2818 – 2823.
[106] D. Chang, D. Han, W. Yan, Z. Yuan, Q. Wang, L. Zou, RSC Adv. 8 (2018) 13722-13727.
[107] J. Liu, X. Jiang, X. Huang, L. Zou, Q. Wang, Colloid Polym Sci. 294 (2016) 1243–1249.
[108] S. Choi, J. W. Lee, Y. H. Ko, K. Kim, Macromolecules 35 (2002) 3526-3531.
[109] Y. Tan, S. Choi, J. W. Lee, Y. H. Ko, K. Kim, Macromolecules 35 (2002)7161-7165.

[110] Z.-S. Hou, J. Xu, Y.-S. Chen, Y. B. Tan, C.-Y. Kan. Chin. J. Org. Chem. 28 (2008) 1937-1942.

[111] H. Yang, Y. Tan, J. Hao, H. Yang, F. Liu, Polym Chem. 48 (2010) 2135–2142.

[112] H. Yang, J. Hao, Y. Tan, *J. Polym. Sci. A:* Polym. Chem. 49 (2011) 2138–2146.

[113] E. A. Appel, J. del Barrio, J. Dyson, L. Isaacs, O. A. Scherman, Chem. Sci. 3 (2012) 2278-2281.

[114] U. Rauwald, O. A. Scherman, Angew. Chem. Int. Ed. 47 (2008) 3950 –3953.

[115] J. Geng, F. Biedermann, J. M. Zayed, F. Tian, O. A. Scherman, Macromolecules 44 (2011) 4276–4281.

[116] H. Qian, D.-S. Guo, Y. Liu, Chem. Eur. J. 18 (2012) 5087 – 5095.

[117] E. A. Appel, J. Dyson, J. del Barrio, Z. Walsh, O. A. Scherman, Angew. Chem. Int. Ed. 51 (2012) 4185 – 4189.

[118] Z. Ji, J. Liu, G. Chen, M. Jiang, Polym. Chem. 5 (2014) 2709–2714.

[119] L. Zhang, T.-Y. Zhou, J. Tian, H. Wang, D.-W. Zhang, X. Zhao, Y. Liu, Z.-T. Li, Polym. Chem. 5 (2014) 4715–4721.

[120] L. Wang, Z. Sun, M. Ye, Y. Shao, L. Fang, X. Liu, Polym. Chem. 7 (2016) 3669–3673.

[121] S. Ahmed, N. Singha, B. Pramanik, J. H. Mondal, D. Dasm, Polym. Chem. 7 (2016) 4393–4401,

[122] K. Madasamy, D. Velayutham, M. Kathiresan, ACS Omega 4 (2019) 8528−8538.

[123] Q. Qi, B. Yang, C.-G. Xi, X. Yang, D.-W. Zhang, S. Liu, Z.-T. Li, ChemistrySelect 1 (2016) 6792 – 6796.

[124] K. Kim, D. Kim, J. W. Lee, Y. H. Ko, K. Kim, Chem. Commun. (2004) 848–849.

[125] R. J. Coulston, S. T. Jones, T.-C. Lee, E. A. Appel, O. A. Scherman, Chem. Commun., 47 (2011) 164–166.

[126] J. Zhang, R. J. Coulston, S. T. Jones, J. Geng, O. A. Scherman, C. Abell, Science 335 (2012) 690-694.

[127] C. Hu, Y. Zheng, Z. Yu, C. Abell, O. A. Scherman, Chem. Commun. 51 (2015) 4858-4860.

[128] C. Hu, F. Tian, Y. Zheng, C. S. Y. Tan, K. R. West, O. A. Scherman, Chem. Sci. 6 (2015) 5303–5310.

[129] C. Hu, Y. Lan, K. R. West, O. A. Scherman, Adv. Mater. 27 (2015) 7957-7962.

[130] I. Hwang, K. Baek, M. Jung, Y. Kim, K. M. Park, D.-W. Lee, N. Selvapalam, K. Kim, J. Am. Chem. Soc. 129 (2007) 4170-4171.

[131] V. Valderrey, M. Wiemann, P. Jonkheijm, S. Hecht, J. Huskens, ChemPlusChem 84 (2019) 1324–1330.

[132] H. Chen, S. Hou, H. Ma, X. Li, Y. Tan, Scientific Reports 6 (2016) 20722.

[133] A. Tabet, R. A. Forster, C. C. Parkins, G. Wu, O. A. Scherman, Polym. Chem. 10 (2019) 467–472.
[134] E. A. Appel, F. Biedermann, U. Rauwald, S. T. Jones, J. M. Zayed, O. A. Scherman, J. Am. Chem. Soc. 132 (2010) 14251–14260.
[135] E. A. Appel, X. J. Loh, S. T. Jones, C. A. Dreiss, O. A. Scherman, Biomaterials 33 (2012) 4646-4652.
[136] E. A. Appel, X. J. Loh, S. T. Jones, F. Biedermann, C. A. Dreiss, O. A. Scherman, J. Am. Chem. Soc. 134 (2012) 11767−11773.
[137] H. Yang, H. Chen, Y. Tan, RSC Adv. 3 (2013) 3031–3037.
[138] Y. Lin, L. Li, G. Li, Carbohyd. Polym. 92 (2013) 429–434.
[139] M. J. Rowland, E. A. Appel, R. J. Coulston, O. A. Scherman, J. Mater. Chem. B 1 (2013) 2904–2910.
[140] K.-D. Zhang, J. Tian, D. Hanifi, Y. Zhang, A. C.-H. Sue, T.-Y. Zhou, L. Zhang, X. Zhao, Y. Liu, Z.-T. Li, J. Am. Chem. Soc. 135 (2013) 17913−17918.
[141] E. A. Appel, X, J. Loh, S. T. Jones, C. A. Dreiss, O. A. Scherman, Biomat. 33 (2012) 4646-4652.
[142] J. R. McKee, E. A. Appel, J. Seitsonen, E. Kontturi, O. A. Scherman, O. Ikkala, Adv. Funct. Mater. 24 (2014) 2706-2713.
[143] E. A. Appel, R. A. Forster, A. Koutsioubas, C. Toprakcioglu, O. A. Scherman, Angew. Chem. Int. Ed. 53 (2014) 10038 -10043.
[144] Z. Yu, J. Zhang, R. J. Coulston, R. M. Parker, F. Biedermann, X. Liu, O. A. Scherman, C. Abell, Chem. Sci., 6 (2015) 4929–4933.
[145] X. Xu, E. A. Appel, X. Liu, R. M. Parker, O. A. Scherman, C. Abell, Biomacromol. 16 (2015) 2743−2749.
[146] J. Cao, L. Meng, S. Zheng, Z. Li, J. Jiang, X. Lv, *Int. J. Polym. Mater.* Polym. Biomat., 65 (2016) 537-542.
[147] H.-L. Ma, H. Chen, S.-Z. Hou and Y.-B. Tan, *Chin.* J. Polym. Sci. 34 (2016) 1251−1260.
[148] C. Liu, G. Xiang, Y. Wu, S. J. Barrow, M. J. Rowland, D. E. Clarke, G. Wu, O. A. Scherman, Polym. Chem. 7 (2016) 6485-6489.
[149] E. Kim, D. Kim, H. Jung, J. Lee, S. Paul, N. Selvapalam, Y. Yang, N. Lim, C. G. Park, K. Kim, Angew. Chem. 122 (2010) 4507-4510.
[150] S. Barman, G. Das, V. Gupta, P. Mondal, B. Jana, D. Bhunia, J. Khan, D. Mukherjee, S. Ghosh, Mol. Pharmaceutics 16 (2019) 2522-2531.
[151] C. Sun, H. Zhang, L. Yue, S. Li, Q. Cheng, R. Wang, ACS Appl. Mater. Interfaces 11 (2019) 22925-22931.
[152] I. Ghosh, W. M. Nau, Adv. Drug Deliv. Rev. 64 (2012) 764–783.
[153] Z. Huang, H. Zhang, H. Bai, Y. Bai, S. Wang, X. Zhang, ACS Macro Lett. 5 (2016) 1109−1113.
[154] H. Bai, H. Chen, R. Hu, M. Li, F. Lv, L. Liu, S. Wang, ACS Appl. Mater. Interfaces 8 (2016) 31550−31557.
[155] T. Zhang, S. Sun, F. Liu, Y. Pang, J. Fan, X. Peng, Phys. Chem. Chem. Phys. 13 (2011) 9789–9795.

[156] Y. Huang, Q.-H. Hu, G.-X. Song, Z. Tao, S.-F. Xue, Q.-J. Zhu, Q.-D Zhou, G. Wei, RSC Adv. 4 (2014) 3348–3354.
[157] F. Biedermann, U. Rauwald, M. Cziferszky, K. A. Williams, L. D. Gann, B. Y. Guo, A. R. Urbach, C. W. Bielawski, O. A. Scherman, Chem. Eur. J. 16 (2010) 13716 – 13722.
[158] X. J. Loh, J. del Barrio, P. P. C. Toh, T.-C. Lee, D. Jiao, U. Rauwald, E. A. Appel, O. A. Scherman, Biomacromol. 13 (2012) 1, 84-91.
[159] Y. Lin, L. Li, G. Li, Carbohyd. Polym. 92 (2013) 429–434.
[160] X. J. Loh, M.-H. Tsai, J. del Barrio, E. A. Appel, T.-C. Lee, O. A. Scherman, Polym. Chem. 3 (2012) 3180–3188.
[161] Y. Liu, Z. Huang, K. Liu, H. Kelgtermans, W. Dehaen, Z. Wang, X. Zhang, Polym. Chem. 5 (2014) 53–56.
[162] X. J. Loh, J. del Barrio, T.-C. Lee, O. A. Scherman, Chem. Commun. 50 (2014) 3033-3035.
[163] Q.-L. Li, S.-H. Xu, H. Zhou, X. Wang, B. Dong, H. Gao, J. Tang, Y.-W. Yang, ACS Appl. Mater. Interfaces 7 (2015) 28656−28664.
[164] C. Sun, H. Zhang, S. Li, X. Zhang, Q. Cheng, Y. Ding, L.-H. Wang, R. Wang, ACS Appl. Mater. Interfaces 10 (2018) 25090−25098.
[165] B. Xiao, Y. Fan, R.-H. Gao, P. Chen, J.-X. Zhang, Q.-D. Zhou, S.-F. Xue, Q.-J. Zhu, Z. Tao, RSC Adv. 5 (2015) 33809–33813.
[166] H. Zheng, Z. Li, J. Zhang, J. Ma, Y. Zhou, Q. Jia, RSC Adv. 5 (2015) 5850–5857.
[167] C. Zou, T. Gu, P. Xiao, T. Ge, M. Wang, K. Wang, Ind. Eng. Chem. Res. 53 (2014) 7570−7578.
[168] L. Zhou, C. Zou, T. Gu, X. Li, Y. Shi, J. Petrol. Sci. and Eng. 149 (2017) 65–74.
[169] T. Ogoshi, K. Masuda, T.-A, Yamagishi, Y. Nakamoto, Macromol. 42 (2009) 8003–8005.
[170] U. Rauwald, J. del Barrio, X. J. Loh, O. A. Scherman, Chem. Commun. 47 (2011) 6000–6002.
[171] M. Idris, M. Bazzar, B. Guzelturk, H. V. Demir, D. Tuncel, RSC Adv. 6 (2016) 98109–98116.
[172] T. Erdem, M. Idris, H. V. Demir, D. Tuncel, Macromol. Mater. Eng. 302 (2017) 1700290.
[173] D. Tuncel, M. Artar, S. B. Hanay, J. Polym. Sci. A: Polym. Chem. 48 (2010) 4894–4899.
[174] R. H. Gao, Y. Fan, B. Xiao, P. Chen, J. X. Zhang, Q.-D. Zhou, S. F. Xue, Q. J. Zhu, Z. Tao, RSC Adv. 5 (2015) 65775–65779.
[175] L.-J. Meng, X. Tian, S. Huang, R.-L. Lin, X.-H. Liu, Q.-J. Zhu, Z. Tao, J.-X. Liu, ChemistrySelect 3 (2018) 9211 –9217.
[176] Z. Gao, J. Zhang, N. Sun, Y. Huang, Z. Tao, X. Xiao, J. Jiang, Org. Chem. Front. 3 (2016) 1144–1148.

[177] J. del Barrio, J. Liu, R. A. Brady, C. S. Y. Tan, S. Chiodini, M. Ricci, R. Fernandez-Leiro, C.-J. Tsai, P. Vasileiadi, L. Di Michele, D. Lairez, C. Toprakcioglu, O. A. Scherman, J. Am. Chem. Soc. 141 (2019) 14021−14025.

[178] Y. Xu, M. Guo, X. Li, A. Malkovskiy, C. Wesdemiotis, Y. Pang, Chem. Commun. 47 (2011) 8883–8885.

Graphic for table of contents